Why Make Fat?: The Impact of *de novo* Fatty Acid Synthesis on Fat Storage, Reproduction, and Longevity in *C. elegans*

Carissa Perez Olsen

A dissertation
submitted in partial fulfillment of the
requirement for the degree of

Doctor of Philosophy

University of Washington

2011

Program Authorized of Offer Degree:
Molecular and Cellular Biology

University of Washington
Graduate School

This is to certify that I have examined this copy of a doctoral dissertation by

Carissa Perez Olsen

and have found that it is complete and satisfactory in all respects,
and that any and all revisions required by the final
examining committee have been made.

Chair of the Supervisory Committee:

Marc R. Van Gilst

Reading Committee:

David M. Hockenbery

Brian K. Kennedy

Marc R. Van Gilst

Date: 5/26/11

In presenting this dissertation in partial fulfillment of the requirements for the doctoral degree at the University of Washington, I agree that the Library shall make its copies freely available for inspection. I further agree that extensive copying of the dissertation is allowable only for scholarly purposes, consistent with "fair use" as prescribed in the U.S. Copyright Law. Requests for copying or reproduction of this dissertation may be referred to ProQuest Information and Learning, 300 North Zeeb Road, Ann Arbor, MI 48106-1346, 1-800-521-0600, to whom the author has granted "the right to reproduced and sell (a) copies of the manuscript in microform and/or (b) printed copies of the manuscript made from microform."

Signature 

Date 06/01/2017

University of Washington

Abstract

Why Make Fat?: The Impact of *de novo* Fatty Acid Synthesis on Fat Storage, Reproduction, and Longevity in *C. elegans*

Carissa Perez Olsen

Chair of the Supervisory Committee:
Professor Marc Van Gilst
Assistant Member, Basic Science Division, FHCRC

Metabolic flux analysis allows for the understanding of how multiple pathways are integrated onto the core metabolism of an animal as it encounters different environmental and physiological challenges. Here, we have developed and implemented a stable ^{13}C isotope approach in *C. elegans* that allows us to monitor how the animals are utilizing their diet. This "mixed isotope" strategy can specifically quantify various aspects of fatty acid metabolism and can accurately determine whether the fats of the animals are absorbed directly from the diet or synthesized *de novo*. We have used this mixed labeling strategy to define how known fat storage genes, such as the insulin receptor, impact lipid metabolism pathways. In doing so, we have been able to establish that elevated *de novo* fatty acid synthesis is the main driver of fat accumulation in *daf-2* animals. Additionally, this type of analysis allowed us to determine that the longevity and fat storage phenotypes of the *daf-2* animals are separable.

In addition, we have used this strategy to identify several novel regulators of *de novo* fatty acid synthesis. These regulators include oxidative phosphorylation and peroxisomal β-oxidation, which have not been previously implicated in the regulation of lipogenesis. In

addition, we found that reproduction is also a key driver of *de novo* fatty acid synthesis as adult animals have significantly more synthesized fatty acids than their larval counterparts. Because reproduction requires a large amount of resources, we hypothesize that a lipogenic shift is an important component for successful progeny production and continued somatic maintenance. Finally, we have also found that RNAi of the *fatty acid synthase* gene results in a reduction in the adult lifespan indicating an important function for lipogenesis in the adult.

Table of Contents

List of Figures

List of Tables

Acknowledgements

I would like to thank all the members of the Van Gilst lab for their ideas, suggestions, and help along the way. I would particularly like to thank the people who have generated data presented here including Felix Nau Jr, Alex Lin and Ngoc Tran.

Dedication

To Phil
who is there for me always

and

To My Parents
who have supported me in everything I have done

CHAPTER I: Lipid Metabolism Pathways and Fatty Acid Allocation

An animal must utilize its dietary resources to produce energy and to generate biomolecules for maintenance, growth, and repair. In addition, resources must be allocated for long-term storage and reproduction. An imbalance in how an animal juggles these requirements may have a significant impact on its health, fecundity and longevity. In this work, we use the model system, *Caenorhabditis elegans,* to understand how genes and pathways contribute to the regulation of dietary nutrient allocation, in particular the regulation of *de novo* fatty acid synthesis. To do this, it was necessary to develop a strategy to track how an animal processes and partitions its dietary nutrients. Elegant stable ^{13}C isotope labeling strategies have been developed in other systems that monitor flux through metabolic pathways, and we have developed such an approach to define the relative contribution of dietary fat absorption and *de novo* fatty acid synthesis to the fatty acid pool in *C. elegans*. The development of the mixed isotope strategy has allowed us to interrogate how various genes and pathways influence nutrient utilization and to investigate how imbalances in the partitioning of dietary resources can impact fat storage, aging and reproduction. Here, we discuss the lipid metabolism pathways that impact dietary allocation of nutrients as well as the consequences of their perturbation.

Inappropriate Nutrient Allocation Impacts Fat Storage

Fatty acids from the diet are used for a number of important processes including the generation of large quantities of energy when they are broken down by mitochondrial β-oxidation. In addition to providing an organism with sufficient levels of ATP, fatty acids are also essential components of cellular membranes (phospholipids), long-term energy storage reserves (triglycerides) and even function in signaling pathways (glycolipids) (Figure 1.1). The amount of fatty acid allocated to each fate must be carefully regulated, as too much or too little fat in any branch can be problematic. Perhaps, the most familiar example of an imbalance in these pathways is in the total amount of fat storage in an animal. It has been well recognized that the increased allocation of fatty acids to triglycerides contributes to accumulation of excess fat stores and the resultant disorders such as metabolic disease and obesity. However, it is often forgotten that too little fat can also have serious consequences, as energy reserves are required for surviving even short periods of fasting. Genetic mutations that result in the reduced capacity to store fat can result in severe diseases

including lipodystrophy (Halaschek-Wiener et al., 2005). Additionally, mutations in mitochondrial β-oxidation enzymes that reduce an individual's ability to access fat stores can result in severe hypoglycemia and even sudden death if not managed properly (Kompare et al., 2008).

Here, we will consider the impact of excess fat stores as obesity and metabolic disorders have become increasingly prevalent in the last century with over 30% of the United States population being considered obese in 2008 (Flegal et al., 2010). Excess body weight has a negative impact on an individual's overall health and is associated with an increased incidence of many prevalent diseases including type II diabetes, cardiovascular disease, hypertension, and many cancers (Wang et al., 2011; Watts, 2009). In fact, obesity increases the overall likelihood of death by 20% (Shi et al., 2004). Total fat storage can be influenced by both dietary fat absorption and the *de novo* synthesis of fatty acids, and, because increased flux through either of these pathways can have dramatic impacts on fat storage, both fat metabolism pathways have been explored as potential pharmacological targets to combat obesity and metabolic disorders.

Although environmental factors play a substantial role in determining body weight, there is a large genetic component that has been estimated at 40% to 70% (McPherson, 2007). In fact, the genetic basis for obesity is equal to or greater than the genetic basis of height (Ashrafi, 2007). The genetics of fat storage are highly polygenic with mutations in single genes accounting for a very small proportion of obesity cases, making it difficult to define the genetic determinants of fat storage. Additionally, studies in mammals and other model systems have identified hundreds of genes that impact fat accumulation; however, the sheer number of genes makes it difficult to determine how each individual gene impacts fat storage (Ashrafi et al., 2003; McPherson, 2007). In theory, genes that impact total fat storage can do so by affecting three major processes: (1) synthesis of new fats, (2) food intake and absorption, and (3) breakdown of fats by β-oxidation (McPherson, 2007). These metabolic pathways are coordinated to allow the proper balances of glucose and fat synthesis and breakdown (Figure 1.2).

De Novo Fatty Acid Synthesis

Fatty acids can be synthesized *de novo* from carbohydrate precursors via the function of two enzymes, acetyl-CoA carboxylase (ACC) and fatty acid synthase (FASN-1). The first and rate-limiting step of fatty acid biosynthesis is the generation of a malonyl-CoA primer by

the ATP-dependent carboxylation of acetyl-CoA by the ACC enzyme. The FASN enzyme is a homodimeric multidomain enzyme that then catalyzes the condensation of acetyl-CoA molecules to generate the 16-carbon fatty acid, palmitate (C16:0) (Figure 1.3A). The resulting palmitate can then be modified into a diverse set of fatty acids by a series of fatty acid elongation and desaturation enzymes (Figure 1.3B).

Expression of the fatty acid synthase enzyme can be found in almost every adult tissue; however, its function is limited in most contexts. There is high expression of the fatty acid synthase protein in hormone-sensitive tissues and in metabolically active tissues including the liver and adipose, where FASN is responsible for converting excess dietary carbohydrates to fats (Menendez et al., 2007; Shi et al., 2004). FASN also generates the fatty acids for a number of specialized functions like supplying fatty acid components of milk during lactation and synthesizing fatty acids for surfactant production in the lungs (Kusakabe et al., 2000). Although fatty acid synthesis is limited in most adult tissues, *de novo* fatty acid synthesis does play an essential role in development. FASN is broadly expressed in the mouse embryo with the highest levels of expression coinciding with areas of tissue-tissue interaction, tissue outgrowth and progressive modeling/remodeling (Chirala et al., 2003). Additionally, fatty acid synthesis is essential during embryonic development as homozygous mutation of the *fasn* locus results in embryonic lethality. The heterozygous FAS mutants (Fasn $^{+/-}$) were recovered at lower than expected frequency (~70% fewer animals) indicating partial haploid insufficiency as well (Chirala et al., 2003). In these mice models, it was further demonstrated that dietary supplementation of saturated fatty acids did not fully rescue these phenotypes, presumably because transport of fatty acids through the placenta is limited. Not only do these studies indicate the importance of fatty acid synthesis in embryonic development, but they also highlight the need to consider teratogenic consequences of reducing fatty acid synthase activity.

The expression of fatty acid synthase is tightly linked to the diet of an animal with FASN expression being induced by the presence of carbohydrates and suppressed by fat. The modulation of FASN expression is largely regulated transcriptionally by the activity of the sterol response element binding protein (SREBP); however, post-translational mechanisms of regulation also impact FASN abundance including protease degradation (Menendez et al., 2007). A number of signaling and hormone pathways have been found to affect the overall levels of fatty acid synthesis through the modulation of the enzyme itself or through

the SREBP transcription factor including both the PI3-Kinase and epidermal growth factor (EGF) pathways.

Food Intake and Dietary Absorption

The majority of fatty acids can be obtained directly from the diet, and because fat absorption requires less energy than *de novo* fatty acid synthesis, fatty acids inhibit FASN activity. Although nematodes do not contain leptin or any other neuropeptides known to regulate mammalian food intake, many of the enzymes required for the absorption of dietary fat are intact (Mullaney et al., 2009). The absorption of dietary triglycerides (TAGs) and phospholipids (PL) requires partial breakdown of the molecule. In animals, TAGs are broken down by gastric and pancreatic lipases which enzymatically cleave the fatty acid tails from the head group to allow for efficient absorption. Phospholipases function similarly on PL to generate free fatty acids which can then be absorbed. Fatty acid transport proteins and fatty acid binding proteins then facilitate the transport of fatty acids throughout the animal.

Fatty Acid Utilization by Mitochondrial β-Oxidation

Fatty acids can be broken down in the mitochondria and/or the peroxisome by β-oxidation pathways, although mitochondrial oxidation is the only energy production pathway. The resulting acetyl-CoA molecules are fed into the TCA cycle for the production of NADH and $FADH_2$. When the amount of fatty acid funneled into β-oxidation is reduced, there is an ultimate accumulation of fat stores in the animal. When an animal is starved, increase lipase expression frees fatty acids from TAG stores, so they can be oxidized for ATP production. Under well-fed conditions, high levels of malonyl-CoA inhibit the transport of fats to the mitochondria and prevent their breakdown.

Targeting Fatty Acid Metabolism Pathways

In order to treat obesity, there have been many attempts to establish drugs that target various aspects of fatty acid metabolism. The majority of developed therapies have been unsuccessful and/or have been withdrawn as treatments due to the danger of side-effects (Ioannides-Demos et al., 2011). So far, only one drug, orlistat, is approved for long-term obesity treatment. Orlistat (also known as Alli) inhibits the activity of pancreatic and gastric

lipases which results in an ~30% reduction in fat absorption and an overall reduction in body mass (Shi et al., 2004).

Because fat synthesis can also contribute to overall fat stores, a number of drugs that can target fatty acid synthase effectively have been explored in animal models. Fatty acid synthase inhibitors like cerulenin and C75 have shown promise in animal studies; however, they have limited utility as a therapy in humans due to low stability, low bioavailability and/or undesirable side-effects (Menendez et al., 2007). In particular, a major challenge to inhibiting fatty acid synthase is the established role for fatty acid synthesis in reproduction and other undiscovered functions for this pathway.

Additionally, the mechanism of fat storage reduction is not clear upon fatty acid synthase inhibition. One leading hypothesis that has been proposed is that the reduction in fat stores in treated animals occurs due to the buildup of products like malonyl-CoA which can suppress the appetite (Shi et al., 2004). Nevertheless, a better understanding of how fat metabolism pathways are regulated and how they interact will be critical for the development of viable therapies.

Relationships Between Metabolism, Reproduction and Lifespan

Not only does the total amount of fat storage impact an animal's health and lifespan, but how nutrients are utilized can also have dramatic affects. In times of growth and reproduction, there are added demands on dietary resources, and these added strains might impact the availability of resources for other processes. The best example of such tradeoffs is the general observation in the aging field that animals with increased longevity tend to have reduced fecundity. This "cost of reproduction" is thought to result from multiple processes competing for the same resources. Therefore, as the demands for offspring production increase, there are fewer resources available for somatic maintenance and repair, growth and movement (Partridge et al., 2005). Two of the most well studied lifespan extension mechanisms are reduced insulin/IGF-1 signaling and dietary restriction, which are known to increase lifespan in *C. elegans, Drosophila,* and rodent models. As well as increasing lifespan, these animals also have delayed and/or reduced fecundity. Interestingly, in *Drosophila*, increased nutrient availability drives an increase in reproductive activity (Piper et al., 2005). Although there is evidence for a relationship between metabolism, reproduction and aging, further studies are needed to establish how these processes impact each other.

Altered Fatty Acid Metabolism in Cancers

In normal cells, the majority of fatty acids are derived directly from the diet; however, in cancer cells, almost none of the fatty acids are dietary in origin (Ookhtens et al., 1984). Increased expression of the FASN gene has been found in the majority of cancers tested including prostate, breast, lung and gastric cancers (Flavin et al., 2011; Kusakabe et al., 2002; Menendez et al., 2007). In cancer cells, fatty acid synthase is not susceptible to normal repressive mechanisms and, although FASN is normally downregulated by fat in the diet, fat synthesis in cancers functions independent of dietary cues (Kuhajda, 2000). The elevated fatty acid synthase expression seems to convey an advantage to cancer cells as elevated FASN expression is correlated with increased metastasis and poor prognosis.

The increase in *de novo* fatty acid synthesis seen in cancers may be directly connected to the glycolytic metabolism of the cancer cell. The vast majority of tumors rely almost exclusively on sugar-based metabolism as first described by Otto Warburg in the 1920s (Warburg et al., 1927). The aerobic glycolysis driven metabolism results in an imbalance of the NADH:NAD+ ratio, which can be alleviated by the function of lactate dehydrogenase or by *de novo* fatty acid synthesis. Additionally, it has been suggested that the increase in lipogenesis is also important for the generation of membranes for the rapidly dividing cancer cells. Regardless of its exact function, it is clear that *de novo* synthesis provides the tumor with an advantage, and inhibition of FASN results in apoptosis in tumor cell lines (Horiguchi et al., 2008; Pizer et al., 1998). Additionally, FASN inhibition in mouse models results in tumor growth inhibition and suppression of metastasis (Flavin et al., 2011; Murata et al., 2010). Because of the susceptibility of cancers to FASN inhibition, many studies in animal models have focused on the potential for treatment of cancers with FASN inhibitors; however, there has not been any successful FASN inhibitors trials in humans as of yet.

C. elegans as a Model for Studying Fat Metabolism

A complete understanding of the genetic regulation of metabolism requires a genetically tractable model to deconvolute complex pathway dynamics. The nematode, *C. elegans*, has recently been established as a model for studying genetic regulation of fat storage. Many core metabolic pathways including food intake, digestion, fatty acid synthesis, fatty acid processing, glycolysis, β-oxidation and lipid signaling are conserved between nematodes and mammals (Mullaney et al., 2009). Because *C. elegans* has been

successfully used to elucidate genetic pathways and to screen for unidentified regulators, there has been a growing interest in using the nematode to understand how genes and the environment impact fat storage and metabolism. To do this, a number of tools have been established to monitor fat storage in the animals including lipophilic dyes, fat analysis by gas chromatography/mass spectrometry and direct imaging by CARS microscopy (Ashrafi et al., 2003; Brock et al., 2006; Hellerer et al., 2007; Yen et al., 2010). Additionally, qRT-PCR panels have been established to monitor the expression levels of metabolic enzymes (Van Gilst et al., 2005).

The nematode also has many genetic tools that make defining genes and pathways that regulate various aspects of fatty acid metabolism feasible. For example, genome-wide RNAi screens have identified over 400 genes that influence total fat accumulation (Ashrafi et al., 2003). Of the genes identified in that screen, over 50% have human homologs that have not been implicated in fat metabolism previously. Additionally, the short generation time and lifespan of the animal makes it possible to monitor different aspects of fat metabolism over development (egg to egg in 72 hours) and over aging (mean lifespan is 2-3 weeks).

Although *C. elegans* has been a useful model for studying fat metabolism, there was a need for the development of new methodology. Not only has the validity of some of the current tools for monitoring fat storage been called into question, but there is also a need for novel ways to monitor how the animal obtains and distributes fatty acids (O'Rourke et al., 2009; Yen et al., 2010). Therefore, the establishment of an improved method for studying fatty acid metabolism in the nematode was needed in order to approach many of the topics discussed here.

Metabolomic Analysis

Because many aspects of fatty acid metabolism are impacted by numerous pathways, transcriptional analyses can be difficult to interpret. Therefore, metabolic flux data is important to directly assess the rate of synthesis and breakdown pathways. Traditionally, in order to quantify lipogenesis, *de novo* fatty acid synthesis is quantified by the incorporation of a radio-labeled precursor in the diet and detection of the label in the fats of the animal. Although strategies based on radio-labeling are very sensitive, there is limited data collected on synthesis in different fatty acid species and lipid classes. In order to quantify fatty acid synthesis with greater resolution, we wanted to implement stable isotope techniques that require high enrichment of the stable isotopes. The requirement of greater levels of

enrichment makes this type of study prohibitively expensive in mammalian systems. The nematode *C. elegans* allows for high stable isotope enrichment that allows us to answer many questions about fatty acid synthesis simultaneously. We have developed a mixed stable ^{13}C isotope labeling approach that allows us to monitor fatty acid synthesis in various conditions and genetic backgrounds, making it possible to use nematodes to increase the understanding of fatty acid synthesis (Perez et al., 2008).

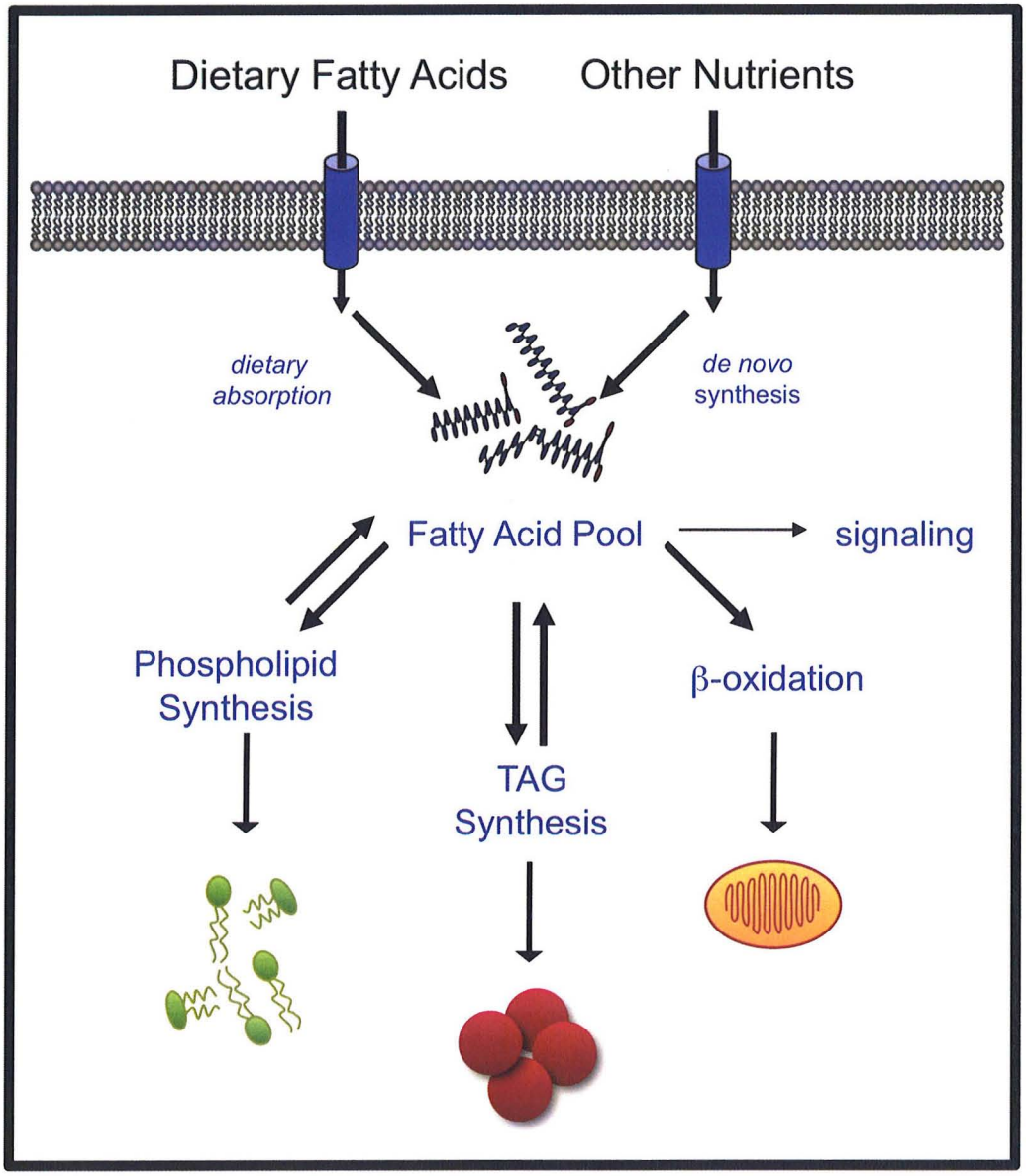

Figure 1.1. Fatty Acid Metabolism and Partitioning: Fatty acids can be absorbed directly from the diet or synthesized *de novo* from dietary carbohydrates. Together, these pathways generate a pool of fatty acids which is then allocated to a number of physiological fates: phospholipid synthesis, triglyceride synthesis and β-oxidation. Fatty acids are also important components of many signaling pathways, but the amount of fatty acid used in signaling pathways is relatively minimal.

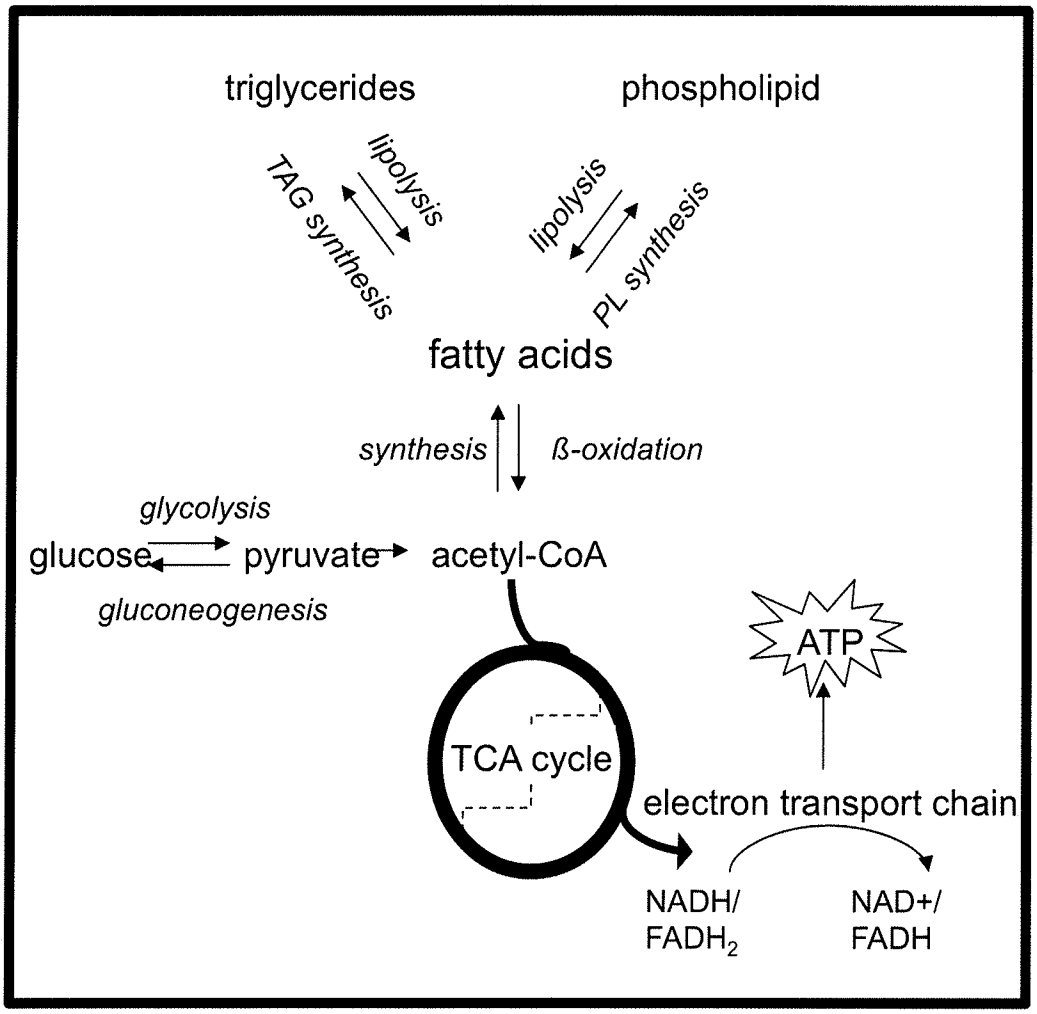

Figure 1.2. Sugar and Lipid Metabolism Pathways: To produce energy, fatty acids and sugars can be broken (by ß-oxidation and glycolysis, respectively) into acetyl-CoA molecules. These acetyl-CoA's then feed the TCA cycle resulting in the production of substrates to drive oxidative phosphorylation. When fatty acid production is required, *de novo* fatty acid synthesis can generate fatty acids from acetyl-CoA molecules. In the nematode, the glyoxylate pathway (represented by the dashed line) can convert fats to sugars by bypassing CO_2-production steps in the TCA cycle. Figure adapted from Ashrafi K (2007).

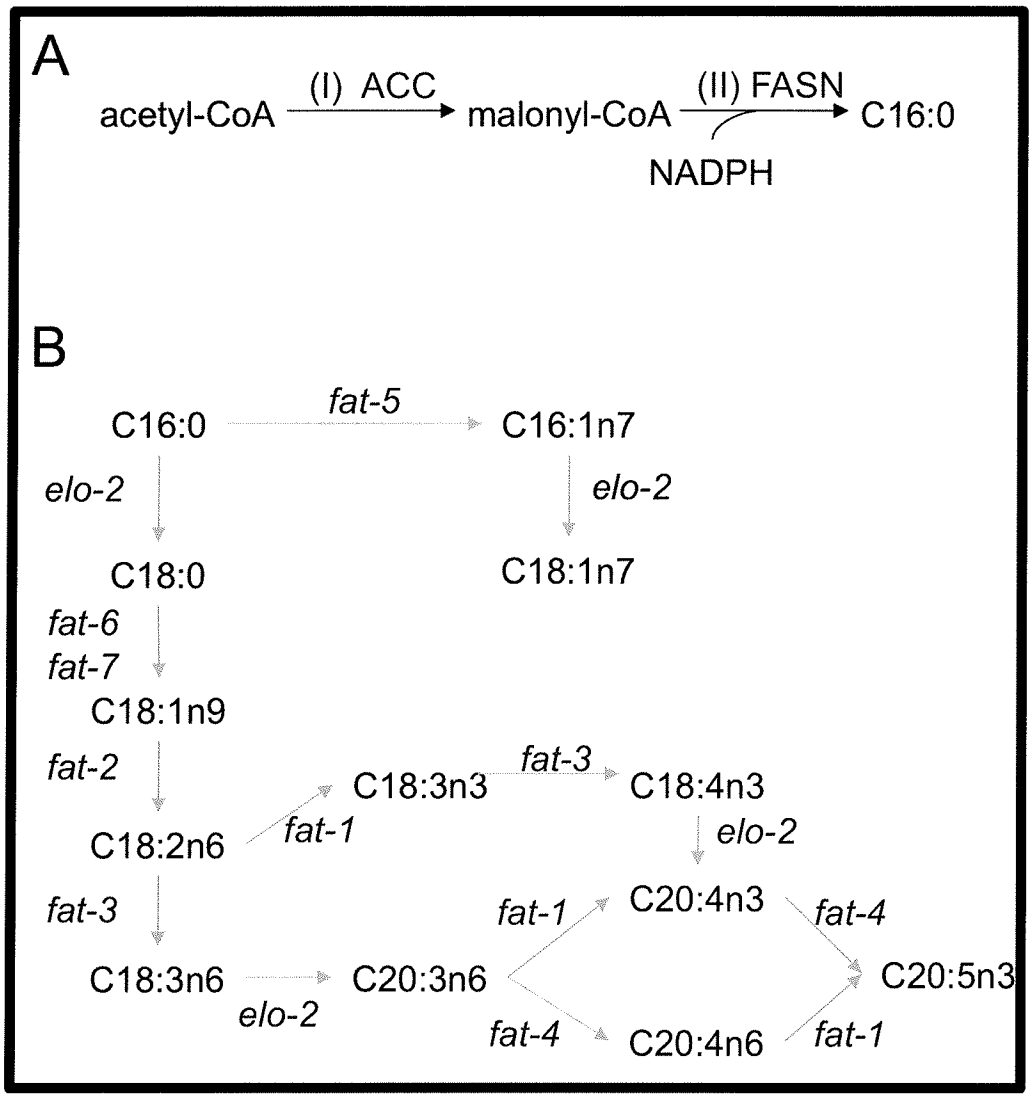

Figure 1.3. Faty Acid Synthesis, Elongation and Desaturation Pathway: (A) Fatty acid synthesis requires two enzymes: (I) acetyl-CoA carboxylase which generates malonyl-CoA (the extender) and (II) fatty acid synthase (FASN) which catalyzes the condensation reaction and results in chain elongation. To generate one fatty acid (C16:0), this reaction consumes 1 acetyl-CoA, 7 malonyl-CoA's, 14 NADPH's and 14 H+. (B) The C16:0 can then be elongated and desaturated to form fatty acids of various lengths and degrees of saturation. The elongases (*elo* genes) and desaturates (*fat* genes) catalyze these reactions in *C. elegans.* The fatty acid nomenclature used here is CX:anb, with "X" indicating the number of carbons in the fatty acid, "a" representing the number of double bonds and "b" indicating the position of the double bond.

CHAPTER II: A Stable ^{13}C Labeling Strategy for Detection and Quantification of *de novo* Synthesized Fatty Acids in *C. elegans*

Modified from an article published in *Cell Metabolism*:
Perez CL and Van Gilst MR. (2008). A ^{13}C isotope labeling strategy reveals the influence of insulin signaling on lipogenesis in *C. elegans*. *Cell Metabolism* Sep;8(3):266-274.

Summary

Metabolic flux analysis allows for the understanding of how multiple pathways are integrated onto the core metabolism of an animal as it encounters different environmental and physiological challenges. Here, we have developed and implemented a stable ^{13}C isotope approach that allows us to monitor how the animals are utilizing their diet. We have developed a "mixed isotope" strategy to specifically quantify various aspects of fatty acid metabolism, and we have found that we can accurately determine whether the fats of the animals are absorbed directly from the diet or synthesized *de novo*. Using this ^{13}C mixed isotope assay, we have determined that *de novo* synthesis can contribute to the generation of each species of fatty acid except for the bacterial cyclopropyl fatty acids. However, the contribution of *de novo* synthesis is minimal in most fat species similar to what is seen in mammalian systems as most fat is obtained directly from the diet. We have further validated this strategy by quantifying fatty acid synthesis in nematodes predicted to have altered fat synthesis, absorption and expenditure due to genetic mutations or drug treatment. With this analysis, we have found that our assay can distinguish the fat metabolism profile in each instance. This mixed isotope labeling strategy will allow the utilization of the nematode, *C. elegans*, as a model for studying the genetic regulation of *de novo* fatty acid synthesis and fat absorption.

Introduction

Excess fat storage increases an individual's likelihood of developing a number of prevalent diseases including Type II diabetes, hypertension, and even many cancers (Wang et al., 2011; Watts, 2009). This impact of fatty acid metabolism on overall health has resulted in many attempts to alter metabolic pathways pharmacologically; however, these efforts have been largely unsuccessful to this point largely because a better understanding of these pathways is needed. In addition to behavioral and environmental factors, it is clear

that genetic background plays a substantial role in determining the propensity for obesity and related complications (McPherson, 2007). Consequently, there is considerable interest in defining genes that affect the partitioning of dietary nutrients for fat storage. Because the genetics of obesity are complex and multifactorial, model systems have been important tools for defining genes and pathways that impact fat storage. Studies in *C. elegans* have characterized numerous pathways that modulate lipid accumulation, including insulin/IGF, serotonin, tubby, and nuclear receptor signaling (Mukhopadhyay et al., 2005; Ogg et al., 1997; Sze et al., 2000; Van Gilst et al., 2005). Furthermore, a genome-wide RNAi screen isolated over 400 genes that influence total fat accumulation, many of which have not been previously implicated in the regulation of fat metabolism (Ashrafi et al., 2003).

In principle, genes could alter fat storage by modulating three factors: (1) how much fatty acid is ingested and absorbed from the diet, (2) how much dietary nutrient is converted to fat via *de novo* lipogenesis, and (3) how much fat is expended through β-oxidation. Because little is known about these processes in nematodes, the ability to elucidate the mechanisms of fat regulatory genes in *C. elegans* has been limited. For example, mutations of the insulin receptor gene, *daf-2*, can increase lifespan and fat storage through inappropriate activation of the FoxO transcription factor DAF-16. Microarray studies have shown changes in the expression of numerous genes predicted to participate in fatty acid metabolism, but it is still not clear how DAF-2 and its regulatory targets actually modulate fat synthesis, absorption, and/or expenditure (Halaschek-Wiener et al., 2005; McElwee et al., 2003)

In order to better understand the mechanisms by which the insulin receptor and other regulatory genes regulate lipid physiology in *C. elegans*, it is essential to develop methods for characterizing and quantifying fatty acid metabolism. Stable isotope-based experiments have been employed to monitor fatty acid flux in numerous biological systems (Brunengraber et al., 1997; Kelleher, 2001; McCabe et al., 2004; Murphy, 2006; Strawford et al., 2004). Furthermore, isotope labeling of food has been applied to globally monitor macronutrient partitioning in an invertebrate model organism, *Drosophila melanogaster* (Min et al., 2006) and (O'Brien et al., 2008). Here, we present a ^{13}C isotope-labeling approach to characterize dietary fat absorption and fatty acid synthesis in *C. elegans* for the first time. We utilize this metholodogy to determine how known regulatory pathways like insulin signaling influence these central aspects of lipid metabolism.

A ^{13}C Enrichment Strategy to Identify and Quantify Dietary and *De Novo* Synthesized

Fatty Acids

We designed a "mixed isotope" assay to quantify the relative contributions of *de novo* synthesis and dietary fat absorption to the total lipid composition in *C. elegans* (Figure 2.1). In principle, animals that are fed a mixture (1:1) of ^{13}C-enriched *E. coli* (OP50) and unlabeled bacteria should obtain approximately half of their nutrients from ^{13}C-labeled bacteria and half of their nutrients from unlabeled ^{12}C bacteria. Therefore, using this strategy, fats absorbed from the diet and directly incorporated into worm lipids will either be fully composed of ^{13}C (if directly obtained from labeled bacteria) or fully composed of ^{12}C (if absorbed from unlabeled bacteria). In contrast, fats synthesized *de novo* in *C. elegans* will contain a statistically definable mixture ^{12}C and ^{13}C since synthesis substrates will be derived from the breakdown of labeled and unlabeled bacterial nutrients. The relative contributions of dietary fatty acid absorption and *de novo* synthesis can therefore be quantified by analyzing the molecular weight (MW) distribution of purified fatty acids by gas chromatography/mass spectrometry (GC/MS).

We prepared mixed isotope "feeding plates" by plating a 1:1 mixture of bacteria grown in standard unlabeled media, and bacteria grown in ^{13}C-enriched media (Isogro-^{13}C Powder Growth Media from Sigma-Aldrich). To confirm the isotope composition of the fatty acids in our feeding plates and to ensure that there was no cross contamination during the labeling assay, we independently analyzed bacterial fatty acids from the feeding plates for each experiment. To do this, we collected bacteria directly from the mixed label feeding plates, extracted the bacterial fatty acids and generated a mass spectrum for palmitate (C16:0) by GC/MS. It is clear from these data that there are no quantifiable peaks in the "synthesized region" of the mass spectrum (Figure 2.2A). The shoulder peaks present at 271–272 and 284–285 are a consequence of natural ^{13}C abundance or ^{12}C contamination in our ^{13}C bacterial growth media. In nature, ^{12}C is 98.9% abundant, and the probability of incorporating ^{13}C into a palmitate methyl ester was determined using a binomial distribution (Kelleher, 2001). Similarly, we calculated the isotope purity of our ^{13}C bacteria enrichment by comparing the fractional abundance of the isotopic peaks at 284 and 285 Daltons (Figure 2.2A). On average, we found that the ^{13}C enrichment of our Isogro media was 98.5% in agreement with manufacturer's specifications. These data confirmed that for the period in which the bacteria reside on the feeding plates, there was no detectable incorporation of contaminating carbon sources, other than natural isotope variation. Thus, dietary fatty acids available to worms grown on mixed isotope feeding plates were either 98.5% composed of

^{13}C or 98.9% composed of ^{12}C.

The primary dietary fatty acid in bacteria is C16:0 (Table 2.1), and, because C16:0 is also the product of *de novo* fatty acid synthesis, we first applied our technique to characterize C16:0 synthesis and absorption. The mass spectrum of C16:0, obtained from worms grown on a mixed isotope feeding plate, revealed C16:0 species with a range of MWs (isotopomers), from 270 Daltons (for a palmitate methyl ester fully composed of ^{12}C) to 286 Daltons (for a palmitate methyl ester fully composed of ^{13}C) (Figure 2.2B). To derive a quantitative model to fit these data, we considered that C16:0 was obtained from four sources (Figure 2.2B). First, dietary absorption: intact C16:0 taken up from unlabeled bacteria and incorporated into worm lipids displayed a MW of 270 Daltons, whereas C16:0 directly absorbed from ^{13}C-enriched bacteria contributed to the isotopomer peak at 286 Daltons (shoulder peaks due to isotope impurities were accounted for in our analysis). Second, C16:0 could be formed in *C. elegans* by elongation of dietary C14:0; molecules generated in this fashion would fall between 270–272 Daltons and 284–286 Daltons (Figure 2.4). Third, C16:0 could be derived from *de novo* synthesis; fatty acids produced by synthesis will display an isotope-labeling pattern that falls into a trinomial distribution, which will depend on the probability of incorporating acetyl-CoA units that are ^{12}C-^{12}C, ^{12}C-^{13}C, or ^{13}C-^{13}C (See Experimental Procedures). Although these probabilities could be determined by fitting the isotopomer data, we were able to independently determine the acetyl-CoA isotopomer distribution by measuring the elongation of C16:0 to C18:0 (Figure 2.3). Finally, since our assays were carried out by placing unlabeled larvae (L1 stage) on mixed isotope bacteria, maternally derived C16:0 that remains in harvested L4 stage animals also contributed to the isotopomer peak at 270 Daltons. Although we can assume the maternally derived fatty acids by accounting for all the other sources of unlabeled C16:0 (MW of 270 Daltons), we also independently confirmed the amount of fatty acid derived from maternal sources. To do so, we grew newly hatched animals (L1s) on fully labeled bacteria (98.5% ^{13}C) until mid-L4 (Figure 2.5). This analysis confirmed the maternal contribution to palmitate is about 5% in the L4 animal.

Taking into account these four possible sources of palmitate, we derived a mathematical model to fit the mass distribution (Figure 2.2B, see Experimental Procedures for a description of the data analysis). Our model revealed that the majority of *C. elegans* C16:0 was derived from direct absorption of bacterial fatty acid. However, *de novo* synthesis did account for 7% of total palmitate.

Origin of Other *C. elegans* Fatty Acid Species

Our findings revealed that dietary fat absorption is the primary source of worm palmitate; however, *C. elegans* contains numerous other types of fatty acids, some of which are not found in its bacterial diet (Table 2.1). Stearate (C18:0), oleate (C18:1n9), linoleate (C18:2n6), and several 20 carbon polyunsaturated fatty acids (PUFAs) are not available in the common laboratory diet (*E. coli* [OP50]) and must be obtained by elongation and desaturation of C16:0 (Figure 2.6) (Watts et al., 2002). Although synthesis accounted for only 7% of the steady-state levels of C16:0, we found a more predominant role for *de novo* synthesis in the production of monounsaturated fatty acids (MUFAs) and PUFAs (up to 19% of total fatty acid) (Figure 2.6). Twenty carbon fatty acids could not be assessed by our method due to extensive fragmentation of these molecules in the mass spectrometer.

We also found that *C. elegans* monomethyl branched-chain fatty acids (mmBCFAs), C15ISO and C17ISO, were >99% derived from *de novo* synthesis. The mmBCFAs are generated by the elongation of a branched chain primer by fatty acid synthase, and these fatty acids have been established to be essential for proper nematode development and growth (Kniazeva et al., 2004). mmBCFAs are not present in the OP50 diet and cannot be produced from modification of bacterial fatty acids. For these reasons, it has been proposed that mmBCFAs must be derived from de novo synthesis (Kniazeva et al., 2004); our results provide direct biochemical confirmation of this hypothesis. In contrast, four *C. elegans* fatty acid species, vaccenate (C18:1n7), palmitoleate (C16:1n7), and two cyclopropane fatty acids (C17Δ and C19Δ), are prevalent dietary fats. We found that 95% of C18:1n7 and C16:1n7 and >99% of the cyclopropyl fatty acids originate from direct absorption of the bacterial fatty acid (Figure 2.6).

Synthesized Fatty Acids Are Distributed Equally to Triglycerides and Phospholipids

De novo fatty acid synthesis contributes more prominently to the generation of MUFAs and PUFAs, which are major phospholipid species in the nematode. Therefore, we considered the possibility that synthesized fatty acids may be funneled preferentially to phospholipid formation. To test this hypothesis, we purified triglycerides (TAG) and phospholipid (PL) fractions from mixed labeled worms. We found that for each fatty acid species, the relative amount of *de novo* synthesis is equivalent for TAG and PL (Figure 2.7). For example, the linoleate (C18:2n6) associated with either TAG or PL is about 18% derived

from *de novo* synthesis. This indicates that synthesized fatty acids are not preferentially allocated to phospholipid synthesis but instead contribute to the generation of the fatty acid pool which is then used to supply phospholipid and triglyceride synthesis.

Biochemical Confirmation of Increased Synthesis in Insulin Signaling Mutants

We next sought to implement this mixed labeling assay with mutants that are predicted to regulate *de novo* fatty acid synthesis. In *C. elegans,* mutations in the insulin receptor gene, *daf-2,* have been shown to regulate lifespan and fat storage through the inappropriate activation of the FoxO transcription factor, DAF-16. Additionally, microarray analysis of *daf-2* mutants has revealed gene expression changes in numerous genes predicted to participate in fatty acid metabolism (Halaschek-Wiener et al., 2005; McElwee et al., 2003; Murphy et al., 2003). Although increased fatty acid synthesis has been predicted as the major influence of fat storage in *daf-2* worms, it is not clear how DAF-2 and it regulatory targets actually modulate fat synthesis, absorption, and/or expenditure.

To determine the mechanism of fat accumulation, we implemented a mixed isotope labeling assay on *daf-2(e1370)* worms. In these animals, we found that there is a significant increase in the proportion of fatty acids derived from *de novo* fatty acid synthesis, suggesting that increased fat storage is due largely to elevated lipogenesis (Figure 2.8). We also established that this elevated synthesis is dependent on the function of the DAF-16 transcription factor as *daf-2(e1370);daf-16(m26)* double mutants displayed levels of fatty acid synthesis that were slightly lower than WT animals (Figure 2.8). Furthermore, mutation of *daf-16(m26)* alone resulted in a slight reduction in *de novo* synthesis. Taken together, these results imply that DAF-16 stimulates fatty acid synthesis, and that activation of the insulin signaling pathway represses synthesis, at least in part, by inhibition of *daf-16.* The role of the insulin signaling pathway in regulating *de novo* fatty acid synthesis is further discussed in Chapter 3.

Decreased Fat Absorption in Triglyceride Lipase Inhibited Animals

Because this method allows us to track both dietary and synthesized fats in the nematode, we next wanted to assay the ability of this stable isotope strategy to discern changes in dietary fat absorption. To do this, we treated nematodes with orlistat to reduce dietary fat absorption. Orlistat is a gastric and pancreatic lipase inhibitor that has been found to reduce dietary fat absorption by 30% in humans (Drew et al., 2007). In these

animals, we found a dose-dependent increase in the ratio of synthesized to absorbed fatty acids. The largest change observed is seen with treatment at 50 μM with a 2.5x increase in relative palmitate synthesis when compared to untreated animals (Figure 2.9A).

Because the ratio of synthesized to absorbed fatty acids will increase when synthesis is increased or when absorption is decreased, we next measured the total amount of fat storage to distinguish these possibilities. With increased fatty acid synthesis, the total amount of fat will increase leading to an overall increase in fat storage; however, with decreased absorption, the total fat will decrease resulting in a decreased TAG:PL ratio. To assay fat storage, we purified TAG and PL populations by column chromatography and compared the relative abundance of fat storage triglycerides using internal standards. We found that treatment with orlistat results in a 47% decrease in TAG:PL suggesting that the amount of fatty acid absorption is decreased, consistent with inhibition of TG lipase activity (Figure 2.9B).

Orlistat has been found to have additional inhibitory effects on fatty acid synthase; however, when we assay the fatty acid composition of the orlistat treated animals, we found decreased abundance of dietary fats and increased relative abundance of *de novo* synthesized fats, the monomethyl branched chain fatty acids, suggesting that the primary impact of orlistat is the triglyceride lipase inhibition, at least in the nematode (Figure 2.9C). Our findings with orlistat treated worms confirmed that the mixed isotope assay could identify changes in dietary fat absorption. Additionally, the efficacy of orlistat in the nematodes provides an example of the homology of fat metabolism pathways in nematodes and mammals and opens the possibility for studying the impacts of various drugs on fat metabolism in worms.

No Change in Isotope Distribution in Mutants with Decreased β-Oxidation

Finally, the remaining contributor to fat storage is fat utilization by mitochondrial β-oxidation. We used *nhr-49(nr2041)* animals which are known to have decreased expression of β-oxidation genes to determine if we can see any changes in isotope distribution (Van Gilst et al., 2005). In these *nhr-49* animals, we detected no change in the ratio of synthesized to dietary fatty acids in all fatty acid species measured (Figure 2.10). Because these animals are high in lipid storage without an increase in *de novo* fat synthesis or dietary fat absorption, it implies that the increased fat accumulation is due to a failure to oxidize the lipids. However, this particular isotope labeling strategy cannot measure this parameter

directly.

Discussion

Using a ^{13}C isotope-labeling strategy, we have provided a thorough description of how *C. elegans* obtains and distributes fatty acids. Elegant stable isotope approaches have been used to measure lipid metabolism in other animal models including humans; what distinguishes this method, however, is that the entire carbon component of a natural food source is labeled, enabling simultaneous monitoring of fatty acid absorption, elongation and desaturation, and *de novo* synthesis. Thus, multiple aspects of nutrient utilization and lipid metabolism can be examined in a single assay with an exceptional degree of detail and precision. Additionally, this approach can survey metabolism over the entire course of development and adulthood; thus, the long-term impact of genetic mutations and dietary manipulations can be readily assessed in high-throughput fashion. We expect this general strategy to be applicable for investigating many different metabolic pathways in *C. elegans,* as well as other model organisms.

We found that worm fatty acids are derived from four sources: (1) direct absorption and incorporation of dietary fats, (2) absorption and modification of dietary fats by elongation and/or desaturation, (3) *de novo* synthesis, and (4) maternal inheritance. When grown on the OP50 strain of *E. coli*, a standard laboratory diet, the majority of fatty acids are directly obtained from ingested bacteria. However, *de novo* synthesis is not a negligible factor, contributing especially to species not available in the diet, such as C18:0 (13%), C18:1n9 (17%), C18:2n6 (19%), and mmBCFAs (>99%). Presumably, worms will modify fatty acid synthesis and absorption patterns to accommodate food sources with different lipid compositions. The fact that the relative contribution of *de novo* synthesis and dietary fat absorption was similar in PLs and TAGs implies that dietary and synthesized fats freely diffuse through the worm such that a common pool is used for the majority of PL and TAG synthesis.

We believe a major advantage of the mixed isotope strategy in nematodes is its ability to define how different genes impact overall fat storage. In order to validate our strategy and to demonstrate the versatility of the mixed isotope assay, we characterized mutants and conditions predicted to regulate aspects of *de novo* fatty acid synthesis and dietary fatty acid absorption. Our success characterizing the impact of genes and drug treatments on fat synthesis indicates that this mixed isotope assay will be a useful tool in characterizing how

genes and drugs impact fat metabolism. Additionally, we can also use this assay to screen for novel regulators of fat synthesis and fat absorption (discussed in Appendix I).

Experimental Procedures

Strains

Worm maintenance and experiments were carried out at 20°C. In these experiments, the following strains were obtained from the Caenorhabditis Genetics Center CGC: wild-type N2 strain (Bristol), CB1370: *daf-2(e1370)*, DR1309: *daf-2(e1370);daf-16(m26)* and DR26: *daf-16(m26)*. *nhr-49 (nr2041)* was a gift from Carl Johnson at Axys Pharmaceuticals.

Growth on Mixed Isotope Feeding Plates

To prepare mixed isotope feeding plates, separate ^{12}C- and ^{13}C-enriched cultures were started by inoculating LB (^{12}C media) and Isogro media (98.5% ^{13}C enriched; from Sigma-Aldrich) with *E. coli* (OP50). Cultures were grown for 16 hr at 37°C, harvested by centrifugation, washed, and then combined 1:1, by weight, in M9 buffer. This mixture was spread onto 15 cm agarose plates (1.5% agarose, 50 mM NaCl, 1 mM $CaCl_2$, 1 mM $MgSO_4$, and 25 mM KPO_4, pH 6.0 buffer). Agarose plates prevent bacterial growth and, thus, the incorporation of exogenous carbon. For labeling assays, 30,000 synchronized L1 larvae were prepared by bleaching gravid adults and allowing embryos to hatch in the absence of food (Van Gilst et al., 2005). 20–24 hr after bleaching, L1s were plated on mixed isotope feeding plates and collected after 44–48 hr of feeding (worms were harvested as mid-L4 larvae). All experiments were carried out at 20°C.

Orlistat Inhibition

An orlistat master stock (from Sigma-Aldrich) was prepared at 13.5 µg/ml in ethanol. In order to spread the drug on NGM plates effectively to the final concentration between 5nM and 50µM, the total volume was increased to 600µl with 1X M9 buffer. We assumed each 6cm plate contains approximately 6ml of media for calculations of the correct drug concentration. Plates were allowed to dry for a minimum of 30 minutes before use. For synthesis analysis, OP50 was also plated on orlistat and the treated bacteria were used to establish the correction factor for these studies.

Lipid Purification and Analysis

For whole-worm fatty acid analysis, total lipids were extracted and converted to fatty acid methyl esters (FAMEs) as described (Watts et al., 2002). For PL and TAG purification, total lipids were extracted with 2:1 chloroform:methanol for 1 hr at room temperature. Next, 0.2 volumes of 0.9% NaCl were added and the mixture was vortexed and allowed to separate for 2 min. The top layer (aqueous) was removed and the bottom layer was dried down under nitrogen. Dried lipids were resuspended in 1 ml of chloroform. Calibrated phospholipid standard (1,2-Dihepatdecanoyl-*sn*-Glycero-3-Phosphocholine, Avanti Polar Lipids) and TAG standard (tritridecanoin, Nu-Chek Prep) were added to the total lipid mixture before extraction. PLs and TAGs were purified by solid phase exchange (SPE) chromatography. Extracted lipid was resuspended in chloroform and loaded onto SPE columns (100 mg capacity, Fisher Scientific) pre-equilibrated with 3 ml of chloroform. TAGs were eluted first with 3 ml of chloroform. Glycosphingolipids were eluted next with 5 ml of a 9:1 acetone:methanol mixture, and phospholipids were eluted last with 3 ml of methanol. Purified lipids were dried, resuspended in methanol/2.5% H_2SO_4, and incubated for 1 hr at 80°C to create FAMEs.

FAMEs were analyzed by gas chromatography/mass spectrometry (GC/MS) (Agilent 6890GC, 5975MS). Isotopomers were monitored in a scanning ion mode customized to each fatty acid species of interest; for example, C16:0 MS scans ranged from m/z = 265 to m/z = 290. To quantify TAG and PL yields, total PL and TAG were compared to the internally added standards. Data were presented as a TAG:PL ratio, which was determined by measuring the sum of all fatty acids found in TAGs versus the sum of all fatty acids found in PLs (Ashrafi et al., 2003).

The relative abundance of each fatty acid species was determined by integrating the area of each fatty acid peak in the gas chromatograph. Fatty acids comprising less than 2% of the total fatty acid were not included in the analysis.

Evaluation of Feeding Plate Isotope Composition, Enrichment, and Purity

For each experiment, the isotope composition of the feeding plates was independently characterized. To do this, a portion of the 1:1 feeding mixture was allocated to a "control" feeding plate. This plate was incubated at 20°C in the absence of worms for the entire course of the experiment. Bacteria were collected from these control feeding plates, total

lipid was extracted, transmethylated, and analyzed by GC/MS according to the same procedures described above.

We also used the feeding plate GC/MS data to calculate the relative ratio of labeled to unlabeled bacterial fatty acid on each set of feeding plates. Although we were careful in our efforts to mix bacteria equally by weight, we found that our cultures were generally not composed of an exact 1:1 mixture. The ratio of fully labeled to fully unlabeled palmitate was often skewed such that there was a slightly higher supply of unlabeled fatty acids, relative to labeled fatty acids (Figure 2.2). For this reason, it was necessary for us to quantify the isotope composition of the bacterial mixture on each set of feeding plates. This information was used to establish a correction factor (CF) for calculations described below.

Calculating the Biosynthetic Origins of Palmitate

To model the mass spectra data, we developed mathematical terms to account for four potential origins of fatty acids in *C. elegans*: (1) *de novo* fatty acid synthesis, (2) direct dietary absorption, (3) absorption and elongation of dietary fatty acid, and (4) maternal inheritance. For palmitate methyl esters, we used Equation 1 to model total isotopomer abundance.

$$(1) \qquad I_n(Tot) = I_n(Synth) + I_n(Abs) + I_n(Elong) + I_n(Mat), \ n=270,\ldots,286$$

where I_n is equal to isotopomers with a MW of n Daltons. $I_n(Tot)$ represents total abundance of each isotopomer. $I_n(Synth)$ equals the abundance of isotopomers resulting from *de novo* synthesis. $I_n(Abs)$ is equal to isotopomers resulting from directly absorbed C16:0. $I_n(Elong)$ represents isotopomers that were generated by elongation of dietary C14:0, and $I_n(Mat)$ takes into account fatty acids supplied by maternal contribution.

Corrections for ^{12}C Isotope Impurity in Labeled Media and Natural ^{13}C Abundance

To begin our analysis, we first determined the abundance of isotopomers due to isotope impurities. Impurity abundance was calculated for I_{271}, I_{272}, I_{273}, I_{283}, I_{284}, and I_{285} using standard binomial distributions (Kelleher, 2001). For our calculations, we used 1.11% as the natural ^{13}C abundance in the unlabeled fatty acids, and 1.5% as the ^{12}C contamination in the labeled fatty acids (see above and Figure 2.2). Isotopomer abundance resulting from

isotope impurity was then subtracted from the data in order to perform the calculations described below. At the end of our analysis, when $I_n(Abs)$, $I_n(Elong)$, $I_n(Synth)$, and $I_n(Mat)$ were determined, isotopomer impurity abundances were then assigned to each of the above terms and added back to create the final model (Figure 2.3). Isotope impurity corrections were not used for isotopomers between 273 and 283 Daltons because the probability of obtaining a dietary fatty acid with MWs in this range is insignificant (Figure 2.2) and because isotopomer peaks resulting from fatty acid synthesis are modeled by acetyl-CoA composition calculations, which take into account both isotope dilution and isotope impurity (see below).

Determining $I_n(Synth)$: Isotopomer Abundance due to Fatty Acid Synthesis

To model the contribution of *de novo* synthesis to C16:0 isotopomer abundance, we considered that C16:0 will be synthesized from eight acetyl-CoAs, and that these two-carbon substrates will be composed of ^{12}C-^{12}C, ^{12}C-^{13}C, or ^{13}C-^{13}C. Therefore, the MW of a synthesized C16:0 molecule will depend on the specific number of (^{12}C-^{12}C) substrates, (^{12}C-^{13}C) substrates, and (^{13}C-^{13}C) substrates, termed A, B, and C, respectively, incorporated into that molecule. Since a total of eight two-carbon units are used to synthesize a C16:0 molecule, the specific number of each substrate will range from 0 to 8, and the sum of A, B, and C must be 8. Thus, a population of synthesized C16:0 will yield an isotopomer distribution that depends on the relative fractions of ^{12}C-^{12}C, ^{13}C-^{12}C, and ^{13}C-^{13}C substrates. The following trinomial expression was used to model the isotopomer distribution:

(2)

$$P(A,B,C) = \left(\frac{8!}{A!B!C!}\right) P_a^A P_b^B P_c^C$$

where P_a equals the probability of incorporating a [^{12}C-^{12}C], P_b equals the probability of incorporating a [^{13}C-^{12}C], and P_c equals the probability of incorporating a [^{13}C-^{13}C]. Although P_a, P_b, and P_c could be theoretically determined by fitting the isotopomer data, we were able to experimentally measure these values directly by examining the elongation of C16:0 to C18:0 (see next section). Next, the probability of each combination of A, B, and C was determined and used to calculate the probability of obtaining isotopomers (P_n) from 270 to 286 Daltons.

(3)

$$P_n = \sum_{n} P(A, B, C), \text{ where } n = 270 + (B + 2C)$$

These probabilities were then used to model the contribution of *de novo* synthesis to the isotopomer distribution using the following equation:

(4) $I_n(Synth) = (NF * P_n)$

where P_n represents the probability of obtaining an isotopomer with MW of n, and NF is a normalization factor that translates the probability of obtaining each isotopomer into total isotopomer abundance. The NF was determined by the following equation:

(5) $NF = I_{276}(Tot)/P_{276}$

The I_{276} peak was used for normalization because this isotopomer is exclusively derived from synthesized fatty acid molecules; therefore $I_{276}(Tot)$ is equal to $I_{276}(Synth)$. Because our feeding mixture generally contained higher levels of ^{12}C bacteria and because worms also carried ^{12}C derived from the mother, two carbon units carried a disproportional amount of ^{12}C, causing the synthesis distributions to be skewed toward "lighter" isotopomers. This was well modeled by our analysis (Figure 2.3). Importantly, our data were also well modeled using experimental determination of P_a, P_b, and P_c. The ability of experimentally measured probability values to correctly fit our synthesis data provides independent confirmation of the analysis.

Modeling $I_n(Elong)$: The Contribution of Dietary Fat Elongation to Isotopomer Abundance

In our palmitate mass spectra, even after removal of peaks due to isotope impurity, we consistently observed peaks at 272 and 284 Daltons that were significantly bigger than would be expected from synthesized palmitate (Figure 2.3). We deduced that these peaks resulted from elongation of dietary C14:0, a fatty acid species found in the *E. coli* diet (Table 2.1). Since this event must take place in *C. elegans,* elongation could occur with labeled, partially labeled, or unlabeled two-carbon units (Figure 2.5). Palmitate molecules created by

elongation of dietary C14:0 would thus yield isotopomers of 270, 271, and 272 (if an unlabeled C14:0 is elongated) or 284, 285, and 286 (if a labeled C14:0 is elongated). The accumulation of fatty acid synthesis-independent isotopomers at 282 Daltons was insignificant, suggesting that elongation of dietary C12:0 is not a major contributor to *C. elegans* palmitate. To calculate the contribution of C14:0 elongation to the palmitate isotopomer distribution, we first quantified the elongation of fully labeled C14:0 to C16:0 (Equation 6).

$$(6) \qquad I_{284}(Elong) = I_{284}(Tot) - I_{284}(Synth) - I_{284}(Abs)$$

Because dietary palmitate (when isotope impurity peaks are removed) will not contribute isotopomers of 284 Daltons, $I_{284}(Abs)$ can be dropped from this equation. Next, $I_{285}(Elong)$ and $I_{286}(Elong)$ can be calculated using the relative abundance of [^{12}C-^{12}C], [^{13}C-^{12}C or ^{12}C-^{13}C], and [^{13}C-^{13}C] substrates available for elongation (Equations (7) and (8)).

$$(7) \qquad I_{285}(Elong) = I_{284}(Elong) * (P_b/P_a)$$
$$(8) \qquad I_{286}(Elong) = I_{284}(Elong) * (P_c/P_a)$$

where P_a is the probability of elongating with a [^{12}C-^{12}C] substrate, P_b is the probability of elongating with a [^{13}C-^{12}C or ^{12}C-^{13}C] substrate, and P_c is the probability of elongating with a [^{13}C-^{13}C] substrate. The same methodology is used to calculate the abundance of I_{270}, I_{271}, and I_{272} isotopomers due to elongation of unlabeled C14:0. In this case, we use I_{272} abundance (after correction for isotope impurities) to calculate I_{271} and I_{270}.

Modeling $I_n(Abs)$: The Contribution of Dietary Palmitate Absorption

After taking into account synthesized fatty acids and elongated C14:0, the remainder of isotopomer abundance at I_{286} is attributable to the direct absorption of fully labeled dietary C16:0 (the probability of obtaining an isotopomer of 286 Daltons via fatty acid synthesis is extremely low, so this term can be excluded from the equation).

$$(9) \qquad I_{286}(Abs) = I_{286}(Tot) - I_{286}(Elong)$$

Because maternal inheritance of C16:0 contributes to isotopomers at I_{270}, we cannot use the

same formula to calculate $I_{270}(Abs)$. However, we can determine the amount of dietary fat at 270 Daltons using the relative proportion of labeled to unlabeled palmitate available to *C. elegans* (as determined in our analysis of the bacterial culture described above).

$$(10) \quad I_{270}(Abs) = I_{286}(Abs) * CF$$

The assumption in this case is that the amount of labeled and unlabeled fatty acids absorbed by *C. elegans* will be proportional to the relative abundance of labeled and unlabeled fatty acids in the bacterial diet. This ratio is determined by analyzing the bacterial feeding plate in order to obtain a CF. This CF is obtained by calculating the ratio of ^{12}C-labeled palmitate to ^{13}C-labeled palmitate in the mixed isotope bacterial cultures (see Figure 2.2).

Modeling $I_n(Mat)$: The Contribution of Maternal Fatty Acid

After accounting for the above three factors, there was a remaining fraction of C16:0 abundance at 270 Daltons, i.e., fully unlabeled fatty acid. Since our worm growths were initiated by placing L1 larvae on mixed label feeding plates, some of the biomass in these L1 larvae may persist into the L4 stage of development. As L1 larvae biomass is entirely derived from unlabeled mothers, maternally contributed fatty acid must be completely unlabeled. Therefore, we concluded that the remaining fatty acid at 270 Daltons (generally around 5% of total fatty acid) was due to maternal contribution.

$$(11) \quad I_{270}(Mat) = I_{270}(Tot) - I_{270}(Abs) - I_{270}(Elong) - I_{270}(Synth)$$

As an independent means of calculating maternal contribution we transferred L1 larvae, which were hatched in the absence of food, to fully labeled ^{13}C bacteria. In this assay, any new fatty acids generated during the feeding period will contain ^{13}C isotope and therefore possess an MW greater than 270 Daltons. The amount of palmitate remaining at 270 Daltons was then determined at different time points during development as an indicator of maternally contributed fatty acid. Our data confirm that, by the L4 stage of development, the maternal contribution of palmitate is generally around 5% of total palmitate (see Figure 2.6). This provides a satisfying secondary confirmation of our data analysis.

Experimental Determination of Acetyl-CoA Isotope Composition

In principle, the acetyl-CoA isotope composition could be obtained by fitting fatty acid synthesis data with a trinomial distribution while allowing the acetyl-CoA isotope composition to vary. However, we chose to experimentally assess isotope composition. The *E. coli* (OP50) diet of *C. elegans* contains insignificant levels of stearate (C18:0); therefore, the primary means by which *C. elegans* obtains C18:0 is by elongation of C16:0 fatty acids. We exploited this property to calculate the isotope composition of acetyl-CoA units for each experiment (Figure 2.3A and 2.3B). If a fully labeled C16:0 is elongated to stearate in *C. elegans*, the MW of stearate will directly reflect the fractions of ^{12}C-^{12}C, ^{13}C-^{12}C, and ^{13}C-^{13}C acetyl-CoA units. Thus, by quantifying the abundance of C18:0 (I_{314}), C18:0 (I_{315}), and C18:0 (I_{316}), we can determine the probability of incorporating the different isotopomers of acetyl-CoA (Equations (12), (13) and (14)). These numbers were calculated after correction for isotope impurity.

$$(12) \quad P_a = I_{314}(Tot)/(I_{314}(Tot) + I_{315}(Tot) + I_{316}(Tot))$$

$$(13) \quad P_b = I_{315}(Tot)/(I_{314}(Tot) + I_{315}(Tot) + I_{316}(Tot))$$

$$(14) \quad P_c = I_{316}(Tot)/(I_{314}(Tot) + I_{315}(Tot) + I_{316}(Tot))$$

where P_a equals the probability of incorporating a [^{12}C-^{12}C], P_b equals the probability of incorporating a [^{12}C-^{13}C or ^{13}C-^{12}C], and P_c equals the probability of incorporating a [^{13}C-^{13}C]. The fact that this method for determining acetyl-CoA isotope composition produced models that correctly predicted both synthesized and elongated isotopomer distribution in C16:0 independently confirms our analyses and also argues that the same pool of acetyl-CoA is used for elongation and for *de novo* synthesis.

Determination of Synthesis Levels for Other Fatty Acids in WT and Mutant Strains

For the majority of our study, we present data as the fraction of fatty acid that was generated through *de novo* fatty acid synthesis. This number was expressed as the total amount of synthesized fatty acid over the total dietary fatty acid taken up or synthesized during the feeding assay. Equation 15 represents the method used to calculate percent synthesis for palmitate.

(15)

$$\%\,\mathrm{FA\ Synthesis} = \frac{\sum_{270}^{286} I_n(Synth)}{\sum_{270}^{286} I_n(Tot) - I_{270}(Mat)} * 100$$

For all fatty acid species, the trinomial distribution described in the previous section was used to calculate total fatty acid synthesis. For 18 carbon fatty acids, we used a trinomial distribution that accounted for the assembly of nine acetyl-CoA units.

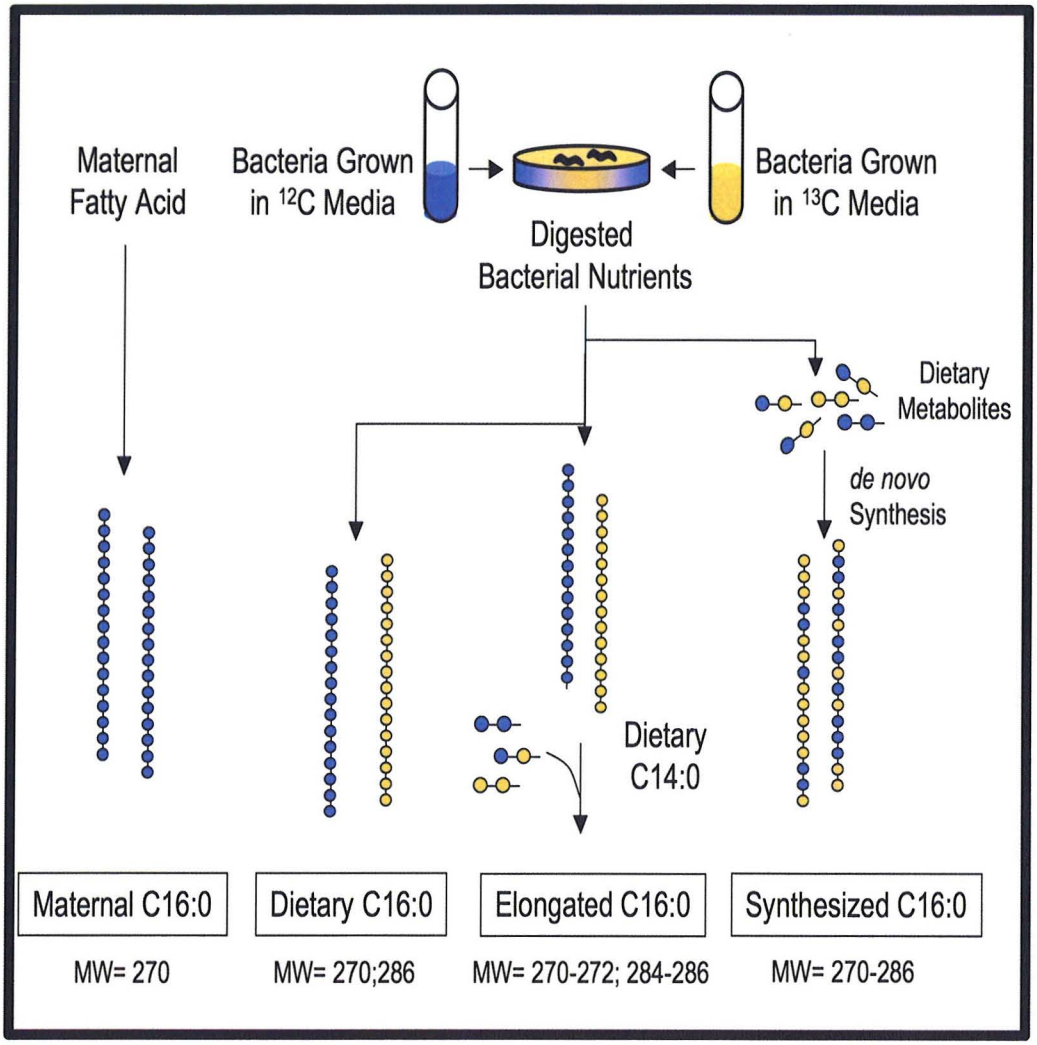

Figure 2.1. "Mixed Isotope" Labeling Strategy: *C. elegans* palmitate (C16:0) can be obtained from four distinct sources, and, by feeding worms a 1:1 mixture of ^{12}C- and ^{13}C-enriched bacteria, each of these sources will produce fatty acids with a specific MW signature. Because we subsequently analyze fatty acid methyl esters, the MW for each C16:0 isotopomer reflects that of the corresponding methyl ester. Directly absorbed C16:0 will either be fully unlabeled (MW = 270) or fully labeled (MW = 286). C16:0 produced in C. elegans from elongation of dietary C14:0 will involve fusion of a fully unlabeled or fully labeled 14-carbon backbone with labeled, partially labeled, or unlabeled acetyl-CoA; consequently, C16:0 created by elongation of C14:0 will generate isotopomers ranging from MW = 270–272 and MW = 284–286. Third, fatty acids synthesized *de novo* from dietary metabolites will have a statistical distribution of C16:0 isotopomers ranging from MW = 270–286 that depends on the isotope composition of the acetyl-CoA pool. Fourth, maternally inherited palmitate will be fully unlabeled (MW = 270).

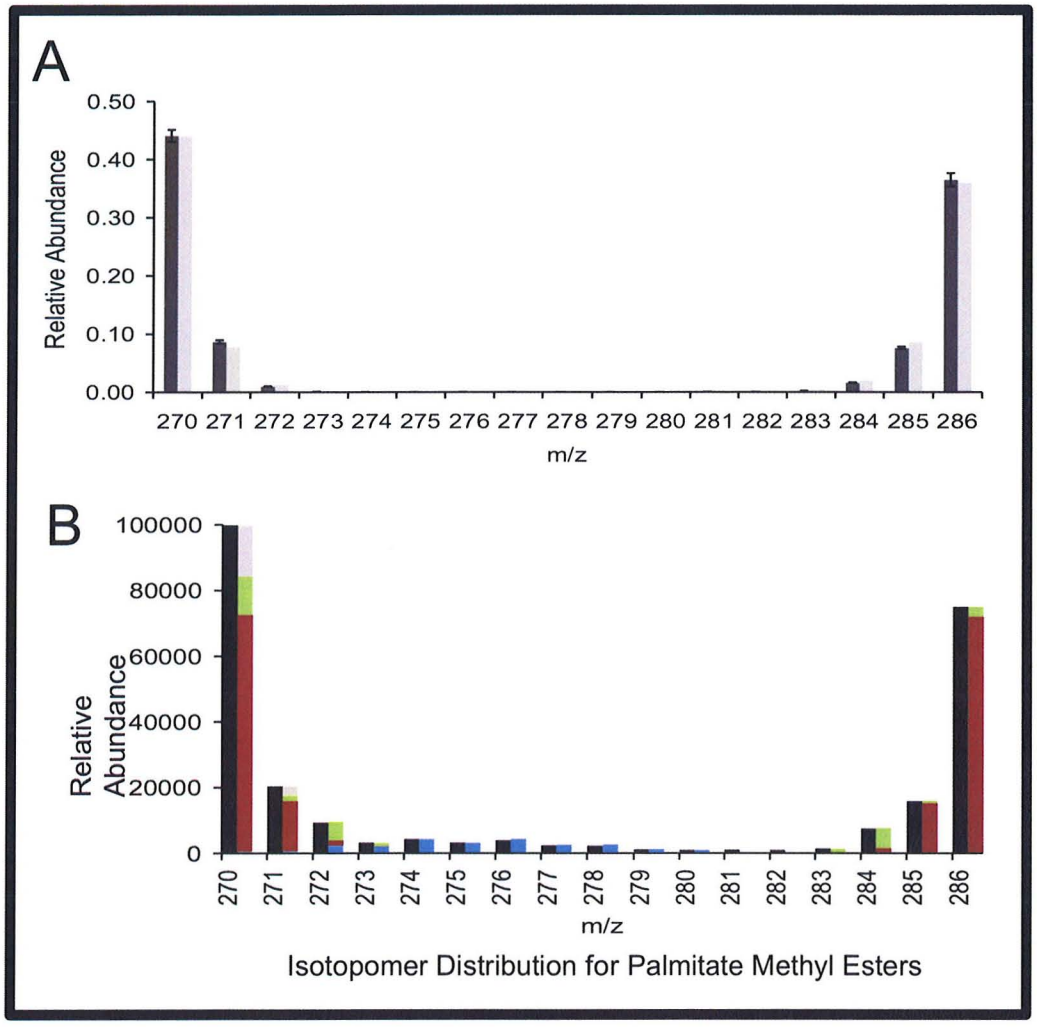

Figure 2.2. Characterization of Palmitate Absorption and Synthesis: (A) Mass spectra of C16:0 obtained from bacteria on control feeding plates were averaged (n > 10) and are displayed here (black bars) as mean fraction of total abundance (± standard deviation [SD]). The peak at 270 Daltons represents C16:0 from bacteria grown in fully unlabeled media, and the peak at 286 Daltons represents C16:0 from bacteria grown in ^{13}C-labeled media. The gray bars represent calculation of isotopomer peaks resulting from natural ^{13}C isotope in unlabeled media (1.11%) and ^{12}C isotope impurity in the ^{13}C media (1.5%). Importantly, the absence of detectable peaks between 272 and 284 Daltons shows that no mixing of isotope label occurred on the feeding plates. (B) A mass spectrum of C16:0 methyl ester obtained from the total lipid of worms grown on a mixed isotope diet from the L1 to the L4 stage of larval development (black). In order to model these data, we accounted for (1) dietary fat absorption (red), (2) *de novo* synthesis (blue), (3) elongation of dietary fat (green), and (4) maternal contribution (gray). Our analysis accounted for shoulder peaks due to natural ^{13}C abundance in the unlabeled media and ^{12}C isotope impurity in the ^{13}C media.

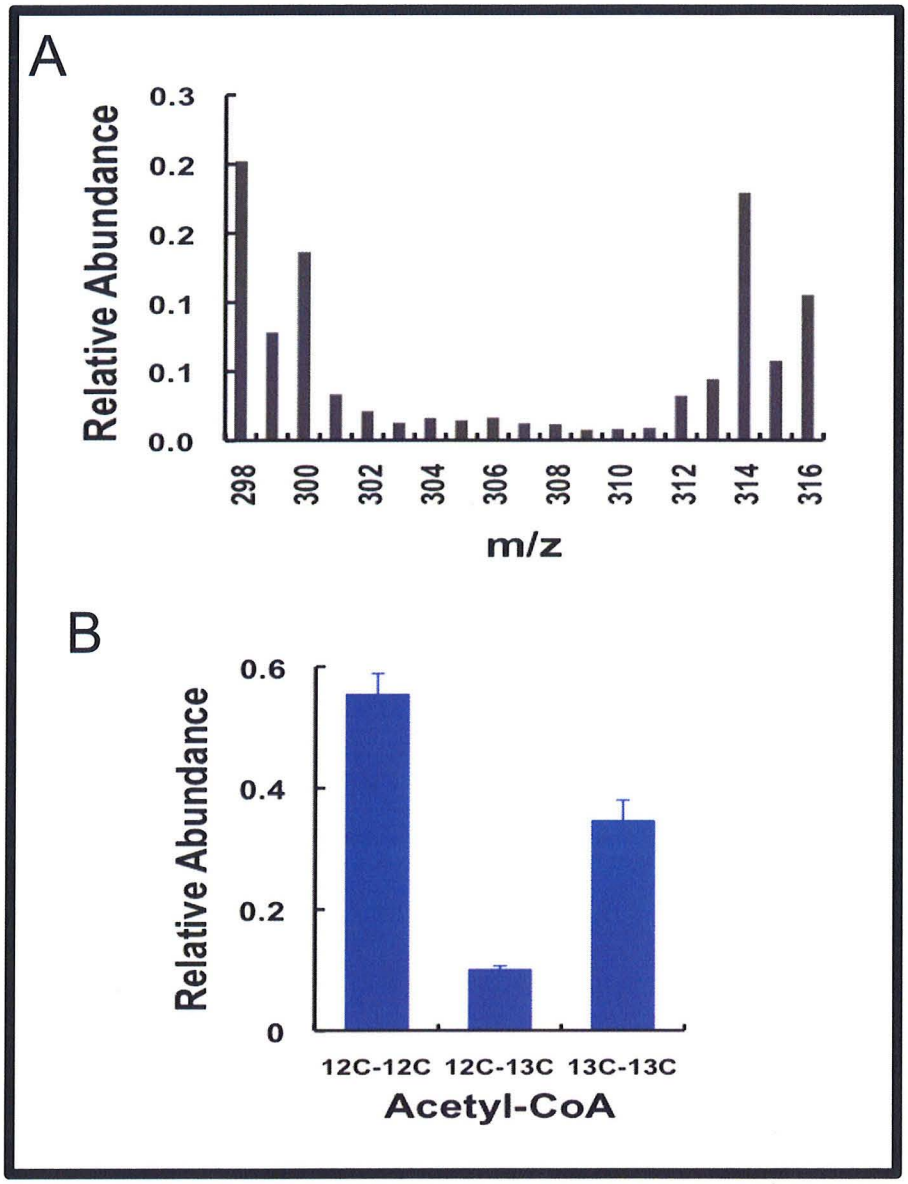

Figure 2.3. Determining Acetyl-CoA Composition: (A) A mass spectrum of stearate (C18:0) obtained from L4 larvae that had been grown on mixed label feeding plates from the L1 stage of development. (B) By examining the relative abundance of isotopomer peaks at 314, 315, and 316 Daltons, we calculated the probability of incorporating unlabeled (^{12}C-^{12}C), partially labeled (^{12}C-^{13}C), and fully labeled (^{13}C-^{13}C) acetyl-CoA isotopomers. Data are the compilation of three experiments and are presented as the mean ± SD.

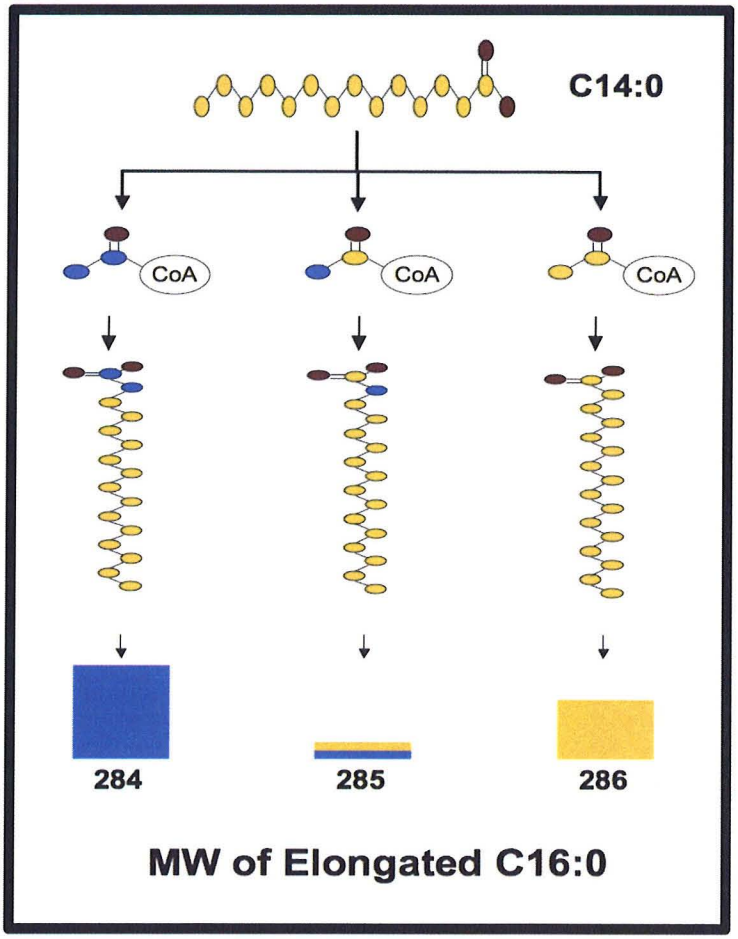

Figure 2.4. Generation of Palmitate by Elongation of Dietary C14:0: Bacterial C14:0 can be elongated in *C. elegans* by the addition of a two-carbon unit. Thus, the final molecular weight of a palmitate generated from a fully labeled C14:0 precursor (284, 285, or 286 Daltons) will depend on the probability of incorporating a ^{12}C-^{12}C, a ^{13}C-^{12}C, or a ^{13}C-^{13}C unit.

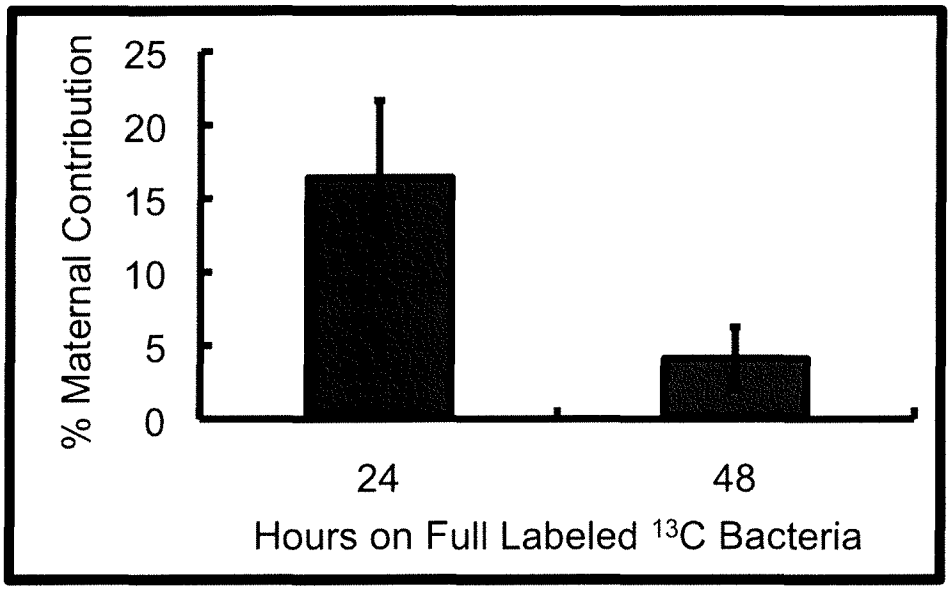

Figure 2.5. Secondary Confirmation of Maternal Contribution: A population of synchronized L1 larvae, derived from unlabeled mothers, was grown on fully labeled ^{13}C bacteria for 24 or 48 hours. After 48 hours when the animals have reached late L4, approximately 5% of the original unlabeled ^{12}C fatty acid remained.

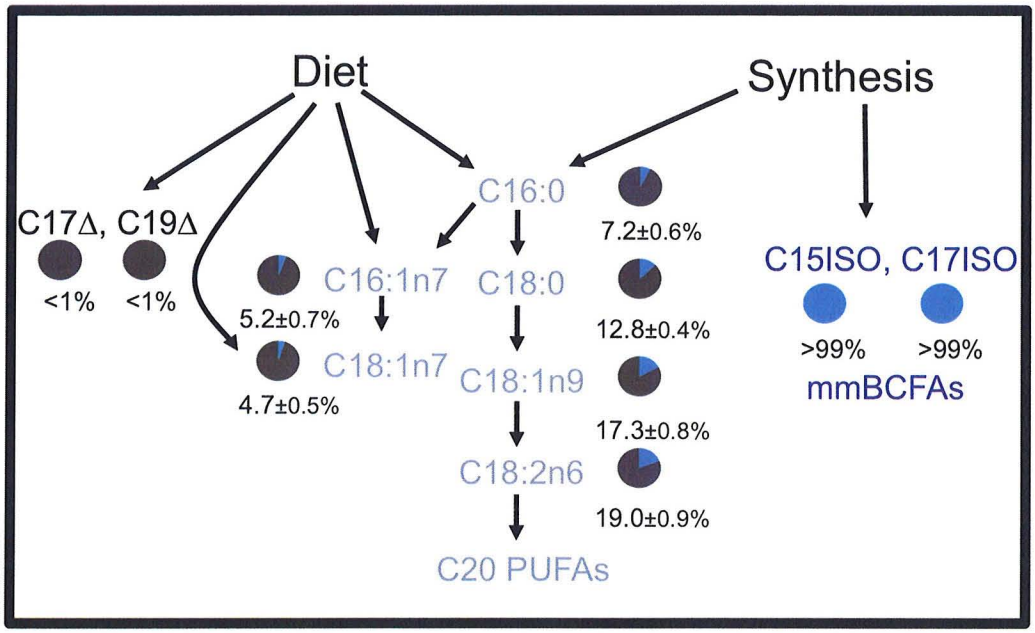

Figure 2.6. Biosynthetic Origin of *C. elegans* Lipids: The most abundant *C. elegans* fatty acids are shown here along with their biosynthetic origins. The proportion of fatty acid derived from synthesis is represented in blue in the pie graphs and numerically indicated below. Fatty acid obtained from absorption and/or modification of dietary fatty acid is displayed in gray. Data represent the compilation of five experiments and are displayed as the mean ± standard error of the mean (SEM).

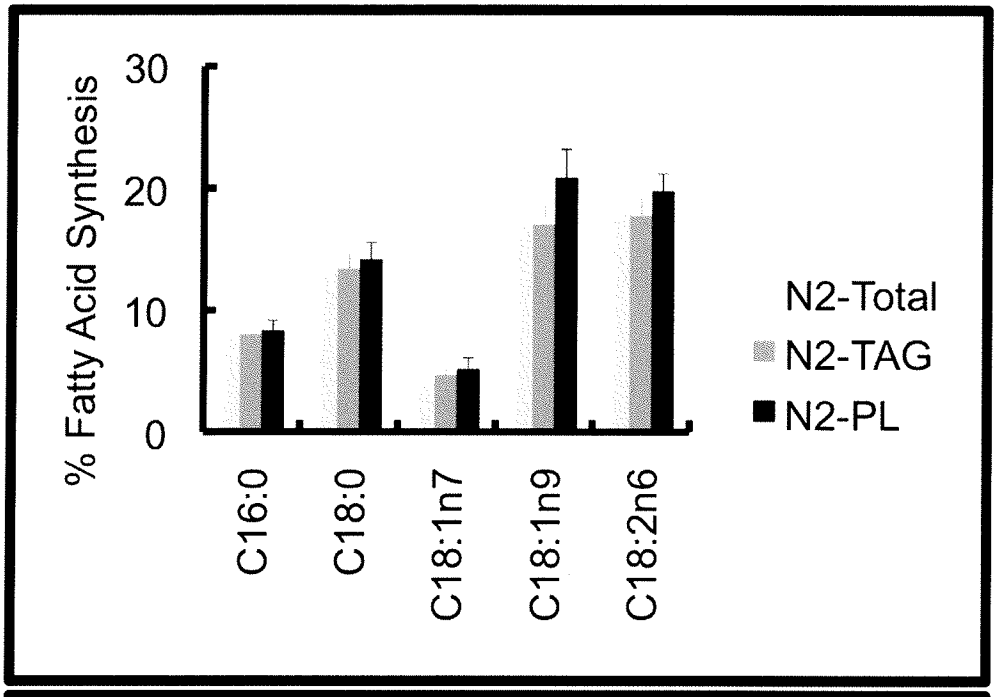

Figure 2.7. Synthesis Contributes Equally to TAG and PL: The percentage of fatty acids derived from *de novo* synthesis in phospholipid (PL), TAG (triacylglyceride), and total lipid is shown for WT (N2). Data are presented as the mean of three experiments with SEM shown.

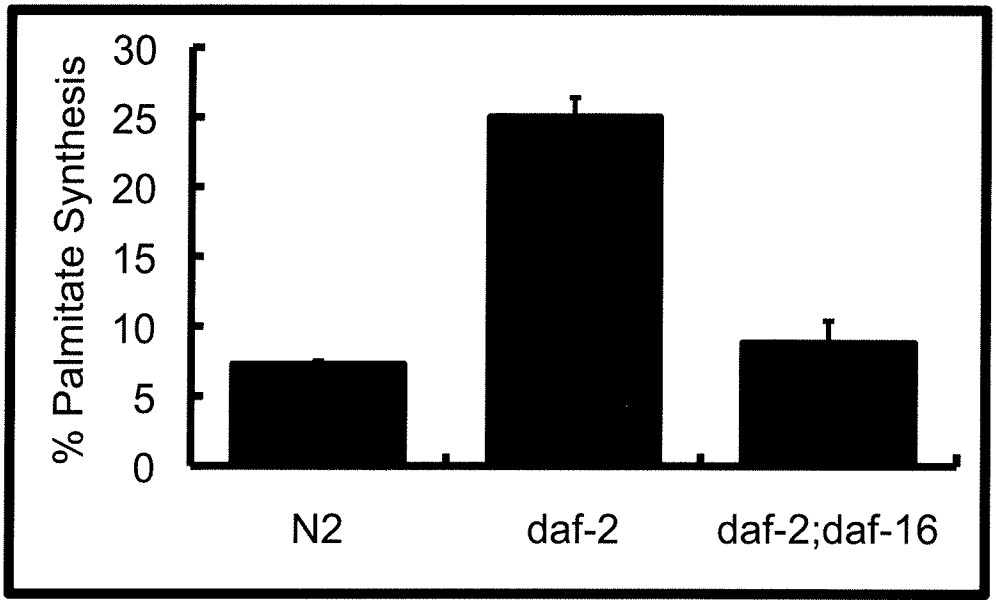

Figure 2.8. Increased Synthesis in *daf-2* Animals: We assayed synthesis in *daf-2 (e1370)* mutant animals and found an increase *de novo* fatty acid synthesis represented here by % palmitate synthesis. However, the synthesis increase is observed in all fatty acid species measures (see Chapter 3). We also found that the synthesis increase was dependent on the presence of the DAF-16 transcription factor with no increase in synthesis seen in *daf-2(e1370);daf-16(m26)* double mutants. Data is from at least 3 replicates with SEM shown.

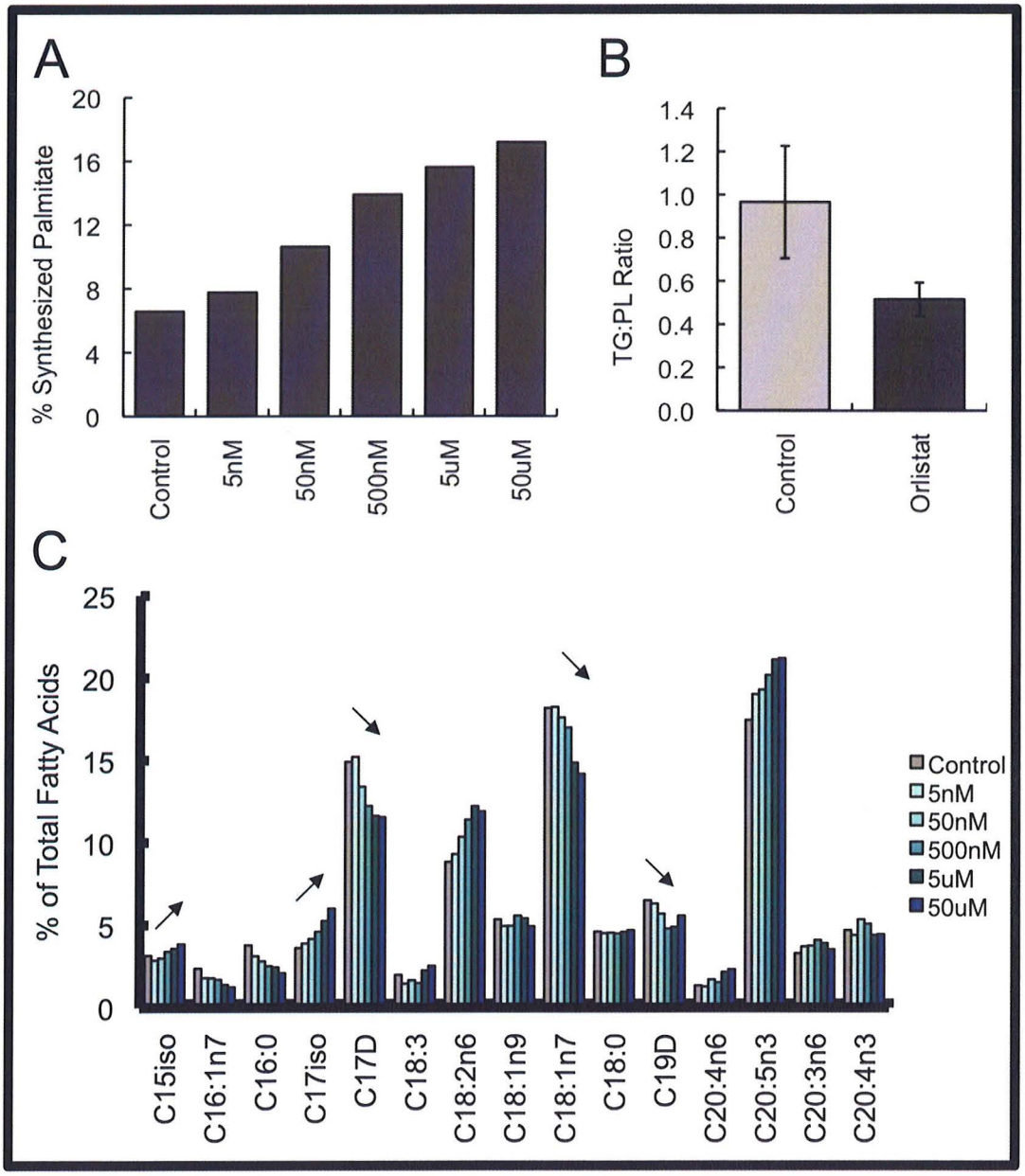

Figure 2.9. Inhibition of TAG Lipase Activity Results in Decreased Fat Absorption: (A) Increasing concentration of the lipase inhibitor, orlistat, results in a dose-dependent increase in the ratio of synthesized to absorbed fatty acids. Data shown for palmitate synthesis. (B) This skewed ratio can be assigned to decreased fat absorption as the TAG:PL ratio decreases indicating reduced fat storage. (C) Changes in the fatty acid composition of the treated animals show a relative increase in the abundance of synthesized fatty acids (C15iso, C17iso) and a relative decrease in the amount of dietary fatty acids (C17D, C18:1n7, C19D).

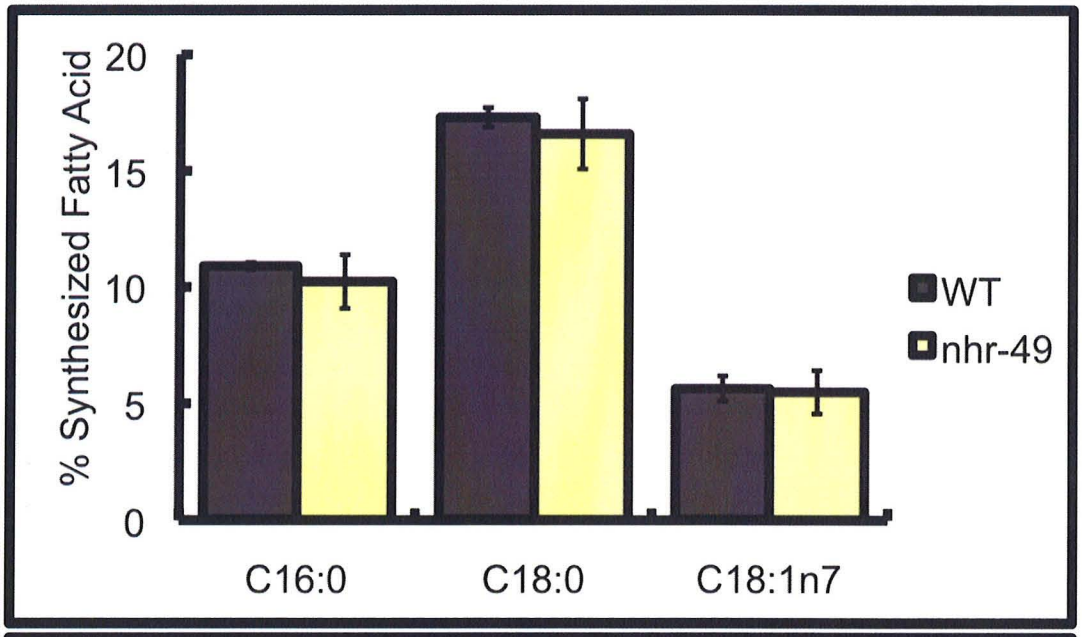

Figure 2.10. Decreased β-oxidation Mutants Show No Change in the Source of Fatty Acids: Although our method can not directly detect changes in fat utilization, we used *nhr-49 (nr2041)* (yellow) to demonstrate that the ratios of synthesis and absorbed fatty acids are unaffected compared to N2 (black). The data shown is from a minimum of 3 experiments with SEM.

Fatty Acid Species	*E. coli*	*C. elegans*
C12:0	7.5 ± 0.9	<2%
C14:0	8.7 ± 0.5	<2%
C15iso	<2%	3.8 ± 0.2
C16:1n7	3.9 ± 1.1	2.1 ± 0.3
C16:0	36.6 ± 3.2	3.7 ± 0.5
C17iso	<2%	5.8 ± 0.3
C17Δ	16.4 ± 0.6	14.9 ± 0.1
C18:2n6	<2%	8.1 ± 0.7
C18:1n9	<2%	4.3 ± 0.5
C18:1n7	15.6 ± 3.0	19.7 ± 1.6
C18:0	<2%	2.5 ± 0.9
C19Δ	7.5 ± 1.5	6.8 ± 0.5
C20 PUFAs	<2%	25.4 ± 1.1

Table 2.1. Fatty Acid Composition of *E. coli* and *C. elegans*: Total fatty acids from *E. coli* and *C. elegans* were purified, transmethylated, and analyzed by GC/MS as described (Watts and Browse, 2002). The relative abundance of each fatty acid species is displayed as % of total fatty acid. Data are the compilation of 3 experiments and are expressed as the mean +/- SEM. The four different *C. elegans* C20 polyunsaturated fatty acids have been grouped together in this table.

CHAPTER III: A ^{13}C Labeling Strategy Reveals the Influence of Insulin Signaling on Lipogenesis in *C. elegans*

Sections on DAF-2 pathway are modified from an article published in *Cell Metabolism*: Perez CL and Van Gilst MR. (2008). A 13C isotope labeling strategy reveals the influence of insulin signaling on lipogenesis in *C. elegans. Cell Metabolism* Sep;8(3):266-274.

Sections on TGF-β pathway were published in *Cell Metabolism:*
Greer ER, Perez CL, Van Gilst MR, Lee BH and Ashrafi K. (2008). Neural and molecular dissection of a *C. elegans* sensory circuit that regulates fat and feeding. *Cell Metabolism* Aug;8(2):118-131.

Summary

Although studies in *C. elegans* have identified numerous genes involved in fat storage, the next step is to determine how these factors actually affect *in vivo* lipid metabolism. We have developed a ^{13}C isotope assay to quantify the contribution of dietary fat absorption and *de novo* synthesis to fat storage and membrane lipid production in *C. elegans*, establishing the means by which worms obtain and process fatty acids. Next, we applied this method to characterize how insulin/IGF signaling affects lipid physiology. Several long-lived mutations in the insulin receptor gene, *daf-2,* resulted in significantly higher levels of synthesized fats in both triglycerides and phospholipids. This elevation of fat synthesis was completely dependent upon the DAF-16/FoxO transcription factor. However, other long-lived alleles of *daf-2* did not increase fat synthesis, suggesting that site-specific mutations in the insulin receptor can differentially influence longevity and metabolism. Importantly, the separation of these phenotypes demonstrates that elevated lipid synthesis is not required for the longevity of *daf-2* mutants. To establish how the lipid metabolism and lifespan are regulated distinctly by DAF-2, we measured fatty acid synthesis in a panel of strains with mutations in genes encoding components which function downstream of the insulin receptor including the AGE-1 and SGK-1 kinases. In doing so, we found that lipid synthesis levels were wild-type in *age-1* mutants but elevated in *sgk-1* animals, suggesting a potential mechanism for the distinct regulation of the longevity and lipid synthesis phenotypes. Additionally, we were able to establish that the impact of insulin signaling on lipogenesis requires, at least partially, the function of the TGF-β transcription regulator, DAF-3, as well as the nuclear hormone

receptor, DAF-12. Ultimately, we propose a model which defines DAF-12 as a major regulator of lipogenesis, functioning downstream of the insulin/IGF and TGF-β pathways.

Introduction

In addition to its regulation of lifespan and dauer formation, the insulin/IGF signaling pathway in *C. elegans* also plays a key role in the regulation of fat metabolism (Ashrafi et al., 2003; Hellerer et al., 2007; Ogg et al., 1997). Under nutrient rich conditions, the insulin receptor, DAF-2, positively regulates the PI3 kinase, AGE-1, which generates pools of PIP_3 signaling molecules. The PIP_3 interacts with a suite of kinases including AKT-1 that phosphorylates the DAF-16 transcription factor and prevents its translocation into the nucleus. When the *daf-2* pathway is inhibited, DAF-16 can move into the nucleus and orchestrate a transcription program that is important for entry to and survival of the dauer state. Dauer, an alternative long-lived larval stage, is associated with increased stress resistance and altered metabolism. Additionally, adult animals with altered insulin signaling have transcriptional changes that result in lifespan extension and metabolic reprogramming similar to the dauer animals (Burnell et al., 2005; McElwee et al., 2006; Murphy et al., 2003). Mutations in the insulin-like receptor gene, *daf-2*, result in an accumulation of lipid, and, like many other *daf-2* phenotypes, the increased fat storage requires the activity of the FoxO homologue, DAF-16 (Ogg et al., 1997; Yen et al., 2010). However, it remains unclear what types of metabolic changes cause the fat accumulation in the *daf-2* animals and what impact the altered metabolism has on lifespan.

The question of how *C. elegans daf-2* regulates lipid metabolism is of particular interest given its potential to inform us about how insulin signaling controls longevity. In fact, it has been proposed that the changes in fat storage may impact the lifespan of the *daf-2* animals. Like *C. elegans*, knockout of the insulin receptor increases longevity in mice (Holzenberger et al., 2003; Katic et al., 2007; Kenyon et al., 1993). The conservation of metabolic regulation, however, is less clear, as the effect of insulin signaling on fat storage in mammals appears to vary based on tissue and context (Bluher et al., 2002; Bruning et al., 2000; Bruning et al., 1998); consequently, defining the relationship between insulin receptor control of lipid metabolism and longevity, in both *C. elegans* and mammals, requires further study.

Although the insulin signaling pathway is important for sensing nutrient availability, it does not function in isolation. The TGF-β pathway acts synergistically with the daf-2

pathway to coordinate a transcriptional response to changing environmental conditions. Mutations in the TGF-β ligand, DAF-7, and its receptor, DAF-1, have also been shown to impact fat storage in the nematode through the transcriptional regulator, DAF-3 (Greer et al., 2008; Ogg et al., 1997). Together, DAF-16 and DAF-3 impact the function of the nuclear hormone receptor, *daf-12*, the main component of the steroid hormone pathway. DAF-12 integrates the inputs from both the insulin and TGF-β pathways to regulate the decision between reproductive growth or dauer diapause. DAF-12 has been found to function downstream of the majority of other proteins that regulate the dauer arrest; however, it is unclear how these pathways may interact to regulate fat storage.

In order to better understand the mechanisms by which any fat storage gene impacts lipid physiology, tools were needed that allowed for the characterization and quantification of fatty acid metabolism in the nematode. To address this need, we have established a ^{13}C stable isotope labeling strategy that has allowed us to determine how the nematode processes and allocates its diet (Perez et al., 2008). Here, we have implemented this mixed isotope technology to define how the insulin signaling pathway and related pathways regulate *de novo* fatty acid synthesis and fat storage.

Disruption of Insulin Signaling Leads to Increased *De Novo* Fatty Acid Synthesis

In order to determine how the insulin signaling pathway impacts fat storage, we used a "mixed isotope" labeling strategy to determine the sources of fat in *daf-2* mutants (method described in Chapter 2). Worms harboring the commonly studied *e1370* allele of *daf-2* contained a >2-fold higher proportion of synthesized fatty acids (Figure 3.1A). The increase in the proportion of synthesized fatty acid is seen in all fatty acid species measured (Figure 3.1B). A higher fraction of synthesized fatty acid might not necessarily reflect an absolute increase in *de novo* synthesis but rather a reduced contribution of dietary fat to the total lipid pool. This scenario, however, would result in less total fat storage. Under our conditions, we found approximately 80% higher levels of triglycerides (TAGs) in *daf-2(e1370)* animals demonstrating the *daf-2* animals have increased fat synthesis (Figure 3.1C). These data are consistent with previous reports, which implemented different strategies to show a similar impact of *daf-2(e1370)* mutation on fat storage (Ashrafi et al., 2003; Hellerer et al., 2007; Ogg et al., 1997). Taken together, we have established a clear role for *daf-2* in the regulation of *de novo* fatty acid synthesis.

Contribution of Lipid Synthesis to Fat Storage in *daf-2* Animals

Because *daf-2(e1370)* animals have elevated fat storage, we considered the possibility that synthesis was specifically increased in these animals and directly allocated to TAG production. To address this question, we analyzed the relative abundance of synthesized and dietary fatty acids in TAGs and phospholipids (PLs). We previously found that wild-type (WT) animals displayed a similar fraction of synthesized and dietary fatty acids in both lipid types ((Perez et al., 2008) and Chapter 2). In the *daf-2(e1370)* animals, we found a higher proportion of synthesized fatty acids in both TAGs and PLs (Figure 3.1B). This result implies that synthesized and absorbed fatty acids contribute to a common pool that feeds both membrane synthesis and fat storage. Thus, in *daf-2(e1370)* mutants, more synthesized fatty acid is available for PL production and for TAG storage.

We next determined how much of the elevated fat storage observed in *daf-2(e1370)* animals originated from *de novo* synthesis. When broken down into synthesized and absorbed components, it is clear that there are 3-fold higher levels of synthesized fatty acids in *daf-2(e1370)* TAGs than in WT TAGs (Figure 3.1D). This increased supply of synthesized fatty acids is sufficient to account for a significant proportion (>60%) of the elevated fat storage found in *daf-2(e1370)* mutants. Additionally, *daf-2(e1370)* mutants also contain higher levels of dietary fatty acids in their TAGs. Much of this increase is likely due to the fact that more dietary fatty acid is free for TAG storage because of the larger contribution of synthesized fat to PL production. However, because increased fatty acid synthesis often inhibits fatty acid β-oxidation via malonyl-CoA, it is probable that reduced β-oxidation is also a factor contributing to the excess fat stores of *daf-2(e1370)* worms.

Alternative *daf-2* Alleles Have Distinct Impacts on Fatty Acid Synthesis

In addition to the *daf-2(e1370)* mutation, other long-lived alleles of *daf-2* have been isolated that contain in site-specific amino acid substitutions in different domains of the receptor (Gems et al., 1998; Patel et al., 2008). Although these alleles all cause life-span extension, they have variable impacts on other aspects of worm physiology, including reproduction, pharyngeal pumping, hypoxia resistance and motility (Gems et al., 1998; Mabon et al., 2009; Patel et al., 2008). We found that several of these alleles displayed dramatically different effects on lipogenesis. Specifically, we found two *daf-2* alleles (*m577* and *e1368*) that did not affect fatty acid synthesis, two alleles (*m596* and *e1371*) that caused a moderate increase in synthesis and one allele (*m41*) that stimulated fatty acid synthesis as

strongly as *daf-2(e1370)* (Figure 3.2A). The level of fatty acid synthesis observed in the different *daf-2* mutants did correlate with the amount of TAG storage in the animals, further supporting the conclusion that the elevated fat storage caused by *daf-2* mutation is primarily due to changes in *de novo* synthesis (Figure 3.2B).

In order to establish that the regulation of fatty acid synthesis was independent of lifespan, we confirmed that all of these *daf-2* alleles led to increased life span under our experimental conditions (Figure 3.2C). Furthermore, we did not find any correlation between the amount of synthesis increase and the degree of lifespan extension. These results demonstrate that increased *de novo* fatty acid synthesis is not required for lifespan extension in *daf-2* animals. Notably, the *daf-2(m41)* animals have the highest levels of synthesized fatty acids, but under our conditions, their lifespan extension is the smallest. Moreover, because *de novo* synthesis is responsible for the majority of the increased fat storage, we believe that longevity in these animals is also independent of total amount of fat stores.

Insulin Regulation of Fatty Acid Synthesis Depends on DAF-16/FoxO But Is Independent of the AGE-1 Kinase

Because the fat synthesis and lifespan phenotypes of *daf-2* are genetically separable, we next wanted to define if their regulation required distinct downstream effectors. In order to further address the genetic pathways by which insulin/IGF signaling impacts fatty acid synthesis, we examined *age-1* and *daf-16* mutants. The impact of insulin signaling on longevity is dependent upon both the AGE-1 PI3 kinase and the DAF-16/FoxO transcription factor (Kenyon et al., 1993; Larsen et al., 1995). When activated, the insulin receptor activates AGE-1, which then leads to AKT phosphorylation of DAF-16, and sequestration of this FoxO factor from the nucleus (Lee et al., 2001). Thus, inactivation of *age-1* enhances longevity by leading to the activation of DAF-16, which we confirmed under our conditions (data not shown). Moreover, deletion of *daf-16* is sufficient to suppress the longevity of both *daf-2* and *age-1* mutants (Dorman et al., 1995). We found that the effect of the *daf-2(e1370)* mutation on fatty acid synthesis was completely dependent upon *daf-16*, as a *daf-2(e1370);daf-16(m26)* double mutant displayed WT levels of fatty acid synthesis. Furthermore, mutation of *daf-16(m26)* alone resulted in a slight reduction in *de novo* synthesis (Figure 3.2A). In contrast, examination of *age-1(hx546)* mutants demonstrated no impact of this long-lived allele on fatty acid synthesis (Figure 3.3). We conclude that the *C.*

elegans FoxO homolog, DAF-16, can act as a potent stimulator of fatty acid synthesis, and that, under fed conditions, insulin signaling suppresses *de novo* synthesis by inhibiting DAF-16. The fact that the *age-1(hx546)* allele did not affect fatty acid synthesis implies again that site-specific mutants in the insulin signaling pathway may differentially modulate DAF-16 activity, such that some mutants may impact DAF-16 so as to affect longevity and fatty acid synthesis, and other mutants may activate DAF-16 longevity pathways, but not *de novo* fatty acid synthesis. Taken together, these results imply that *daf-16* stimulates fatty acid synthesis, and that activation of the insulin signaling pathway represses *de novo* synthesis, at least in part, by inhibition of *daf-16*.

The Role of SGK-1 In Regulating Synthesis

In order to understand how the DAF-2 receptor regulates synthesis, we tested the requirement of the components of the insulin signaling pathway. When activated, DAF-2 positively regulates the AGE-1 kinase as described above. The phosphatidylinositol kinase catalyzes the phosphorylation of PIP_2 to PIP_3, which in turn activates a number of downstream kinases including the AKT kinase family proteins, AKT-1 and AKT-2, and the serum- and glucocorticoid-inducible kinase homolog (SGK-1) proteins. These kinases phosphorylate the DAF-16 transcription factor, which blocks its ability to move into the nucleus where it can activate its target genes. We quantified the rates of fatty acid synthesis in mutants of these kinases and found no role for AKT-1 or AKT-2 in regulating fatty acid synthesis. However, the *sgk-1(ok538)* animals had a significant increase in the relative abundance of synthesized fatty acids (Figure 3.3A). Therefore, we wanted to test whether SGK-1 regulation of *de novo* fatty acid synthesis was dependent on DAF-16. To do this, we constructed a *sgk-1(ok538);daf-16(m26)* double mutant and found that these animals have wild-type synthesis (Figure 3.3A). *In vitro,* it has been determined that SGK-1 is dependent on the function of a 3-phosphoinosite-dependent kinase called PDK-1 (Hertweck et al., 2004). A gain of function mutant of *pdk-1(mg142)* has been described, and we have preliminary evidence that this activating mutation can fully rescue the high synthesis of the *daf-2(e1370)* mutant. Taken together, we believe that this provides evidence that lipogenesis and lifespan are regulated by distinct signaling pathways with lipogenesis being regulated by the SGK-1 kinase. However, further study is required to elucidate the interactions between the insulin signaling components and to identify unknown players (Figure 3.4).

We thought that other pathways that impact the DAF-16 transcription factor might play a role in regulation of fatty acid synthesis; however, we did not find any change in fatty acid synthesis in mutants of the JNK (c-Jun N-terminal Kinase) or EAK (Enhancer of AKT-1) pathways (Table 3.1). Therefore, we predict that an unidentified pathway may converge on the SGK-1 kinase and DAF-16 transcription factor to regulate fatty acid synthesis. In a screen of known fat storage mutants, we identified a Type II PI3-Kinase that may play a role in regulating synthesis independent of *age-1*; however, we have not yet confirmed the involvement of this kinase in the insulin signaling pathway (described in Appendix I).

DAF-12 as A Master Regulator of Fat Synthesis

In unfavorable environments, the insulin signaling pathway functions through *daf-16* to downregulate the expression of DAF-9, a cytochrome P450 that functions in the biosynthesis of the DAF-12 ligand. *daf-12* encodes a nuclear receptor that regulates the dauer diapause and lifespan (Rottiers et al., 2006). To test whether fat metabolism regulation was mediated by *daf-12*, we assayed synthesis in several *daf-12* mutants. We found that in *daf-12(rh273)*, a dauer-constitutive allele, there is a significant increase in fat synthesis (Figure 3.5A). Another dauer-constitutive allele, *rh274,* results in a much less dramatic increase in fat synthesis. Additionally, in *daf-12(m20)* and *daf-12(rh61rh412)* animals which are dauer-defective, there was no increase in synthesis (Figure 3.5A).

Next, we tested whether *daf-12* activity was essential for the synthesis increase seen in *daf-2(e1370)* animals. In *daf-2(e1370);daf-12(m20)* animals, the increase in synthesis was partially reduced indicating a role for DAF-12 in the regulation of synthesis (Figure 3.5B). This result is particularly intriguing as *daf-12(m20)* enhances the longevity of a *daf-2(e1370)* animal (Patel et al., 2008). Taken together, this data suggested a role for *daf-12* in the regulation of fatty acid synthesis; however, more work needs to be done to fully establish the impact of DAF-12 on lipogenesis.

The TGF-β Pathway Regulates Lipogenesis As Well

The TGF-β pathway is an important nutrient sensing pathway that also regulates lifespan and dauer development that acts synergistically with the insulin-like signaling pathway. The TGF-β receptor, DAF-1, is activated by its ligand, DAF-7, and results in the inhibition of the transcriptional regulator DAF-3. Because the TGF-β pathway also converges on *daf-12*, we measured fatty acid synthesis in mutants of the TGF-β ligand, *daf-7(e1372)* and its receptor,

daf-1(m40). We found an ~3-fold increase in *de novo* fatty acid synthesis in these animals. Additionally, this increase was dependent on the downstream effector, *daf-3,* as abundance of synthesized fatty acids is wild-type in *daf-1(m40);daf3(mgDf90)* animals (published in (Greer et al., 2008); Figure 3.5C). Not only does this data support the role of *daf-12* in regulating synthesis, but this increase also suggests that increased lipogenesis may be a fundamental component that allow dauer larvae survival.

Discussion

There has been considerable interest in the *C. elegans* insulin receptor due to its influence on longevity, stress resistance, and lipid storage (Kenyon et al., 1993; McElwee et al., 2006; Wolkow et al., 2000). The commonly studied *daf-2(e1370)* allele blocks insulin signaling, extends life span, and leads to elevated fat accumulation. We found that *daf-2(e1370)* animals have more than double the amount of synthesized fatty acids in TAG and PL, implying that *de novo* synthesis is the predominant mechanism by which the insulin signaling pathway affects fat storage in *C. elegans*. This conclusion is further supported by a positive correlation between the fatty acid synthesis levels of different *daf-2* mutants and their total fat storage.

Our results with alternative *daf-2* alleles also show that the impacts of the insulin receptor on lifespan and lipogenesis are genetically separable. Thus, the enhanced longevity of *daf-2* mutants does not require increased lipid synthesis. The structural position of the *daf-2* alleles studied here does not provide a clear explanation for their distinct effects on longevity and lipid synthesis (Figure 3.6). The two alleles with the strongest enhancement of de novo synthesis are *m41* and *e1370*. The *e1370* mutation localizes near the active site of the kinase domain, where it could potentially interfere with downstream signaling. The *m41* allele localizes to the L1 domain, which is responsible for ligand interaction; however, *m41* does not alter an amino acid predicted to make direct contact with the insulin ligand. The *m577* and *e1371* mutations both localize to the FnIII2 domain, but only one of these alleles affects *de novo* synthesis. Furthermore, *m596* and *e1368* localize to the L2 domain but also impact lipid synthesis differently. Both the FnIII2 domain and L2 domain reside in the extracellular portion of the insulin receptor and do not directly participate in ligand binding or kinase interaction. Thus, these *daf-2* mutations may directly disrupt interaction with an undefined factor or may indirectly alter ligand binding or kinase activation by differentially perturbing allosteric changes. Alternatively, *daf-2* alleles may

have distinct impacts on protein stability, thus varying the strength of the insulin response. Further genetic and structural investigation will be necessary to establish how these simple site-specific mutations distinctly affect DAF-16/FoxO activity, longevity, and lipogenesis. In any event, the fact that we were able to identify insulin receptor mutants that specifically impacted life span, but not metabolism, suggests that targeted mutations in the insulin receptor may be able to manipulate distinct physiological outcomes; such a finding warrants further investigations in *C. elegans* and mammalian models.

The fact that *daf-16* is required for both longevity and elevated fat synthesis suggests that *daf-16* might respond differently to distinct *daf-2* mutations, such that some mutations activate its capacity to promote longevity but not *de novo* lipogenesis (Figure 3.6A). This could occur because differential modification of *daf-16* is required for its impact on lipogenesis, because of tissue-specific differences in the signaling mechanism, or because *daf-16* control of lipogenesis may be more sensitive to signaling dosage. Alternatively, the effect of the *daf-2(e1370)* mutation on lipogenesis may involve an additional factor that functions together with *daf-16* to stimulate fatty acid synthesis. In this case, some *daf-2* alleles may not influence this additional factor. We found that the *age-1(hx546)* allele, which also results in *daf-16*-dependent lifespan extension, did not impact *de novo* synthesis. These findings demonstrate that site-specific mutations in the insulin receptor or downstream components are able to selectively mediate the longevity enhancing effects of DAF-16/FoxO, without impacting DAF-16/FoxO control of *de novo* fatty acid synthesis. There are several explanations for these observations. First, *age-1* and *daf-2* alleles may be hypomorphic, in that their function is reduced enough to allow DAF-16/FoxO to instill longevity programs, but not reduced enough to enable DAF-16/FoxO to stimulate *de novo* lipogenesis. Second, these mutant alleles may lead to loss of function in tissues that modulate aging, but not tissues that control fatty acid synthesis. This second model may be supported by the findings of Wolkow et al., which showed that tissue specific expression of *daf-2* in muscle could rescue the fat storage phenotype of the *daf-2(e1370)* worms, but not the enhanced longevity (Wolkow et al., 2000). Finally, insulin control of fatty acid synthesis may proceed through an alternative pathway, which does not involve the *age-1* kinase. In this scenario, the specific mutant alleles of *daf-2* that do not affect fatty acid synthesis may be selectively compromised in their ability to activate the AGE-1 pathway that controls aging, but not the pathway that regulates fatty acid synthesis. In order to begin to address these models, we analyzed the impact of other insulin related pathways on lipogenesis. We

did not find a role for either the JNK or EAK pathway in regulating synthesis suggesting that an uncharacterized pathway downstream of the DAF-2 receptor may regulate the lipogenic phenotype. This pathway may involve the function of SGK-1 as we did find increased fat synthesis in the *sgk-1* mutant, which implicates this alternative kinase in fat regulation. However, it is not yet clear how SGK-1 is differentially regulated in this context. Additionally, further genetic analysis will be required to fully distinguish between these models; however, we predict that synthesis regulation will be modulated by a distinct pathway and are currently screening for such a pathway (Figure 3.4).

The mixed isotope labeling strategy also allowed us to define the regulation of *de novo* fatty acid synthesis downstream of *daf-16.* Our studies established a role for DAF-12 and DAF-3 in regulating lipogenesis in *C. elegans* (Figure 3.7). This function is of particular interest as DAF-12 has homology to mammalian nuclear hormone receptors which function in the regulation of lipid metabolism, the liver X receptor alpha and beta (LXRA and LXRB) (Mooijaart et al., 2005). This steroid signaling pathway has also been linked to longevity and to reproduction in *C. elegans*, making future studies in the nematode particularly interesting (further discussed in Chapter IV). It is interesting to note that all of the genes that regulate fatty acid synthesis also play a role in the formation of the dauer larva. The connection of lipogenesis to the dauer state may suggest a requirement of synthesis for dauer initiation and survival.

Experimental Procedures

Strains

Strains were maintained at 20°C on HG plates seeded with *E. coli* (OP50). The following alleles were provided by the CGC: wild-type N2 Bristol, DR1567: *daf-2 (m577),* CB1370: *daf-2 (e1370),* DR1564: *daf-2(m41),* DR1572: *daf-2(e1368),* DR1565: *daf-2(m596),* DR1568: *daf-2 (e1371),* DR1309: *daf-2(e1370);daf-16(m26),* DR26: *daf-16(m26),* CF1038: *daf-16(mu86),* TJ1052: *age-1 (hx546)*, HT941: *jnk-1(+); rol-6(su1066)*, HT942: *jnk-1(+); rol-6(su1066)*, HE1006: *rol-6(su1006)*, AA87: *daf-12(rh273)*, DR20: *daf-12(m20)*, CB1372: *daf-7(e1372),* DR40: *daf-1(m40),* GR1310: *akt-1(mg144),* JT573: *akt-1(sa573),* KQ154: *akt-2(tm812)* and KQ1120: *sgk-1(ok538).* EAK mutants, BQ6: *eak-7(mg338)* and BQ8: *hsd-1(mg345)*, were provide by Patrick Hu from University of Michigan. DR1547: *daf-2(m577);daf-12(m20)* and DR1296: *daf-2(e1370);daf-12(m20)* were provided by David Gems. The *daf-1(m40);daf-3(mgDf90)* strain was constructed and provided by Kaveh

Ashrafi. The *sgk-1(ok538);daf-16(mu86)* was constructed by standard mating and genotyping procedures. The *mu86* allele was chosen because it is a deletion allele that can easily be distinguished by PCR amplification and impact on synthesis is the same.

Mixed Isotope Method

The isotope labeling strategy. lipid extraction procedures and GC/MS detection were implemented as described in the experimental procedure section of Chapter 2. Briefly, separate cultures of bacteria are grown in 12C LB media and 13C Isogro media. Bacteria is harvested, weighed, and mixed in a 1:1 ratio on agarose plates. 30,000 L1 animals are plated on the mixed isotope plates and grown till L4 at 20°C, then collected and frozen. Lipids are then are extracted and analyzed via GC/MS.

Lifespan Analysis

Previous studies had reported the lifespan of the different daf-2 alleles at 18°C and 22.5°C (Gems et al., 1998). Our fatty acid synthesis experiments were all carried out at 20°C. Therefore, because these daf-2 alleles are temperature sensitive, we determined the lifespan of each daf-2 mutant included in our study at 20°C. Lifespan assays were carried out as previously described (Hsin et al., 1999). Bagged and lost animals were excluded from the analysis.

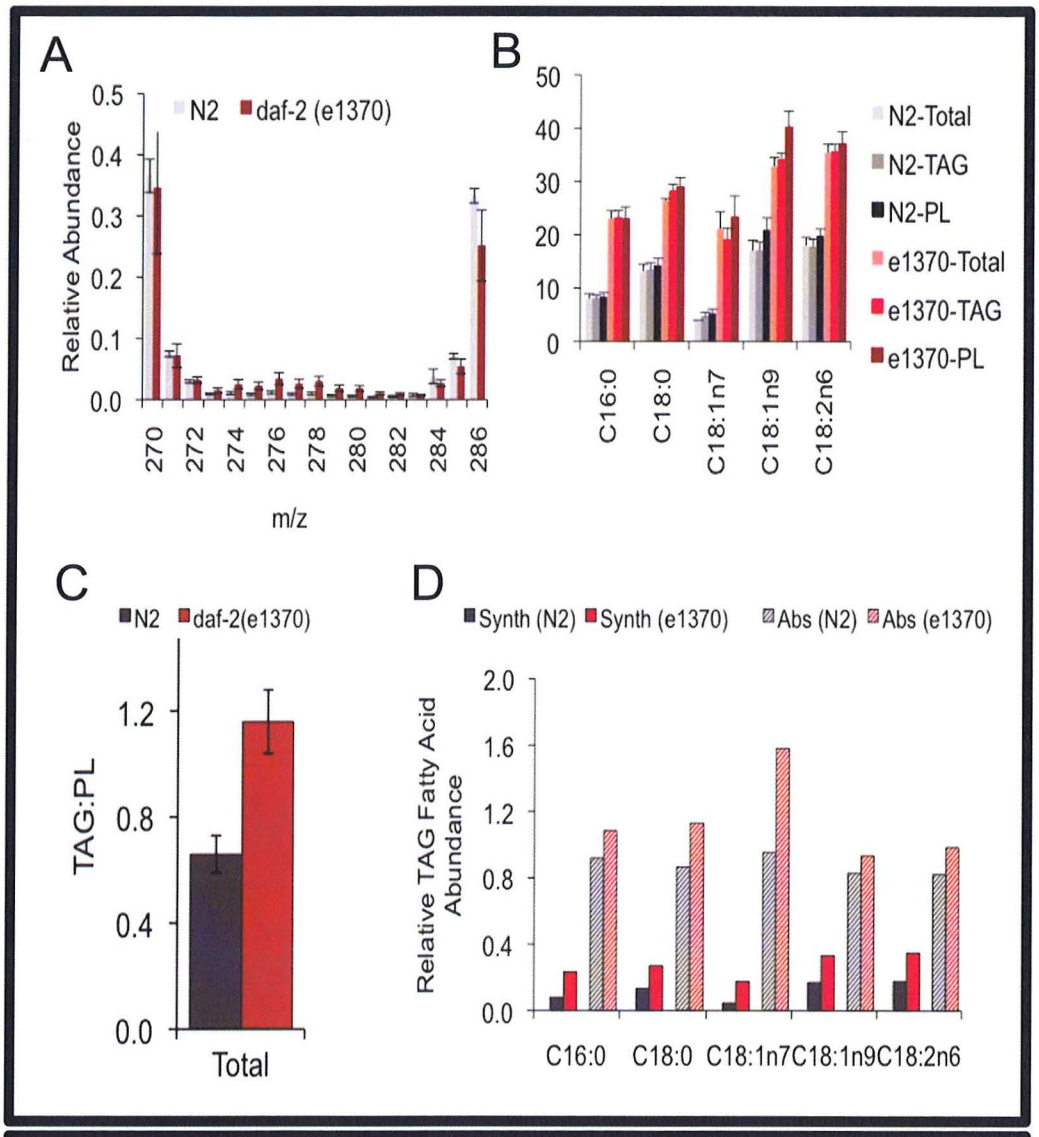

Figure 3.1. Regulation of Fatty Acid Synthesis and TAG Storage by daf-2: (A) Isotopomers exclusively associated with de novo synthesis (MW 274–280) are increased in palmitate isolated from the total lipid of the *daf-2(e1370)* animals (red), as compared to WT animals (gray). Data are the mean of five experiments ± SD. (B) The percentage of fatty acids derived from *de novo* synthesis in phospholipid (PL), TAG (triacylglyceride), and total lipid is shown for WT (N2) and *daf-2(e1370)*. Data are presented as the mean of three experiments ± SEM. (C) The total amount of TAG in N2 and *daf-2(e1370)* mutants. Data are displayed as mean TAG:PL ratio ± SEM. (D) For each fatty acid, we used total TAG measurements along with fatty acid synthesis data to estimate the relative abundance of dietary (Abs) and synthesized fatty acid in the TAG of N2 and *daf-2(e1370)* animals.

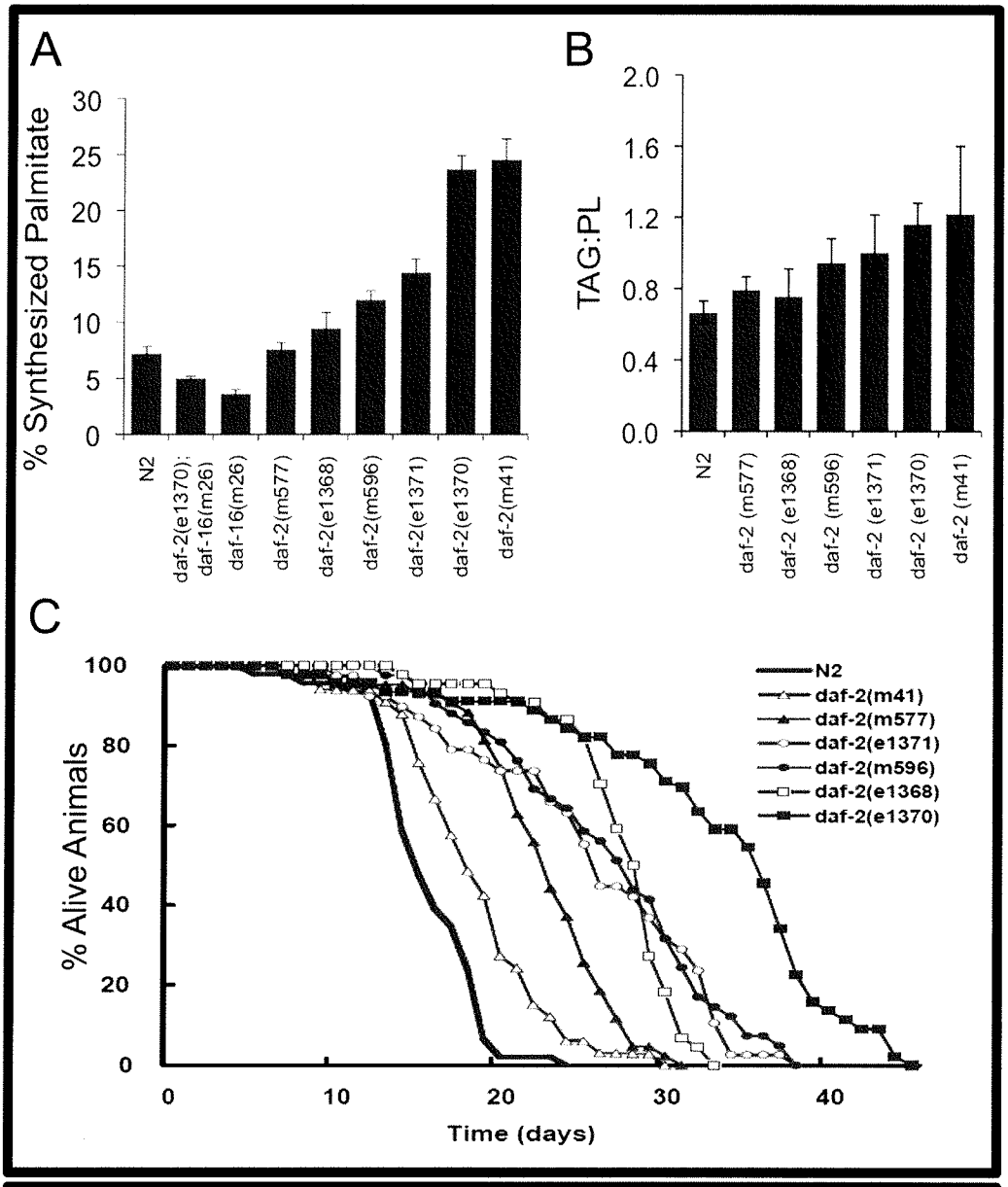

Figure 3.2. Alternative Alleles of *daf-2* Have Different Impacts on Lipogenesis: (A) The relative amount of de novo synthesis in various *daf-2* and *daf-16* mutants. Data presented here are for palmitate; however a similar pattern was observed for most other fatty acid species (data not shown). Data represent the mean of at least five experiments ± SEM. (B) TAG measurements in WT and *daf-2* mutants. Numbers shown represent the mean of at least five experiments ± SEM. (C) Lifespan analysis was performed for all mutant strains at 20°C. The mean lifespans +/- SE are: N2: 16.7±0.49; *daf-2(e1368)*: 28.4±0.6; *daf-2(e1370)*: 34.0±1.3; *daf-2(e1371)*: 26.5±1.2; *daf-2(m41)*: 19.3±0.8; *daf-2(m577)*: 23.7±0.7; and *daf-2(m596)*: 27.6±1.0.

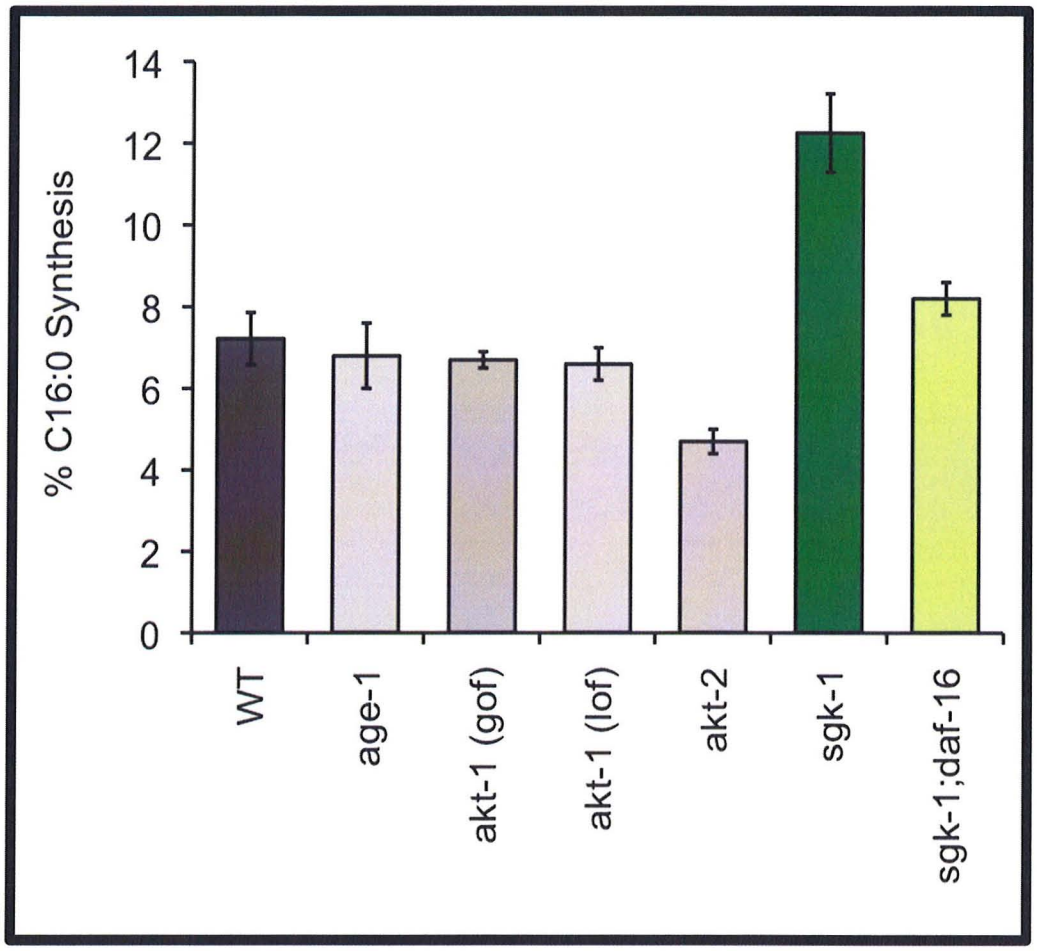

Figure 3.3. SGK-1 Regulates Fatty Acid Synthesis: (A) We quantified *de novo* fatty acid synthesis in mutants of other components of the insulin signaling pathway and found that genes that regulate lifespan (*age-1, akt-1,* and *akt-2*) did not alter the levels of lipogenesis. However, *sgk-1* animals had a 70% increase in the levels of synthesis. This increase was dependent on *daf-16* as determined by the WT synthesis levels found in *sgk-1;daf-16* double mutant.

Gene	C16:0 Synthesis
jnk-1 (lpln1)	5.0 ± 0.5
jnk-1 (lpln2)	6.9 ± 0.5
hsd-1 (mg345)	4.3 ± 0.4
eak-7 (mg338)	5.7 ± 0.4
N2	5.5 ± 1.0

Table 3.1. Palmitate Syntheis in JNK and EAK Pathway Mutants: JNK-1 overexpression lines (lpln1 and lpln2) and mutants in components of the EAK pathway (*hsd-1* and *eak-7*) had wild-type levels of C16:0 synthesis. Data from a minimum of 3 experiments with SEM shown.

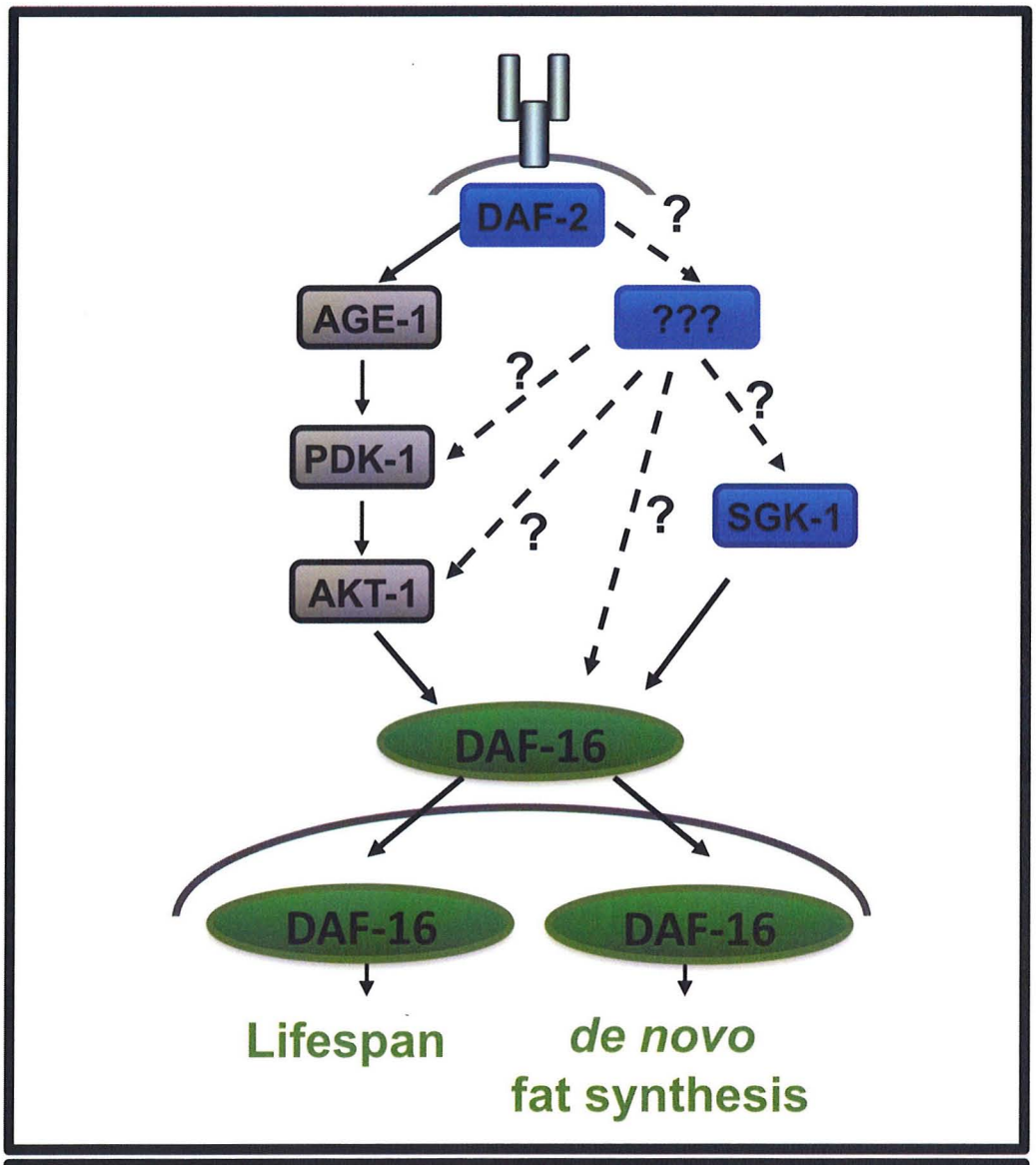

Figure 3.4. Model for the Distinct Regulation of Lifespan and Lipogenesis by DAF-2: Mutants in the insulin pathway that result in high synthesis (blue), wild-type synthesis (grey) and reduced synthesis (green) are shown with unidentified relationships shown with broken lines. Further genetic epistasis analysis will be necessary to complete the pathways that impact lipogenesis.

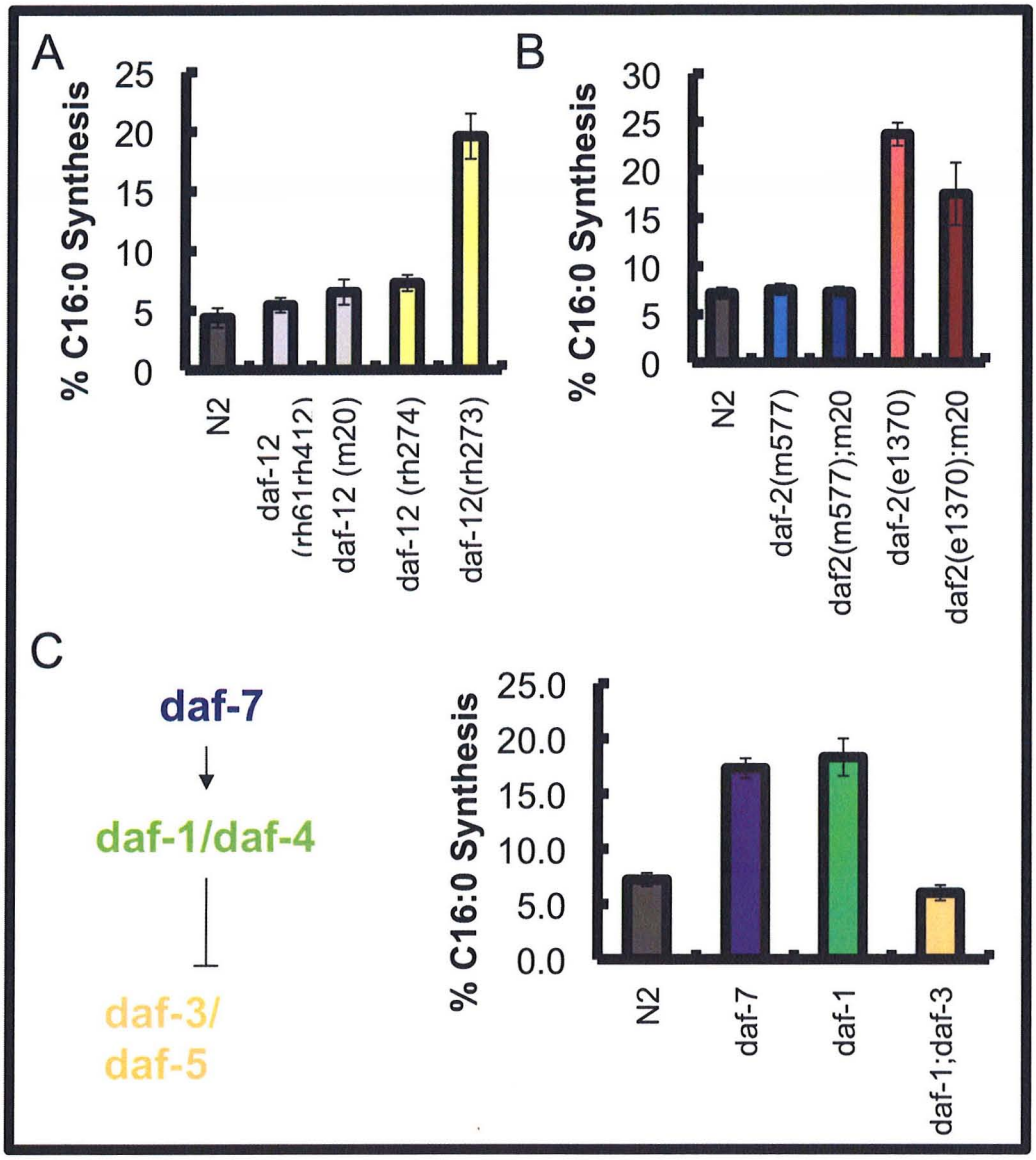

Figure 3.5. Regulation of Fatty Acid Synthesis By DAF-12 and DAF-3: (A) Palmitate synthesis was quantified in a series of *daf-12* alleles with dauer-defective alleles shown in grey and dauer-constitutive alleles shown in yellow. (B) Next, we identified an interaction between the DAF-2 and DAF-12 pathways by measuring synthesis in *daf-2;daf-12* double mutants. (C) Finally, we found synthesis is also regulated by the TGF-β pathway. All synthesis measurements are from a minimum of 4 experiments with SEM shown.

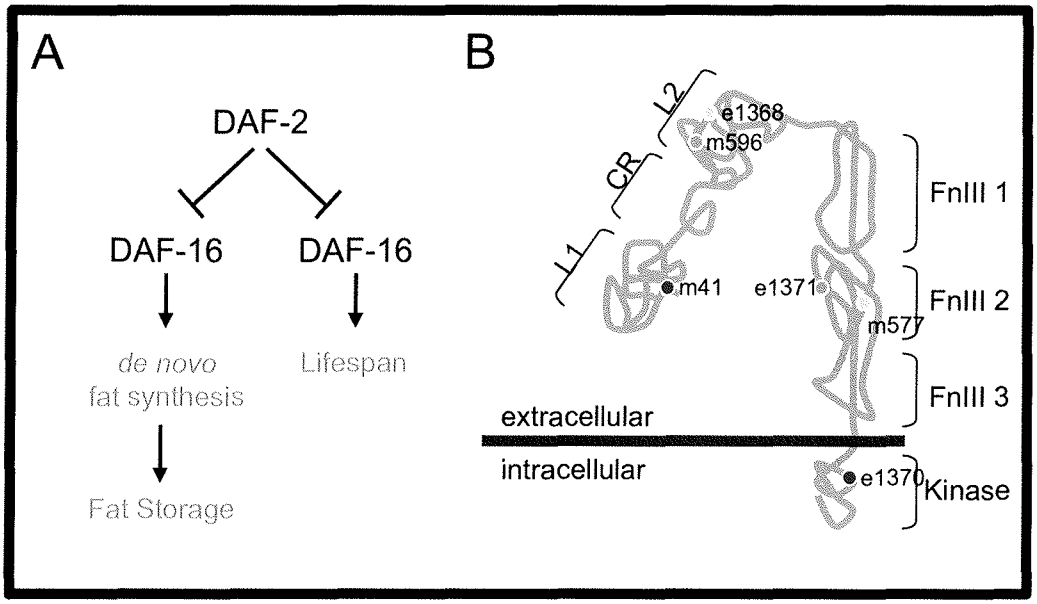

Figure 3.6. Insulin Signaling Mutants Differentially Impact Lipogenesis: (A) Our findings demonstrate that insulin signaling suppresses *de novo* synthesis by inhibiting the lipogenic function of DAF-16/FoxO. Some alleles of *daf-2* increase *de novo* lipogenesis and enhance longevity, whereas other *daf-2* alleles lead to *daf-16*-dependent longevity but do not cause stimulation of *de novo* synthesis. Thus, site-specific mutations in the insulin receptor gene can differentially affect longevity and lipogenesis, implying that the downstream mechanisms utilized to generate these physiological outcomes are, at least partially, distinct. (B) The predicted locations of the *daf-2* alleles used in this study are displayed on a structural diagram of the insulin receptor. The cartoon is based on alignment of the DAF-2 protein with the human insulin receptor (Patel et al., 2008).

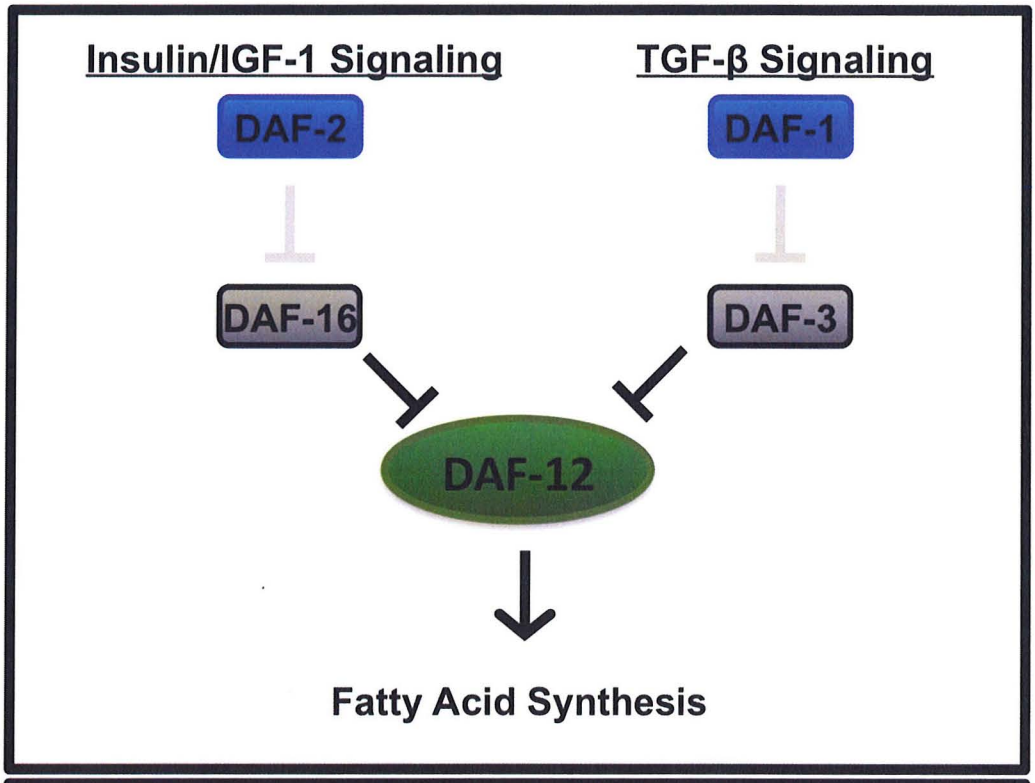

Figure 3.7. Model for Integration of Nutrient Sensing Pathways and Lipogenesis: In favorable environments with plentiful food, both insulin and TGF-β signaling will be on resulting in the suppression of the downstream transcription factors (DAF-16 and DAF-3, respectively). This will result in the promotion of reproductive development by the DAF-12 nuclear receptor and low levels on synthesis. However, in an unfavorable environment, both signaling pathways will be off, resulting in the promotion of increased *de novo* synthesis by DAF-12.

CHAPTER IV: The Impact of *de novo* Fatty Acid Synthesis on Reproduction and Longevity

Summary

An animal must be able to process its diet and allocate the resources appropriately to a number of distinct physiological fates. The partitioning of dietary molecules must be modified as the animal encounters different environmental conditions and metabolic needs, and the ability of an organism to utilize its resources efficiently may have dramatic impacts on growth, homeostasis, reproduction and aging. Because reproduction requires a large amount of resources, a metabolic shift may be an important component for successful progeny production and continued somatic maintenance. We have used a "mixed isotope" labeling strategy in *C. elegans* to define the changes in fat metabolism in reproductive adult animals. This isotope analysis has revealed that, at the onset of adulthood, the relative amount of *de novo* fatty acid synthesis almost doubles indicating a significant change in how the diet is processed. Fatty acid quantification also established that there is an increase in the abundance of monomethyl branched chain fatty acids (mmBCFAs), fat species essential for development, at this time as well. Further analysis has demonstrated that this increase in synthesis correlates with the reproductive period but is not involved in germ cell production or in germline migration. Direct analysis of the embryos themselves found that there is an enrichment of synthesized fatty acids in the triglycerides of the embryo indicating that *de novo* lipogenesis at this time may be important for supplying fatty acids to the developing oocytes. Because of the increase in *de novo* fatty acid synthesis in adults, we also examined the requirement of the *fatty acid synthase (fasn-1)* gene in survival. In doing so, we found that *fasn-1* RNAi results in a reduction in the adult lifespan indicating an important function for lipogenesis in the adult. Taken together, we have established a model that the lipogenic transition in reproductive adults is important for: (1) the generation of mmBCFAs for embryos, (2) provision of fatty acids for TAG synthesis in the germline, and (3) somatic maintenance under the increased demands of reproduction.

Introduction

Reproduction is an energetically costly process, and, in fact, in *C. elegans,* there are many more mitotic divisions required for the production of a full brood than are needed for the growth and development to adult. The large amount of resources needed to produce

progeny may limit the availability of ATP and substrates for other physiological processes. In fact, there have been many studies that have suggested a tradeoff between reproduction and lifespan. Conditions that increase lifespan like dietary restriction, which has been found to extend lifespan in both nematodes and mammals, often result in a decline in fecundity (Flatt, 2009). Additionally, many mutations that result in lifespan extension are also associated with a reduction in reproduction. For example, strong mutations in the insulin/IGF-1 pathway result in a dramatic lifespan extension, but these animals also have a delayed onset of reproduction and reduced brood size (Kenyon, 2010). However, the extension of lifespan is not always at the cost of fecundity, as weaker mutations in the same insulin/IGF-1 pathway also result in longevity phenotypes without any detriment in brood production (Kenyon, 2010). In addition to the correlative relationships between lifespan and fecundity, studies have also found that the reproductive tissues themselves can impact the lifespan of the organism. In *C. elegans,* it has been established that the germline precursor cells and the somatic gonad can play a substantial role in the regulation of lifespan (Arantes-Oliveira et al., 2002; Yamawaki et al., 2010). The relationship between lifespan and reproduction may be explained by differences in the ability to allocate resources to the proper fates.

In fact, there have been a number of indications that the germline can impact lifespan by driving changes in fat metabolism. First, the nuclear hormone receptor, DAF-12, and the FoxO transcription factor, DAF-16, are required for the longevity associated with the loss of germ cells (Yamawaki et al., 2010). Because both of these signaling pathways have been implicated as key regulators of fat metabolism, it is possible that the lifespan extension may be due to their ability to partition nutrients to the germline. We have characterized both DAF-12 and DAF-16 as regulators of *de novo* fatty acid synthesis in larval animals; however, the role of these factors in regulating lipogenesis during reproduction has not been investigated (Chapter III and (Perez et al., 2008)). Additionally, recent studies have found that a lipase is genetically linked to reproduction and aging, and it has been proposed that this lipase affects lifespan through lipid hydrolysis and fat mobilization (Wang et al., 2008). However, these connections have not been explored with direct biochemical approaches. A stable isotope approach in combination with lipid biochemistry would allow the direct monitoring of how these fats are being processed and mobilized for reproduction. A further understanding of how fat metabolism is connected to reproduction may provide key insights into the regulation of aging.

In recent years, a relationship between reproduction, metabolism and aging has started to emerge; however, a clear understanding of these relationships has not been established. The remaining questions have been left unanswered, at least in part, due to the difficulty in directly studying the impacts of metabolism. In particular, the regulation of fat storage by reproduction has been difficult to thoroughly understand, as the tools for monitoring fat storage have yielded varied results. For example, utilization of lipophilic dyes like Nile Red and Sudan Black have found decreased fat storage in germline minus animals (Wang et al., 2008). However, biochemical methods for measuring fat storage have found the same animals have elevated triglyceride to phospholipid ratios indicating higher amounts of fat stores (O'Rourke et al., 2009). We have established a "mixed isotope" labeling strategy that allows us to determine how dietary nutrients are utilized. The advantage of this mixed isotope labeling strategy is that we can directly monitor changes in fatty acid metabolism, and, here, we have implemented this labeling scheme to quantify differences in the fatty acid metabolism of reproductive animals.

Lipogenic Shift Between Larval and Adult Animals

In previous work, we developed stable isotope labeling technology in *C. elegans* that allows us to trace dietary carbons into the fats of the animal. This strategy allows us to accurately quantify the relative abundance of *de novo* synthesized fatty acids and fatty acids absorbed directly from the diet (Perez et al., 2008). We have used this mixed isotope strategy to characterize how L4 nematodes process their diet. However, because these developing animals may allocate nutrients differently than adults, we next wanted to assess how reproductively competent adult animals utilize the same dietary resources. In order to monitor the allocation of dietary nutrients in adults, we utilized the same stable isotope labeling approach to quantify the flux of dietary carbon into the lipids of the adult nematodes. In doing so, we found that there is a dramatic shift in the way the animals process their diet between larvae and adult. In L4 animals, the majority of palmitate (C16:0) is obtained directly from the diet with only 7% coming from *de novo* fatty acid synthesis. However, just 24 hours later, there is an 81% increase in the relative amount of palmitate derived from synthesis (Figure 4.1).

One of the key advantages of this mixed labeling strategy is that we can examine the contribution of fatty acid synthesis to other fatty acid species. This ability allows us to ascertain whether *de novo* synthesis is contributing specifically to the formation of any

particular fatty acid species. Additionally, because elongation and desaturation of palmitate requires additional enzymes, we can detect perturbations in these fatty acid modification pathways concurrently. We found increased fatty acid synthesis in all other fatty acid species measured including stearate (C18:0) and linoleate (C18:2n6) with an 82% and 98% increase in the relative contribution of synthesis, respectively (Figure 4.1). The elevated synthesis observed in these fatty acid species may demonstrate a coordinated upregulation in fatty acid synthesis enzymes and the fatty acid elongation and desaturation pathways. However, when we quantified fatty acid synthesis in the vaccenic (C18:1n7) pathway, we did not see an increase in synthesized fatty acids, indicating that there is not a global upregulation of synthesis activity. These results suggest a regulated increase in fatty acid synthesis and processing in adult animals that has not been recognized as of yet.

Given the timing of the increase in fatty acid synthesis, we wanted to test whether the production of embryos drives the lipogenic increase. Therefore, we tested whether the elevated synthesis is seen only at the onset of adulthood or whether it is a persistent feature of adult metabolism. To do this, we grew wild-type N2 animals on mixed isotope growth plates as far as possible (until day 3 of adulthood when the number of progeny make interpretation difficult), collecting a population of animals on each day of adulthood. We found that the relative contribution of *de novo* fatty acid synthesis increases in the first three days of adulthood (Figure 4.2). Although the largest change in palmitate synthesis is seen between L4 and adult (1.8-fold), the relative amount of palmitate synthesis continues to rise between day 1 and day 2 of adulthood (1.6-fold). Then, the rates begin to level out with the change between day 2 and day 3 being only 1.1-fold. Together, the total increase in fatty acid synthesis is quite dramatic over the first days of adulthood with about a 3-fold increase in the amount of synthesis in C16:0, C18:0, and C18:2n6. In fact, the rates of *de* novo synthesis are among the highest that have been observed in the nematode thus far. Moreover, the rates of fatty acid synthesis are continuing to increase when the majority of progeny are produced, suggesting a potential connection between fatty acid synthesis and reproduction.

Rates of Fatty Acid Synthesis Over the Reproductive Period

Because the wild-type N2 adults are continuously laying fertilized eggs, we wanted to eliminate any possible impact of the hatched progeny's metabolism. Therefore, we utilized the *fem-1;fer-15* temperature sensitive sterile strain which has defects in both

masculinization of the germline and spermiogenesis. The *fem-1;fer-15* animals are therefore sterile at 25°C but have otherwise normal female germline and produce unfertilized embryos. The increase in fatty acid synthesis is intact in the *fem-1;fer-15* animals suggesting that the lipogenic shift is a product of the metabolism of the adult animals and not the developing F1 larvae that have hatched on the plates (Figure 4.2). In fact, the contamination of progeny at day 3 adult in the N2 collections may have artificially reduced the rates of synthesis, as we see a 1.4-fold increase in the *fem-1;fer-15* animals (opposed to the 1.1-fold change seen in N2s).

We next wanted to test whether synthesis rates returned to larval levels after progeny production stopped. The implementation of the *fem-1;fer-15* strain allowed us to extend out analysis until the cessation of egg-laying. In order to quantify synthesis in the adult animals, we plated L1 animals on mixed growth plates and collected the isotope-labeled animals as far out as day 9. The relative abundance of synthesized fatty acids continues to increase during the time period when the animals are actively producing eggs (until about day 3 of adulthood at 25°C). After the fertile period (day 4), there is no significant increase in the amount of *de novo* synthesis after day 3 as seen with palmitate (C16:0) and linoleate (C18:2n6); however, the synthesis rates do not return to their baseline larval levels (Figure 4.3). We do see a reduction in the relative abundance of synthesized C16:0 and C18:2n6 at day 9 to 23% and 30%, respectively; moreover, these numbers are likely overestimates as the feeding rates are also reduced in day 10 animals which would result in a relative increase in synthesis rates due to decreased fat absorption. Nevertheless, this evidence suggests that the lipogenic transition seen at adulthood is tightly connected to reproduction.

Fatty Acid Synthesis Is Not Required for the Production of Germ Cells

There are many aspects of reproduction that might require and/or benefit from a lipogenic metabolism including germ cell formation and development, provision of sufficient fats to the germline or adequate supplies of particular synthesized fatty acid species. It has been established that the main fatty acid synthesis enzymes, *fatty acid synthase (fasn-1)* and *acetyl-CoA carboxylase (pod-2)* are essential for embryonic viability. When either enzyme is depleted by RNAi in the mother, this deficiency leads to embryonic lethality due to a failure in proper polarization of the embryo (Rappleye et al., 2003). Additionally, RNAi of *fasn-1* at L1 leads to permanent L1 arrest and lethality establishing a role for *fasn-1* in larval development as well as in embryonic development. However, there has not been an

established role for *fasn-1* in a reproductive adult. Because of the timing of the lipogenic transition, we theorized that *de novo* synthesis might be important for the formation of germ cells. We tested the impact of *de novo* fatty acid synthesis on germ cell development by treating larval animals with *fasn-1* RNAi. This treatment was initiated after 24 hours of development on control bacteria (L4440) to bypass the larval arrest phenotype. To determine if a full complement of germ cells developed, the number of produced embryos was then counted. We found that, although none of the embryos developed as expected, there was no deficiency in the number of embryos produced, demonstrating that fat synthesis is not required for germ cell production (Figure 4.4).

Additionally, we looked at germline progression by DIC microscopy and did not see any defect in germline migration in animals treated with *fasn-1* RNAi using the same RNAi feeding scheme described above (Figure 4.5). Because of the necessity to bypass the larval arrest, we could not test if there is a requirement for *fasn-1* earlier in germline development. However, because germ cell formation continues into early adult stages, we believe this is evidence that *fasn-1* does not play a role in germline migration and germ cell formation.

The Lipogenic Transition Contributes to the Production of mmBCFAs

We next explored whether fatty acid synthesis was elevated to produced sufficient quantities of a particular fatty acids species. To determine if the abundance of these fatty acids increases during this period, we quantified the relative abundance of fatty acids in L4 and day 1 adults. Between L4 and adult, we did not see a significant enrichment in *de novo* synthesis in any particular fatty acid species (Figure 4.1). Also, there is little change in the relative levels of straight chain fatty acids between L4 and adult (Figure 4.6A). However, there are several types of fatty acids where synthesis rates can not be ascertained directly by our detection methods or labeling strategy including the C20 polyunsaturated fatty acids (PUFAs) and monomethyl branched chain fats (mmBCFAs). We were particularly interested in the mmBCFAs, C15ISO and C17ISO, as they have been found to be essential for larval development (Kniazeva et al., 2004). Because the mmBCFAs are not found in the diet and are fully *de novo* synthesized, we hypothesized that the increase in fatty acid synthesis may function to provide the progeny with appropriate levels of mmBCFAs. The mmBCFAs are synthesized by the same fatty acid synthase enzyme that produces straight chain fatty acids, but their synthesis is initiated by a branched chain primer instead of malonyl-CoA. We

did find an increase in the relative abundance of C17ISO between L4 and adults animals (Figure 4.6A). When we analyzed the fatty acid composition of the embryos themselves, we found a slight but significant enrichment in the mmBCFAs in both TAG and PL (Figure 4.6B and 4.6C). Interestingly, we also detected a decrease in the relative abundance of C16:0 (Figure 4.6A). Because the precursor for mmBCFAs is formed by the same fatty acid synthase enzyme that produces C16:0, we believe that this may indicate a bias in the elongation of branched chain primers which generate mmBCFAs by FASN-1. We are currently testing the importance of mmBCFA synthesis by quantifying the mmBCFA abundance in *fasn-1* RNAi embryos.

The C13ISO generated by FASN-1 requires the activity of elongases (*elo-5* and *elo-6)* to produce full length C15ISO and C17ISO fatty acids. When adult animals are treated with *elo-5* RNAi, there is no larval arrest in their progeny, and, in fact, these F1 animals continue to develop into adults which allows us to learn more about the function of mmBCFAs in germline formation (Kniazeva et al., 2004). Eventually, after the fertilization of very few oocytes (~1-10), there is a defect in oogenesis and a progressive degeneration of the gonad (Kniazeva et al., 2004). Because we do not see defective oogenesis in adult animals treated with *fasn-1* RNAi (Figure 4.4), we believe that mmBCFA formation is not the primary driver of lipogenesis during reproduction. However, we do see deterioration of the adult germline in *fasn-1* treated animals in preliminary experiments suggesting that mmBCFA deficiency may contribute to the overall status of the gonad (data not shown).

Synthesized Fatty Acids Are Distributed Equally to TAG and PL Populations

Because the production of oocytes requires formation of new membranes, we hypothesized that the increase in fatty acid synthesis may be important for the formation of adequate PL pools. Alternatively, it is also possible that *de novo* synthesized fatty acids would be funneled into TAG synthesis to provide the embryo with sufficient long term energy reserves. To assay the contribution of fatty acid synthesis to different lipid classes, we grew animals on mixed isotope labeled food until L4 and adult and then purified neutral lipids (TAG) and phospholipid (PL) populations. This analysis clearly demonstrated that the relative contribution of synthesis is equal for each fatty acid species regardless of whether the fatty acid was associated with TAG or PL (Figure 4.7). For example, the amount of synthesized palmitate is about 7% in both TAG and PL at L4, and there is an equivalent increase in both lipid classes with synthesis contributing to about 13% of palmitate in TAG

and PL of adults. This data suggest that the increase in *de novo* synthesis contributes to the overall pool of fatty acids and is not biased to any particular lipid species.

A Functional Germline Is Not Required for Upregulation of Synthesis

It has been established that signals from the germline can have a dramatic impact on the metabolism of the whole animal. We hypothesized that the status of the gonad may impact the overall rates of *de novo* synthesis. Therefore, we wanted to assess if the developing germline was required for the increase in *de novo* synthesis observed in the reproductive adult. To do this, we utilized the temperature sensitive sterile strain, *glp-1(e2141)* that is required for the mitotic proliferation of germ cells. Therefore, at 25°C, the *glp-1* animals do not form a reproductive germline and have very few germ cells. The *glp-1* animals have wild-type levels of fatty acid synthesis at L4; therefore, we used them to test whether oocyte production is required to stimulate the increase in synthesis seen at adulthood. We found that the *glp-1* animals had increased synthesis at day 1 of adulthood comparable to rates measured in N2 and *fem-1;fer-15* sterile animals (Figure 4.8). We also found that the relative abundance of mmBCFAs increase in the *glp-1* animals between L4 and adult suggesting that mmBCFA formation is not regulated by the reproductive germline either (data not shown). These results demonstrates that the lipogenic shift is intact in germline-minus animals suggesting that the upregulation of the *de novo* fatty acid synthesis pathway is independent of the germline.

In wild-type animals, there is a large amount of cell division and growth occurring in the germline which may suggest that the increases in *de novo* fatty acid synthesis is a result of the increased activity in the gonad. However, the fact that germline minus animals have increased levels of fatty acid synthesis and higher abundance of mmBCFAs as adults demonstrates conclusively that the increased synthesis seen at this time is not occurring specifically in the gonad.

The Synthesized Fatty Acids Are Preferentially Funneled to the Germline

Because of the high metabolic demands of reproduction, we thought that the increase in synthesis might be required to provide the germline with sufficient quantities of fatty acids. We have established that the fatty acids do not contribute preferentially to TAG or PL synthesis in the animal, and next, we wanted to test whether the synthesized fatty acids themselves could be shuttled preferentially to the germline to provide adequate fatty acids

for the membranes and fat stores of the developing oocytes. In order to test this, we compared the distribution of synthesized fats in the whole adult animal versus a population of purified embryos. We did this by growing the animals on mixed labeled bacteria and retaining a sample for whole animal collection, while hypochlorite treating the remaining population of animals to obtain a population of intact eggs. We then extracted total lipid and separated the fats into phospholipid (PL) and triglyceride (TAG). In the analysis of the PL populations, we did not see any significant change in the distribution of synthesized and absorbed fatty acid (Figure 4.9A). This suggested that the synthesized fatty acids are not preferentially funneled into the membranes of the germline.

However, when we quantified synthesis in the TAG associated fatty acids in the embryo, we found a slight but significant difference in the distribution of synthesized fats (Figure 4.9B). In fact, we believe that this analysis underestimates the contribution of lipogenesis to TAG synthesis because we used a fertile strain for this analysis. Therefore, the adults also contain embryos, which would lead to an underestimation of the contribution of synthesis to embryo TAG. Taken together, we propose a model where *de novo* synthesis is increased in the somatic tissues of the animal to provide extra fatty acids for the gonad. Because free fatty acids are transported to the germline, the enrichment of synthesized fatty acids in the TAG would suggest that TAG synthesis is occurring at a faster rate than PL synthesis. To support this idea, we assessed the lipid composition of the embryos and found that they are largely composed of triglyceride with a TAG:PL ratio of 1.3 as opposed to the TAG:PL ratio of 0.5 seen in adults (Figure 4.10).

The Excess Synthesized Fatty Acids May Be Important for Lifespan

Although we believe that *de novo* synthesized fatty acids are funneled preferentially to the germline, the relative enrichment is relatively low, suggesting that increased synthesis may play another role in the adult. In *C. elegans*, the energetic requirements of reproduction are quite high with large amounts of cell division and growth occurring in the germline compared to the somatic tissues. Because of the demands of reproduction, we hypothesized that the lipogenic shift seen in reproductive adults may also function as a compensatory mechanism to allow for sufficient fats to be contributed to the maintenance of the somatic tissues. To test this hypothesis, we decided to assay the lifespan of animals treated with *fasn-1* RNAi. Again, the RNAi treatment was initiated 24 hours into development. We found that N2 animals treated with *fasn-1* RNAi had a reduction in their

mean lifespan of ~2 days, suggesting that fatty acid synthesis is required for a full lifespan (Figure 4.11A). Although the *fasn-1* RNAi treatment is initiated before the completion of gonad migration, the reduction of lifespan in the *glp-1* animals supports the hypothesis that fat synthesis may play a role in the somatic tissues.

To further test this idea, we have started a lifespan assay with animals put on *fasn-1* RNAi after they reach adulthood (after 48 hours of growth at 25°C). In this preliminary analysis, it seems that *fasn-1* RNA will result in about the same reduction in lifespan (~1.5 days) in animals where fatty acid synthesis was compromised only in adulthood. Furthermore, we also performed *fasn-1* RNAi lifespans with the *rrf-1* mutant. *rrf-1* encodes an RNA-directed RNA polymerase which is required for somatic but not germline RNAi. Therefore, using these animals, we can determine the impact of *fasn-1* on the germline alone. Thus far, our analysis shows that *fasn-1* has no impact on the lifespan of the *rrf-1* animals, further supporting the conclusion that fatty acid synthesis is required in the somatic tissues of the adult animal (Figure 4.12). Of course, further studies are needed to determine where the synthesized fatty acids themselves are used. Although we can not discount the possibility that synthesis plays another important role such as mmBCFA formation in adults, we believe this supports the model that the lipogenic transition is important in somatic maintenance.

Because the *glp-1* animals have increased synthesis without the demands of embryo production, we hypothesized that the extended lifespan of the *glp-1* animals might be a result of the extra lipids synthesized during this period. In fact, when we measure the TAG:PL of these animals, we found that they do, in fact, have excess fat storage (up to 2.5x more than controls) (Figure 4.13). Interestingly, the *glp-1* animals have wildtype levels of fat storage at L4 and D1 adult collections, suggesting that the elevated fat storage may be directly attributed to the increase in *de novo* fatty acid synthesis. Also, when the *glp-1* animals are treated with *fasn-1* RNAi, their lifespan is reduced to that of N2 on *fasn-1* RNAi. The reduction in lifespan demonstrates that *fasn-1* is required for healthy aging in the *glp-1* animals. To us, this suggests a model where the excess synthesized fatty acids may be utilized for other demands like tissue maintenance which are normally sacrificed during times of reproduction.

Discussion

There is a dramatic change in how animals process their diet during the reproductive period resulting in a significant increase in the relative abundance of *de novo* synthesized fatty acids in adult animals. Because many of the known regulators of fatty acid synthesis are associated with dauer formation pathways like insulin signaling and TGF-β pathway mutants (Greer et al., 2008), it may suggest an association such that mutations that inhibit reproductive growth result in increased lipogenesis. However, we have shown here that the demands of reproduction may require a shift in fat metabolism that results in an increase in lipogenesis. The demonstration that reproduction impacts the amount of *de novo* fatty acid synthesis in adult animals reveals a previously unknown function of lipogenesis in *C. elegans.*

In this study, we sought to determine the role for *de novo* synthesis during the reproductive period, and we found that synthesis contributes to several processes. We found that the embryos contained an increased proportion of mmBCFAs, which are essential for larval growth (Kniazeva et al., 2004). Because these fatty acids are fully synthesized, we suspected that one of the functions of the increased fatty acid synthesis is to provide the embryos with sufficient quantities of mmBCFAs. In order to test this hypothesis, fatty acid composition of embryos from mothers treated with *fasn-1* RNAi will be required. In addition to providing the germline with mmBCFAs, we found an enrichment of synthesized fatty acids specifically in the TAG of the embryo. Because the embryo contains large quantities of stored fat, we predict that the increase in synthesis is important to provide the germline with excess fatty acids. The enrichment of the synthesized fatty acids in the TAG suggests that the levels of TAG synthesis in the germline are higher than PL synthesis rates.

Although both mmBCFA synthesis and the generation of sufficient pools of fatty acids for the embryos may be important features of the lipogenic increase, these processes may not account for the total increase in *de novo* fatty acid synthesis. We have found that knockdown of *fasn-1* gene in adult animals leads to a reduction of their lifespan. Although further studies are needed to characterize the impact of *fasn-1* RNAi on the animal, we propose a model where the increased lipogenesis seen at the onset of reproduction is needed to provide enough fatty acids for somatic maintenance (Figure 4.14). We also see a reduction of the lifespan of *glp-1* animals that do not have a reproductive germline. Although the *glp-1* animals are normally long-lived, on *fasn-1* RNAi, they are as short lived

as treated N2. We believe that this reduction in longevity suggests that the increased lifespan on the *glp-1* animals is a result of the extra resources for somatic maintenance.

There have been a number of signaling mechanisms described that connect the status of the gonad to the metabolism of the whole animal. It seemed likely that a similar mechanism was regulating synthesis based on the needs of the germline. Surprisingly, we found the lipogenic increase was intact in *glp-1* animals that lack a reproductive germline, demonstrating that there is not a signaling mechanism relaying the status of the developing germ cells. We cannot yet characterize the role of signaling from the somatic germline, which has also been established as an important regulator of longevity and may report on the status of the germline. However, it has been shown that DAF-12 steroid hormone signaling plays an important role in regulation by the somatic germline. Thus, we have tested *daf-12* mutant animals for the ability to drive the synthesis increase, and, thus far, the *daf-12* alleles we have tested have the lipogenic shift. This suggests that the somatic germline may not be required for lipogenic increase, at least not through the DAF-12 pathway. In our search for regulators of this increased synthesis, we have indentified a role for *nhr-69.* In animals that overexpress this gene, there is no increase in fatty acid synthesis between L4 and adult. Interestingly, these animals have a severely compromised brood and a reduction in lifespan, giving support to our model. These results also confirm that there is regulation of this increase by genetic factors (See Appendix I).

Experimental Procedures

Strains

The strains used in these experiments were: wild-type N2 (Bristol), CF512: *fem-1(hc17);fer-15(b26)*, and CB4037: *glp-1(e2141)*. All strains were maintained at 20°C, and sterile strains were shifted to 25°C to induce sterility for the experiments.

Quantification of Fat Synthesis

Stable isotope labeling and quantification was performed as previously described ((Perez et al., 2008) and Chapter 2) except that these experiments were performed at 25°C. In order to label animals into adulthood, more bacteria was plated (0.5g/plate), and the animals were transferred to fresh plates when the food supply was low (~2 to 3 days). Because our interest was in the quantification of *de novo* synthesis and absorption, the % of synthesis calculated as: (synthesized FA/(synthesized FA + dietary FA))*100.

Lipid Extraction and Column Separations

Lipid extraction and detection was performed as described (Perez et al., 2008).

Analysis of Embryos

In order to quantify relative fatty acid synthesis, fatty acid composition and fat storage numbers, a population of purified embryos was harvested. To do this, we grew a population of nematodes to adult on mixed isotope plates (prepared as described in (Perez et al., 2008) and Chapter 2) and then hypochlorite treated the animals to harvest the eggs. Standard bleaching techniques were utilized with a 20% bleach solution.

Brood and Lifespan Analysis

To bypass the *fasn-1* RNAi induced larval arrest, synchronized L1s were transferred to L4440 control bacteria for 24 hours before being transferred to *fasn-1* RNAi bacteria for the duration of the experiment. Brood analysis was conducted by transferring the animals to fresh plates each day and counting the laid embryos (for *fasn-1* treatment) or the hatched L1s (for L4440 control treatment) after 24 hours. The same RNAi strategy was implemented for lifespan analysis. Any bagged or lost animals were not included in the totals.

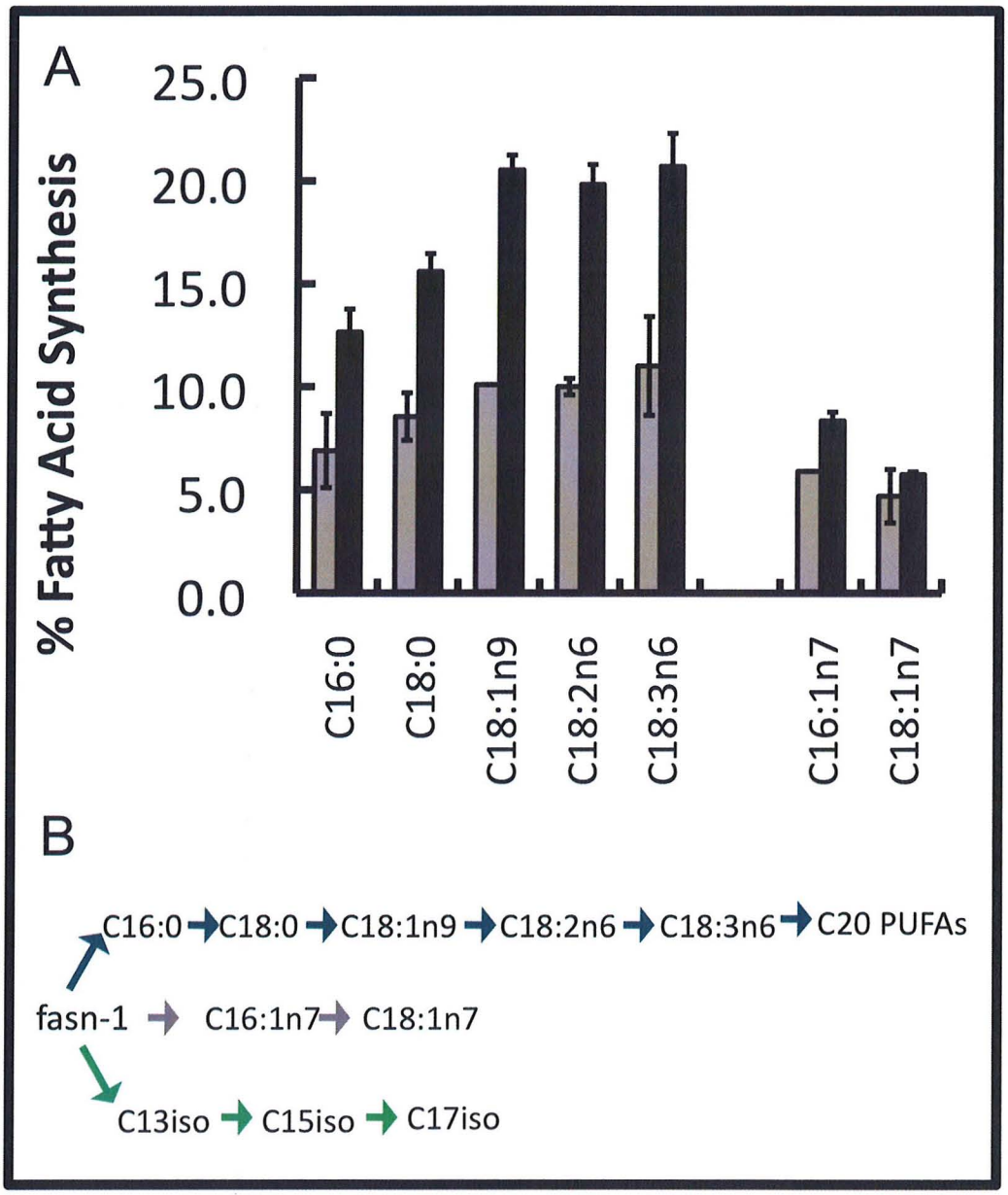

Figure 4.1. Increased Synthesis in Adult Nematodes: (A) The amount of fatty acid synthesis is almost doubled between the late L4 (grey) stage and day 1 adult (shown in black). The increase in synthesis is found in all components of the C20 PUFA pathway but not in the fatty acids of the C18:1n7 synthesis pathway. Data shown is from purified phospholipids with at least 4 experiments. SEMs are shown. (B) Schematic of the C20 PUFA, C18:1n7, and mmBCFA synthesis pathways

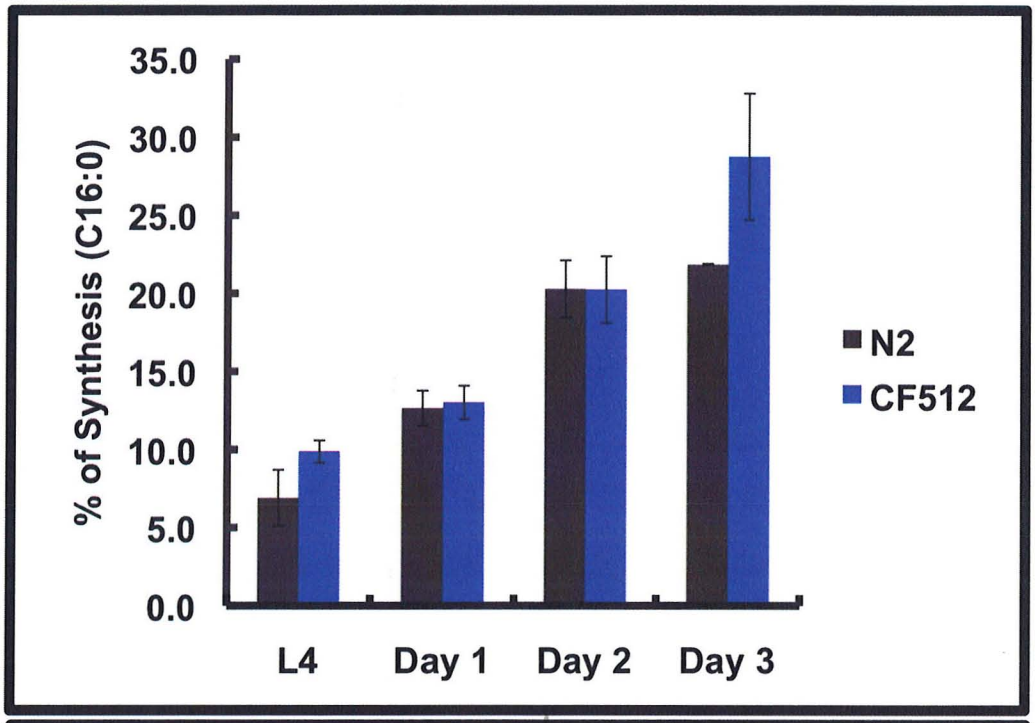

Figure 4.2. Synthesis Continues to Increase in First Days of Adulthood: Animals were grown on mixed isotope media into adulthood, and we found that the relative abundance of synthesized palmitate continues to increase while the animal is still laying eggs. Data shown is from purified phospholipids with at least 3 experiments (except for the Day 3 N2 data point which only had 2 independent collection. SEMs are shown.

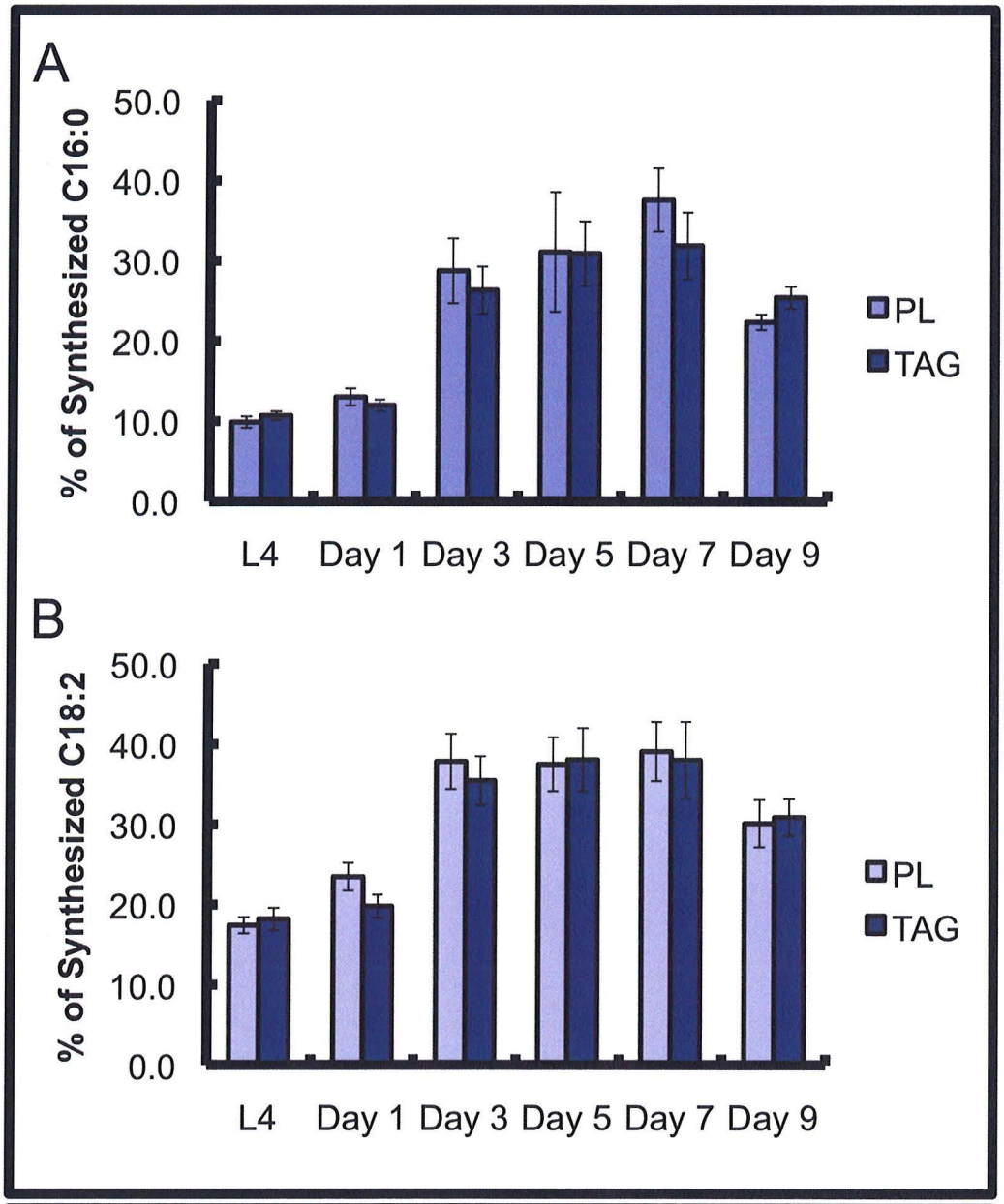

Figure 4.3. Synthesis Over Adulthood: Using *fem-1;fer-15* animals, we quantified synthesis over adulthood for C16:0 (A) and C18:2n6 (B). Data shown is for both purified phospholipids (PL) and triglycerides (TAG) with at least 3 experiments. SEMs are shown.

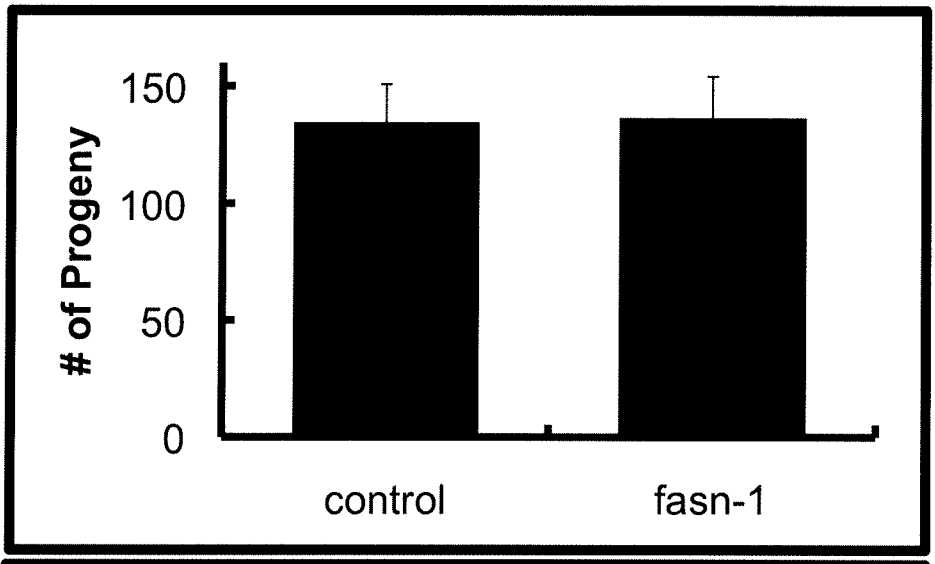

Figure 4.4. Number of Embryos Produced in *fasn-1* Treated Animals Is Normal: In order to determine if germ cell number was affected by *fasn-1* RNAi treatment, we grew larvae past the L1 arrest point (24hr) on control bacteria (L4440) and then plated them on *fasn-1* RNAi. Control animals were transferred at this point to fresh L4440 plates. The number of laid embryos was then counted. Experiments were performed at 25° and progeny from 5 animals were counted.

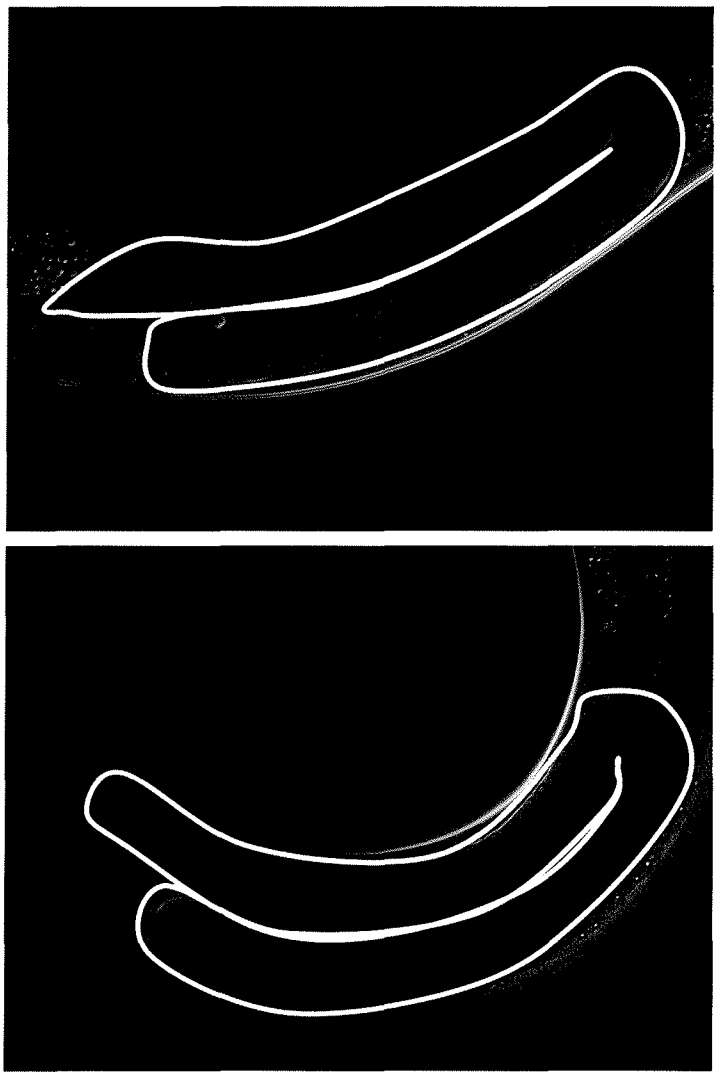

Figure 4.5 Germline Progression Is Normal With *fasn-1* Treatment: In order to determine if the gonad arms could progress normally without *fasn-1*, we switched animals to *fasn-1* after 24hr of growth at 20°C. DIC microscopy showed that gonad migration was intact in these animals. The gonad arm is outlined.

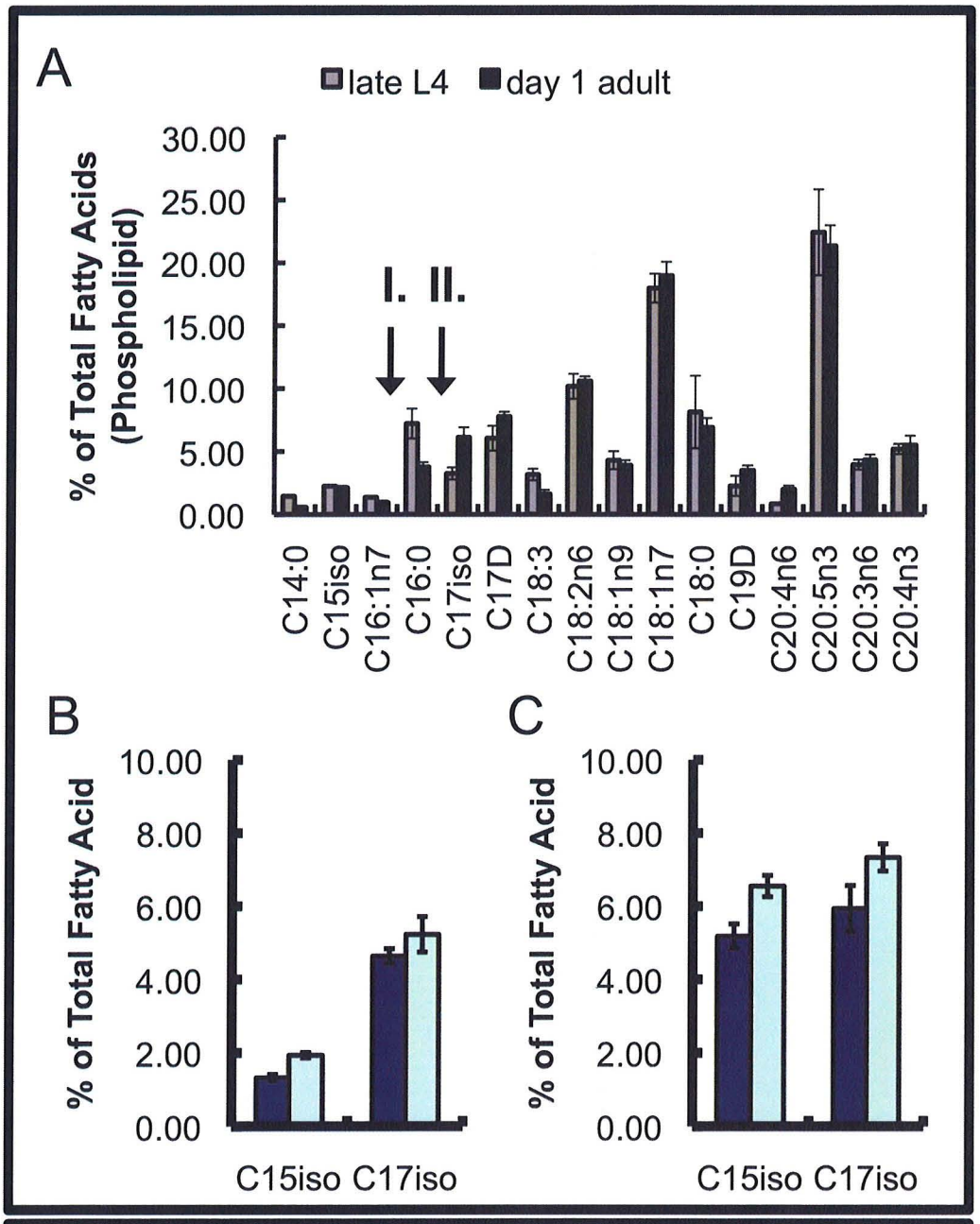

Figure 4.6. Increased mmBCFAs in Embryos: (A) Although the fatty acid composition of the animals does not change dramatically between L4 (grey) and day 1 adult (black), there are two significant changes: (I) decreased abundance of palmitate (C16:0) and (II) increase in the relative abundance of C17iso. We then measured the relative abundance of the mmBCFAs in the embryos and found a slight but significant increase in the C15ISO content in phospholipid (B) and increased abundance of both mmBCFA species in the triglyceride (C).

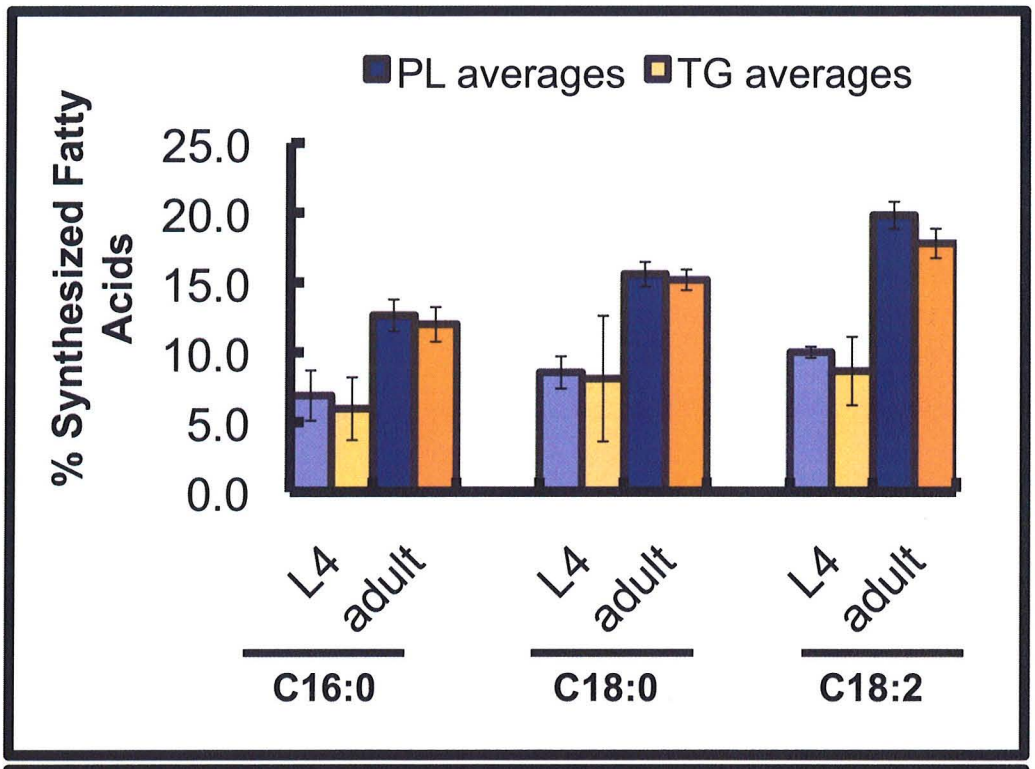

Figure 4.7. Synthesis Contributes Equally to PL and TG Formation: Relative synthesis is equal in the phospholipid (purple) and triglyceride (grey) populations of the nematode at L4 (lighter shades) and in day 1 adults (dark). Data shown is from at least 3 experiments with SEM shown.

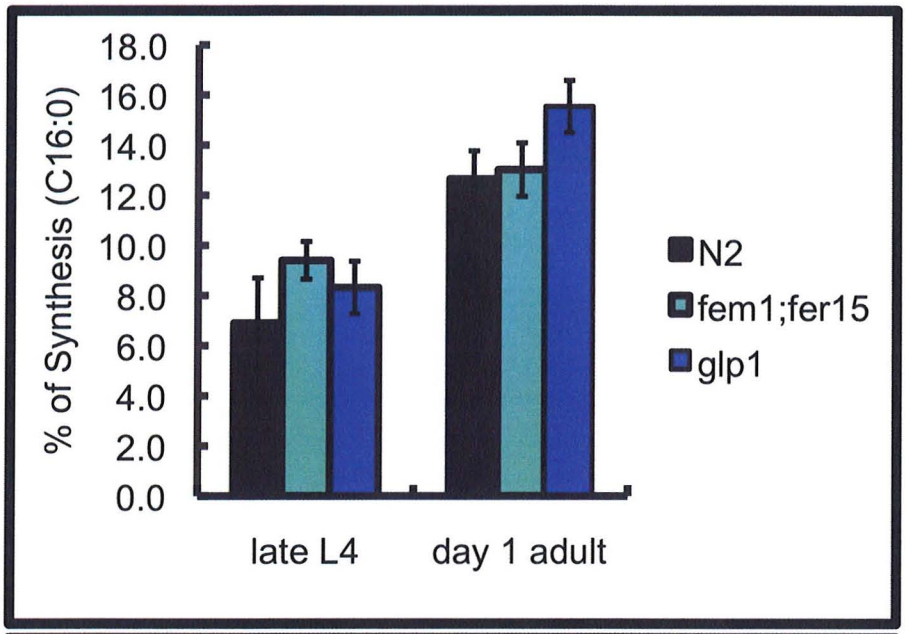

Figure 4.8: Elevated Synthesis Is Independent of Production of Functional Oocytes. The rates of palmitate synthesis in germline minus *glp-1* animals (blue) is comparable to wild-type (N2) animals (shown in black) and *fem-1; fer-15* mutants (green), indicating that the increase in lipogenesis is independent of a reproductive germline. Data shown is from a minimum of 3 experiments with SEM shown.

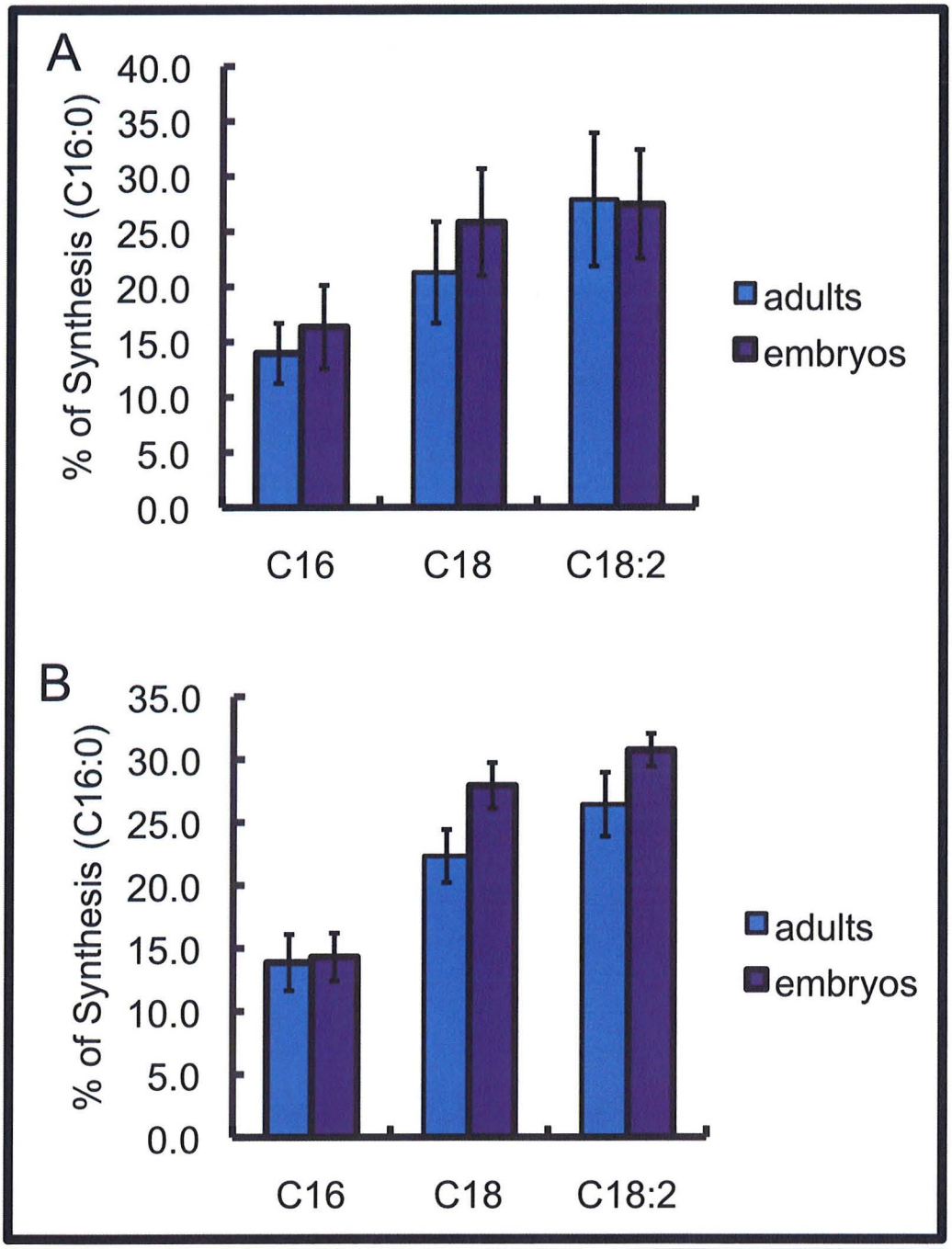

Figure 4.9: The Relative Synthesis in Embryos Is Increased in TAG. The relative amount of synthesized fatty acids is equivalent in embryos (purple) and in adults (blue) in a purified phospholipid population (A). However, there is a significant increase in the relative abundance of synthesized fatty acids in certain species in triglycerides specifically in C18:0 and C18:2n6 (B).

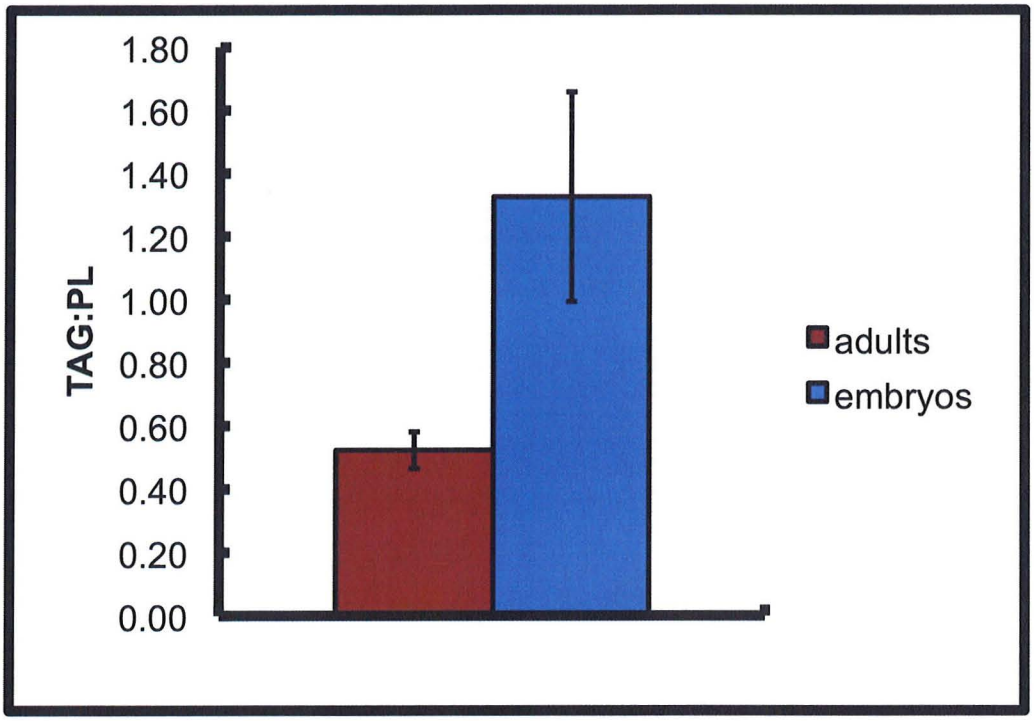

Figure 4.10. Embryos Have A High TAG:PL Ratio: To assess the relative abundance of the lipid classes, we separated lipids by column chromatography for adults (red) and bleached embryos (blue). This analysis demonstrated a significant increase in the abundance of TAG in the embryos compared to the adult population. Additionally, because the adults contain embryos, this difference is an underestimate. The method for purifying embryos is described in experimental procedures. Data shown is from a minimum of 4 experiments with SEM shown.

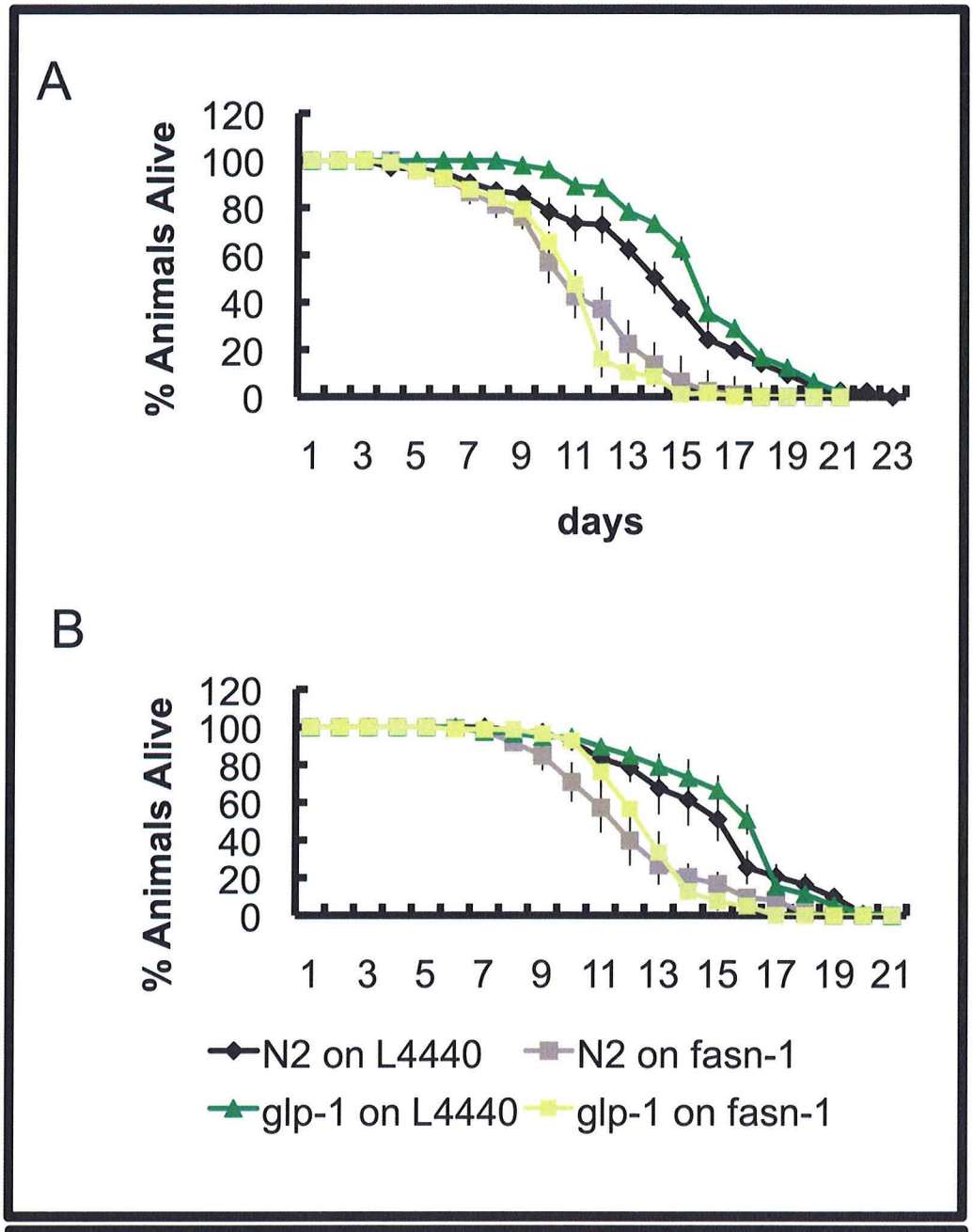

Figure 4.11. *fasn-1* Results in Reduction of Lifespan: (A) *fasn-1* RNAi treated was initiated after 24hr of larval growth. The *fasn-1* RNAi resulted in a reduction of lifespan in N2 and in *glp-1* animals. (B) Lifespan analysis of *fasn-1* RNAi was initiated after 48hr of growth. The trends seen with both 24hr and 48hr RNAi initiation appear to be the same. Curves from three replicates, each with a minimum of 25 animals. All lifespans were performed at 25°C.

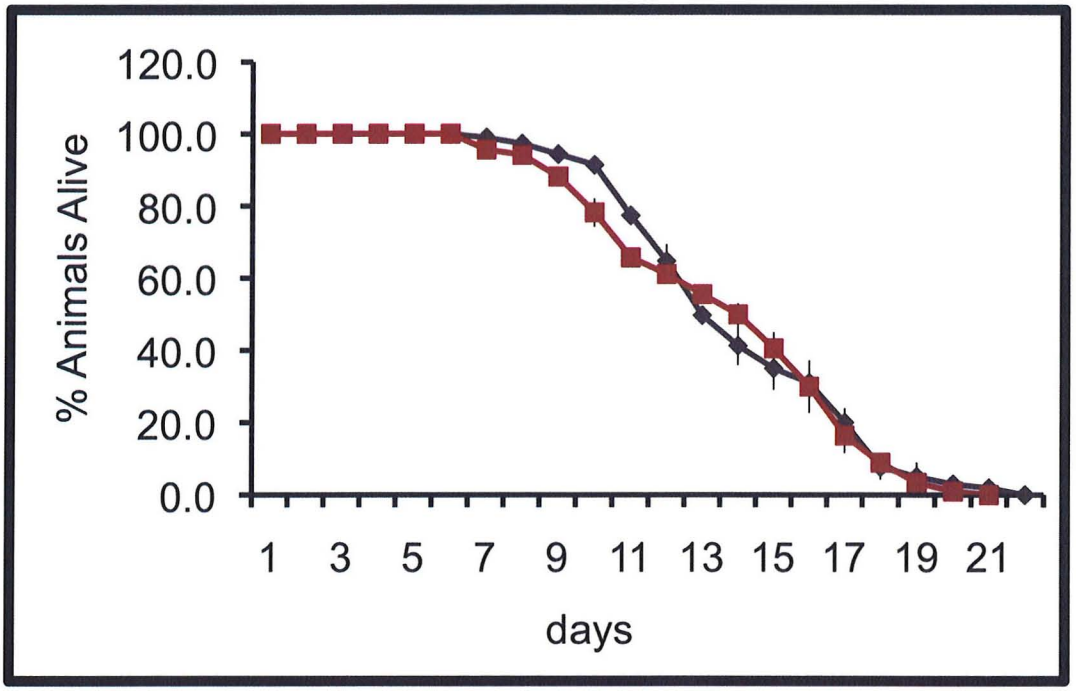

Figure 4.12. *fasn-1* in the Germline Does Not Reduce Lifespan: *fasn-1* RNAi treatment was initiated after 48hr of larval growth in *rrf-1* animals. There is no difference between the lifespan of *rrf-1* animals on control RNAi (black) or fasn-1 RNAi (red), supporting the conclusion that FASN-1 plays a role in the somatic tissues. All lifespans were performed at 25°C. Curves were generated from a minimum of two replicates with at least 25 worms in each.

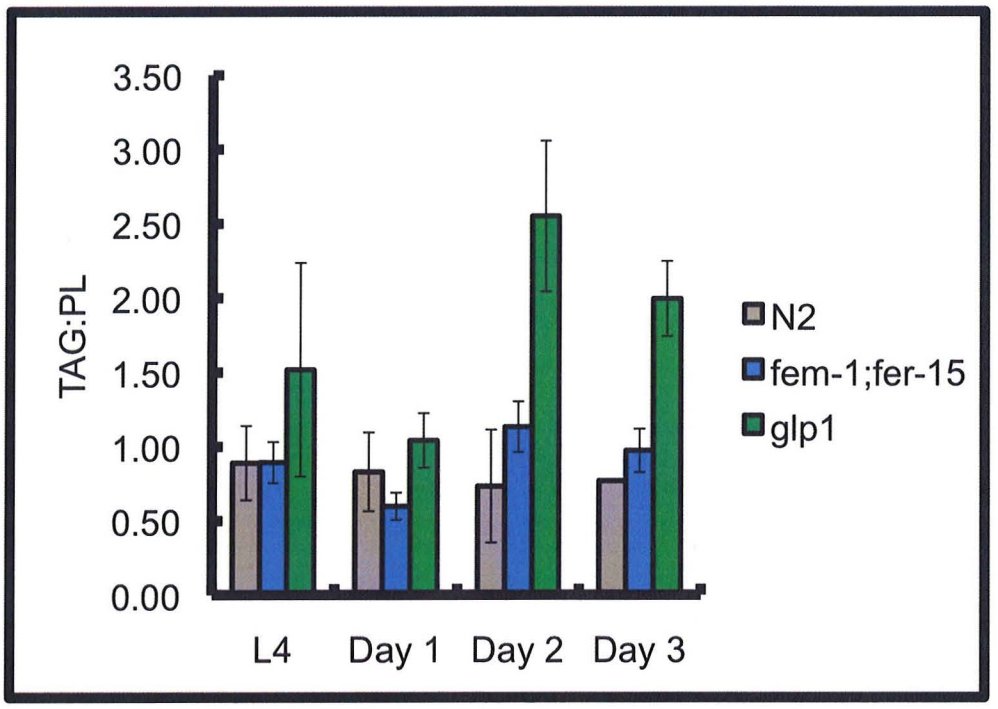

Figure 4.13. TAG Storage in Adult Animals: Sterile adults were harvested at the noted day of adulthood. Total lipids were then extracted and separated into neutral lipids (TAG) and phospholipids (PL). Internal standards were used to correct for recovery and the TAG:PL ratio was calculated for wild-type N2 (grey), *fem1;fer15* animals (blue) and *glp1* mutants (dark green). Although *glp*-1 TAG:PL ratio is relatively normal at L4 and day 1, there is a significant increased in the fat stores of these animals after day 2. Data show is from a minimum of three experiments and SEM is shown for *fem-1;fer-15* and *glp-1* animals. The data for N2 represents two experiments although those animals have been analyzed in similar experiments with the same average TAG:PL.

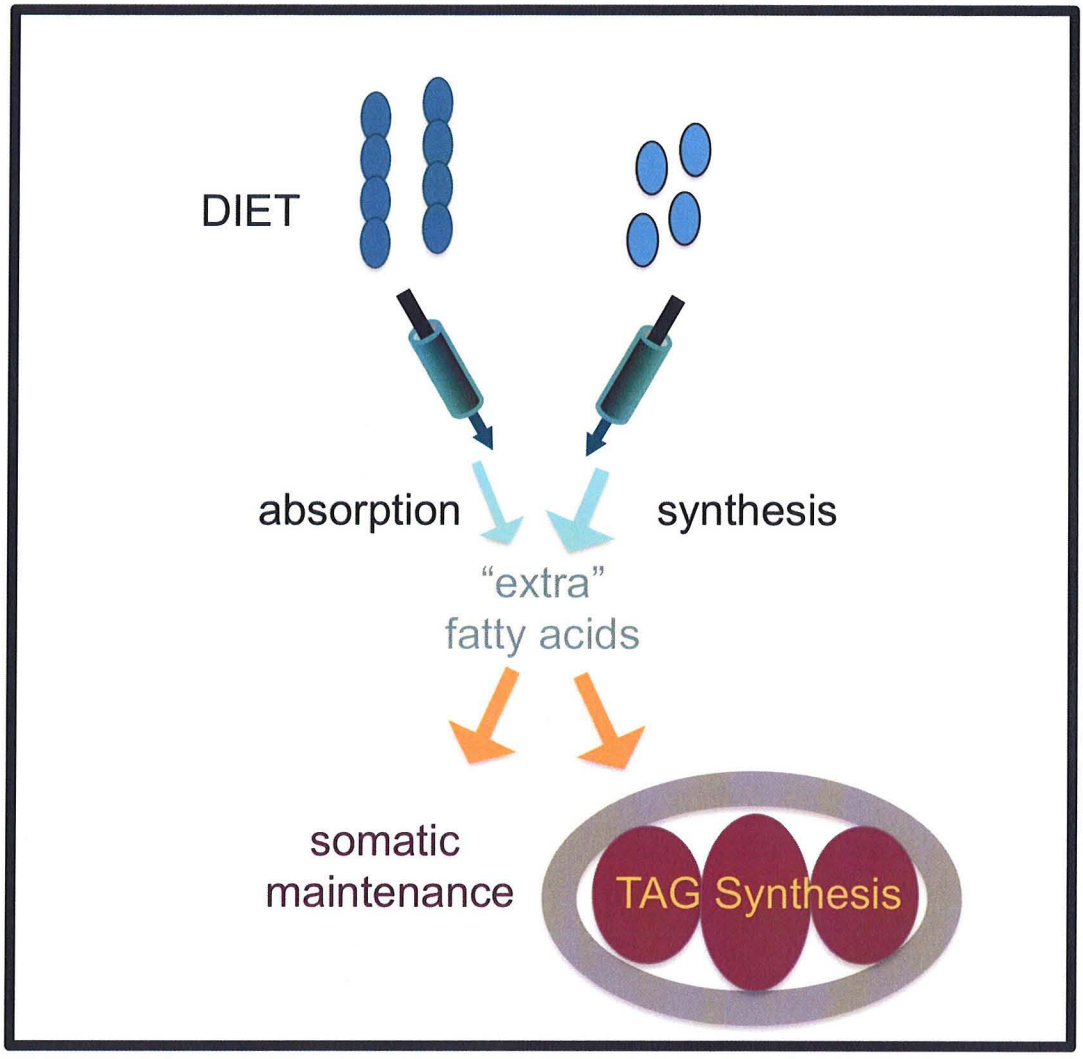

Figure 4.14. Model for Role of Fatty Acid Synthesis in Reproduction: Fatty acid synthesis is increased to generate adequate pools of fatty acids. These fatty acids are funneled to the germline where they are used primarily for TAG synthesis. Any surplus fatty acids can be used for the other functions of the animal like somatic maintenance. We predict that when fatty acid synthesis is compromised, all fatty acids are funneled to the germline, leaving few resources for somatic maintenance.

CHAPTER V: Reduced Oxidative Phosphorylation Drives Lipogenesis in *C. elegans*

Summary

In the 1920s, it was established that cancer cells have a dramatic change in their overall metabolism. Unlike normal cells, cancer cells stop utilizing fat for energy and begin to rely almost exclusively on sugar breakdown. It has been proposed that this metabolic shift results in a growth and survival advantage for the tumor. Another key feature of cancers is that this glycolytic metabolism is accompanied by a tremendous increase in *de novo* fatty acid synthesis. In the redox balance hypothesis, this elevated lipogenesis has been suggested to be a compensatory mechanism that is required for the change in primary energy sources from fat to sugar. Namely, fatty acid synthesis is elevated to restore NAD+ levels necessary to run glycolysis; however, it is not clear what drives lipogenesis in cancer cells. Here, we describe our establishment of nematodes as a model of cancer cell metabolism that will allow us to address many important yet unanswered questions about lipid metabolism in glycolytic states. Using a stable isotope based quantification method, we have found that compromised oxidative phosphorylation is a primary driver of *de novo* fatty acid synthesis. Additionally, we have quantified lipogenesis in a number of electron transport chain mutants (*clk-1, isp-1,* and *mev-1*) and have found a correlation between NAD+:NADH metabolism and increased *de novo* fatty acid synthesis. The genetic tractability of *C. elegans* has allowed us to identify the hypoxia inducible factor, HIF-1, and the transcription factor, DAF-16, as potential mediators of this lipogenic increase. We believe that the nematode will be valuable in probing the activity of different metabolic pathways using stable isotope labeling feeding approaches.

Introduction

Each cancer has a unique set of affected genes and pathways that affect its formation, progression, and metastatic potential; however, there are several unifying features that are constant in the vast majority of cancers. One of these hallmarks was first observed by Otto Warburg in the 1920s when he observed that tumors rely heavily on glycolysis for the generation of energy even in the presence of ample oxygen (Warburg et al., 1927). The reprogramming of energy metabolism to aerobic glycolysis has been observed in the vast majority of tumors tested, and, in fact, the sugar-fueled metabolism is the basis of the PET scan detection methods. The early observation of aerobic glycolysis in cancers has

withstood the test of time, and the Warburg metabolism of tumors has recently been characterized as an emerging hallmark of cancers (Hanahan et al., 2011). However, to run this type of metabolism, there are additional changes in metabolic pathways that are required.

The aerobic glycolysis of the tumor coincides with a severe reduction in the rates of oxidative phosphorylation. This decreased electron transport chain activity results in the accumulation of NADH as its electrons are no longer donated to complex I to drive the formation of a proton gradient. As the imbalance of NADH:NAD+ becomes greater, the cell must initiate pathways to regenerate NAD+ levels in order to continue to run glycolysis which is essential for their survival. One of the ways to regenerate NAD+ is through lactate production by lactate dehydrogenase activity. The lactate produced is then excreted from the cell. However, fatty acid synthesis is another way to regenerate NAD+ levels, and another key feature of tumors is that there is a switch from dietary fat incorporation to *de novo* fatty acid synthesis.

In normal cells, *de novo* fatty acid synthesis is minimal contributing only about 10% of the total fatty acids; however, in cancers, fat synthesis is the primary source of fats contributing over 90% of the total fat available (Menendez et al., 2007). Expression of the main fatty acid synthesis enzyme, fatty acid synthase (FASN) is upregulated in many cancers as demonstrated by immunohistochemistry studies (Kusakabe et al., 2002). In fact, this increase in lipogenesis is one of the most frequent alterations in cancers and has been observed in the majority of cancer types tested including prostate, breast, stomach and lung cancer (Menendez et al., 2007).

The restoration of the redox balance with fat synthesis may provide several distinct advantages to the cancer cells including elimination of the need for high levels of potentially destructive acids. Additionally, growing tumors require high levels of phospholipid synthesis and the increased synthesis of fatty acids would help to provide the fatty acids necessary for membrane synthesis. In support of this role, membrane phospholipids in cancer cells have been shown to have more synthesized fatty acids associated with them than control cells (Hilvo et al., 2011). Both high glycolytic and lipogenic activity provide the cancer with a survival advantage, and these metabolic shifts are associated with higher risk of disease reoccurrence and death (Menendez et al., 2007). In fact, the advantages of aerobic glycolysis are somewhat counterintuitive as reduced respiration also results in a decrease in the production of ATP; however, this metabolic shift may help to facilitate the rapid

generation of biomass needed in growing tumors (Vander Heiden et al., 2009). Because these processes are limited in normal cells, genes involved in the glycolytic and lipogenic transition may provide selective targets for the treatment of cancers. Because these changes are important for the survival of the tumor, disruption of either process results in cancer inhibition in mouse models and cell culture systems. However, a better understanding of the genes and pathways necessary for the metabolic changes will benefit treatment options in the future.

Although it has been established that *de novo* fatty acid synthesis is increased in the majority of cancers, the drivers of this lipogenic shift have not be elucidated. One hypothesis is that the hypoxic conditions in the tumor environment may lead to the increase in FASN expression. Adaptations to hypoxic environments are mediated by the hypoxia inducible factor, HIF-1, which activates a suite of genes and pathways needed for survival in low oxygen environments. One of HIF-1's targets is the *fasn-1* gene, which suggest that the increase in lipogenesis is an important response to low oxygen environments. However, it has also been shown that HIF-1 can activate its targets independent of oxygen availability by acidosis and reactive oxygen species (Lee et al., 2010; Menendez et al., 2007). Because signaling pathways and metabolite levels also impact lipogenesis, these factors must be considered as well.

We have established a stable isotope labeling strategy that allows us to monitor the dynamics of fatty acid metabolism (Chapter 2 and (Perez et al., 2008)). Here, we wanted to apply this method to see if we could mimic the changes seen in cancer cell metabolism. This manipulation would give us a genetically tractable system for identifying genes and metabolic pathways that are important for cancer cell metabolism. Here, we have used *C. elegans* to describe an increase in lipogenesis that mirrors cancer cells and to identify genes that impact this transition.

Decreased Oxidative Phosphorylation Drives *De Novo* Fatty Acid Synthesis

In cancers, the glycolytic state has been hypothesized to be a result of hypoxia and/or mitochondrial dysfunction. Because both of these perturbations impact oxidative phosphorylation, we wanted to determine the role of the electron transport chain on fatty acid synthesis using a mixed isotope labeling assay (described in Chapter 2). To do this, we measured the amount of synthesis in a mutant with diminished electron chain activity. The *clk-1* gene encodes a demethoxyubiquinone (DMQ) hydroxylase that is required for the

synthesis of coenzyme Q (ubiquinone) which functions to transport electrons from Complex I to Complex III in the electron transport chain (Figure 5.1). The *clk-1* animals have been shown to have a mild reduction in the rates of mitochondrial respiration along with lifespan extension and slow growth phenotypes (Braeckman et al., 2009). We grew this animals on mixed isotope labeling plates to determine rates of *de novo* fatty acid synthesis. We found a ~70% increase in palmitate synthesis and a ~80% increase in stearate synthesis in *clk-1(qm30)* animals (Figure 5.2). Because the elevated synthesis is seen upon perturbation of oxidative phosphorylation, this result effectively demonstrates that decreased oxidative phosphorylation leads to an increase in *de novo* fatty acid synthesis.

Because ubiquinone has other functions within the cell, we also assayed synthesis rates in *isp-1*(*qm150*) worms which have a structural defect in complex III of the electron transport chain. In *isp-1* animals, we found that there is an even greater increase in synthesis with a 125% increase measured in palmitate which confirms that the lipogenic phenotype is due to decreased oxidative phosphorylation and not off target effects (Figure 5.2). Because the *isp-1* animals have a more severe reduction in respiration, we believe this suggests there is a dosage dependent effect defining the rates of fatty acid synthesis based on the degree of oxidative phosphorylation inhibition. Taken together, this suggests that the elevated fatty acid synthesis observed is direct result of decreased electron transport chain activity. Additionally, the increased synthesis observed in nematodes with compromised oxidative phosphorylation suggests that *C. elegans* is a useful model for studying cancer metabolism.

The Impact of NADH:NAD+ Metabolism on Fatty Acid Synthesis

Because we found that defects in coenzyme Q (*clk-1)* and complex III (*isp-1*) resulted in increased lipogenesis, we wondered whether any decrease in mitochondrial respiration would cause increased fat synthesis. In addition to decreasing the function of the ETC, coenzyme Q and complex III deficiency would also lead to the backup of both types of reducing equivalents, NADH and $FADH_2$ (succinate). Therefore, we tested whether the increased fat synthesis was a result of a reduction in oxidative phosphorylation directly or an imbalance of metabolites namely NADH and/or $FADH_2$. To do this, we measured *de novo* synthesis in mutants for the succinate dehydrogenase of Complex II, *mev-1*. Because *mev-1* is required to accept electrons from succinate, these animals allowed us to test whether succinate buildup causes increased lipogenesis. These *mev-1* animals did not show any increase in fatty acid synthesis, suggesting that succinate imbalances do not impact

lipogenesis (Figure 5.2). This result also demonstrates that fatty acid synthesis is not a response to a generalized decrease in mitochondrial respiration function. However, the impact of succinate on the ETC has not been established in nematodes, so further experiments are required to determine if compensation by the NADH pathway can relieve the requirement of succinate.

In order to test if the reverse is true and the succinate pathway can compensate for a reduction in the NADH pathway, we quantified lipogenesis in animals treated with rotenone, a Complex I inhibitor. In doing so, we found a dose-dependent increase in fat synthesis upon rotenone treatment (Figure 5.3). The lipogenic response upon Complex I inhibition demonstrates that the succinate pathway cannot compensate for a reduction in NADH metabolism. Additionally, this result demonstrates that there is a graded response to reduced ETC activity, which is consistent with the graded synthesis increase observed in the *clk-1* versus *isp-1* animals. In considering the components of the ETC that we have tested thus far, we believe that our data suggests a role for the ratio of NADH:NAD+ in the regulation of fatty acid synthesis upon inhibition of oxidative phosphorylation.

The Role of HIF1 in Regulating Synthesis

To identify genes that are essential for the increased lipogenesis, we began by testing the requirement of the HIF-1 transcription factor for this adaptation. A recent study demonstrated that the hypoxia-inducible factor HIF-1 is required for the lifespan extension seen in *clk-1* and *isp-1* animals, suggesting that HIF-1 is active in these ETC mutants (Lee et al., 2010). Although the main HIF-1 stabilization mechanism is mediated by limited oxygen conditions, this group demonstrated that the impaired respiration increases HIF-1 activity under normoxia (Lee et al., 2010). In mammalian cell culture, HIF-1 has also been described to regulate FASN-1 through the SREBP transcription factor (Furuta et al., 2008). Therefore, we tested the involvement of the hypoxia-inducible factor (HIF) in mediating the lipogenic response to ETC inhibition. To do this, we quantified synthesis in *hif-1(ia04)* mutant animals treated with the Complex I inhibitor, rotenone. The untreated *hif-1* mutants have wildtype levels of synthesis suggesting that HIF-1 does not regulate *de novo* synthesis under normal conditions. However, there is no increase in *de novo* synthesis when they are treated with rotenone (Figure 5.4). Under the conditions used, the wild-type animals have over 2x the amount of synthesized palmitate. This result suggests that *hif-1* is the main driver of lipogenesis when the electron transport chain is inhibited. Because we performed

these experiments in oxygen-replete conditions, the stabilization of HIF-1 by hypoxia is not required for the increase in synthesis.

The Interactions Between Electron Transport Chain Mutants and the Insulin/IGF Signaling Pathway

The FoxO transcription factor homolog, DAF-16, is activated by stress and nutrient depletion, and because we have already established that *daf-16* is a regulator of fat synthesis (see Chapter 2 and (Perez et al., 2008)), we wanted to test its involvement in regulating lipogenesis when mitochondrial respiration is inhibited as well. To do this, we quantified synthesis in both *clk-1(qm30);daf-16(m26)* and *isp-1(qm150);daf-16(m26)* double mutants. In preliminary experiments, we found a reduction in amount of palmitate synthesis in both strains although the decrease was greater in the *clk-1;daf-16* animals (Figure 5.5A). This suggests that the full upregulation of fatty acid synthesis requires not only the activity of HIF-1, but also the activity of DAF-16.

Next, we tested if the reduction of electron transport chain activity could further increase the elevated fatty acid synthesis seen in mutants of the DAF-2 insulin receptor. In the *clk-1;daf-2* animals, we found that these pathways were partially additive, suggesting that the function, at least, in part through different mechanisms (Figure 5.5B). However, the *isp-1;daf-2* double mutants have decreased synthesis compared to either of the parent strains (Figure 5.5B). Although further study is required to determine how these pathways impact lipogenesis, the different interactions of the *clk-1* and *isp-1* gene with the insulin/IGF pathway suggests that *isp-1* and *clk-1* may regulated lipogenesis through distinct mechanisms.

Using *C. elegans* to Probe the Function of TCA Cycle Intermediates

Under normal respiring conditions, the TCA cycle functions to produce reducing equivalents that are then converted to ATP by oxidative phosphorylation. There is no net loss of carbon through the TCA cycle; however, when oxidative phosphorylation is compromised, the intermediates of the TCA cycle can be diverted to other metabolic pathways. In order to generate fatty acids, there needs to be a supply of carbon as well as NADPH. Using *C. elegans* and rotenone treatment, we are now able to test the requirements of alternative metabolic pathways for fatty acid synthesis induced by decreased mitochondrial respiration.

The glyoxylate cycle is an anabolic pathway that allows the generation of sugar from fat. This pathway bypasses several step in the TCA cycle that result in carbon loss via CO_2. We reasoned that this cycle may be akin to glutamine feeding into the TCA cycle, which is thought to be a critical pathway for cancer cell metabolism. To test the requirement of the *gei-7* gene in inducing fatty acid synthesis, we quantified fatty acid synthesis in animals subjected to rotenone treatment. In *gei-7* animals, there is a synthesis increase upon rotenone treatment, suggesting that the glyoxylate pathway is not required for lipogenic metabolism with reduced oxidative phosphorylation (Figure 5.6). However, this experiment indicated that we can effectively probe the requirement of various metabolic pathways in oxidative phosphorylation compromised nematodes.

Discussion

In ETC mutants, we have found a dramatic increase in the relative abundance of *de novo* synthesized fatty acids. In these animals, there is reduced oxidative phosphorylation and therefore an increased reliance on glycolysis. One of the primary effects of this altered metabolism is the accumulation of NADH whose electrons are no longer donated to Complex I of the ETC. Because NAD+ is no longer produced at Complex I, adequate NAD+ pools must be restored by lactic acid production or by fatty acid synthesis. In fact, we found that mutations in the ETC that do not impact NADH:NAD+ ratio, *mev-1* animals, do not have increased fatty acid synthesis. This altered metabolic state mirrors very closely the metabolism of cancer cells which are known to rely primarily on glycolysis and have also been shown to have very high rates of fat synthesis. The ability of FASN to restore the NADH:NAD+ ratio has been described in the "Redox Imbalance Hypothesis", and we believe that the increase in fatty acid synthesis associated with decreased oxidative phosphorylation provides a genetic model for the study of cancer cell metabolism. In support of this model, studies on the effect of rotenone of lipogenesis in the 1960s found that rates of fatty acid synthesis were linearly related to the resulting NADH:NAD+ ratio with rotenone treatment in rabbit heart mitochondria (Hull et al., 1967). Future studies on the relative importance of lactate synthesis and lipogenesis will be important to a full understanding of this altered metabolism.

Our finding that the HIF-1 transcription factor is important in regulating the lipogenic response to decreased oxidative phosphorylation suggests that oxygen availability may also impact synthesis rates. In fact, studies in *C. elegans* have found an increase in fat storage

after anoxia treatment through the SREBP (Sterol Response Element Binding Protein) transcription factor (Taghibiglou et al., 2009). Early experiments have found a role for SREBP in mediating the synthesis increase we see with decreased electron transport chain activity (data not shown). Although we have shown that the influence of HIF-1 on fat synthesis is independent of oxygen availability, this response pathway may also respond directly to a reduction in oxygen levels. Hypoxic cycles have been demonstrated to be a feature of the tumor environment which suggests that low oxygen availability may influence fat synthesis in tumor cells as well. Our attempts at measuring synthesis in worms grown in hypoxia have, thus far, been inconclusive.

The increase in lipogenesis in cancer cells requires the activity of several other pathways; however, the relative importance of these pathways has not been fully investigated. For example, there are several enzymatic reactions that produce NADPH including the pentose phosphate shunt, the malic enzyme and isocitrate dehydrogenase. Using the nematode and isotope flux analysis, it will be possible to determine the relative importance of each of these pathways as well as if they can compensate for each other. Additionally, although it is clear that glutamine is a contributor to the TCA cycle during glycolytic periods, the same setup can be utilized to determine how glutamine impacts the metabolism of the cell (Figure 5.7).

The identification of mediators of this lipogenic transition will allow for studies to interrogate the importance of these pathways in nematode survival under reduced oxidative phosphorylation. We predict that *de novo* synthesis may be an important response to hypoxic environments. In support of this idea, different *daf-2* animals have distinct resistance to hypoxia, and there is a correlation between the degree of hypoxia resistance and amount of *de novo* fatty acid synthesis (Mabon et al., 2009).

Although cancer cells are a clear example of decreased electron transport chain activity, there are other contexts where these studies would be informative. For instance, chronic exposure to hypoxia in individuals with sleep apnea or asthma has been associated with increased incidence of obesity. Moreover, in nematodes, exposure to anoxic environments results in an accumulation of fat storage. This fat accumulation is dependent on the activity of the transcription factor SREBP that is known to regulate the fatty acid synthase gene. Taken together, hypoxia induced fat accumulation may be explain the increase of *de novo* fatty acid synthesis when the electron transport chain is compromised (Taghibiglou et al., 2009).

Experimental Procedures

Strains

The strains used in these experiments were maintained at 20°C. The strains provided by the Caenorhabditis Genetics Center (CGC) are: N2 Bristol, CB4876: *clk-1(e2519)*, MQ130: *clk-1(qm30)* and MQ887: *isp-1(qm150)*, TK22: *mev-1(kn1)*, RB766: *gei-7(ok531)*, ZG31: *hif-1(ia04)*, MQ1050: *isp-1(qm150);daf-16(m26)*, MQ876: *isp-1(qm150);daf-2(e1370)*, XXX: *clk-1(qm30);daf-16(m26)* and MQ513: *clk-1(e2519);daf-2(e1370).*

Mixed Isotope Feeding Assay, Lipid Purification and Analysis

All experiments were performed as described in the Experimental Procedures in Chapter 2. Because many of these strains are slow growing and have some asynchronous development, the animals were harvested when the majority of the worms were at mid-L4. These experiments were conducted before our discovery of the increase in synthesis that coincides with the onset of adulthood (discussed in Chapter 4); therefore, more carefully staged collections would be warranted to ensure accurate synthesis numbers.

Rotenone Treatment

A rotenone stock was made at 0.5 mg/ml in DMSO, and top spread on the mixed labeled plates. The rotenone stock was made fresh for each experiment as we found significant variability that we attributed to instability of the drug. Inconsistencies were still seen between experiments. Therefore, with each experiment, a titration was performed.

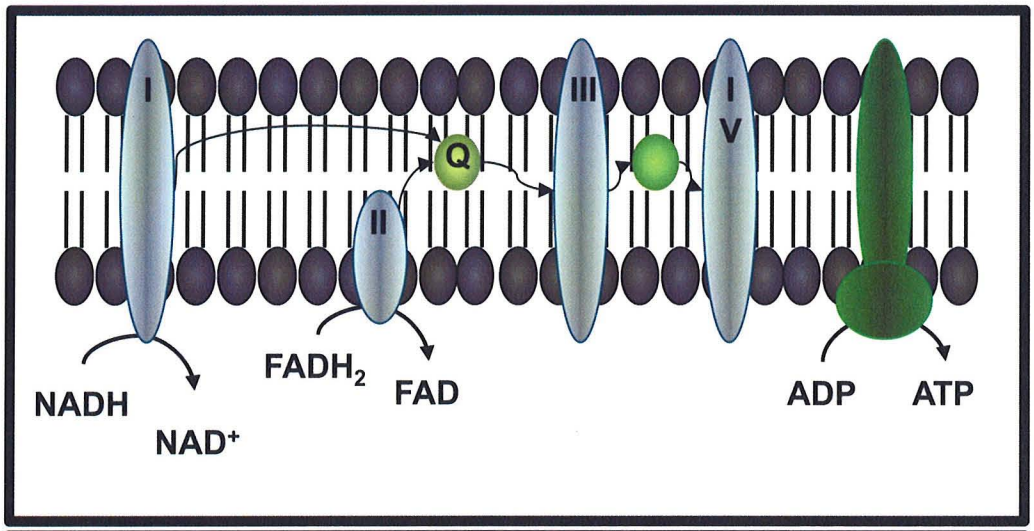

Figure 5.1: Schematic of the Electron Transport Chain. Electrons are donated from NADH to Complex I of the ETC to drive the formation of a proton gradient that is ultimately utilized to produce ATP. The electrons are transferred from Complex I through coenzyme Q to Complex III. There is an alternate pathway involving the transfer of electrons from $FADH_2$ to Complex II and then to coenzyme Q. Strains with mutations in genes encoding components of the ETC were used in this study: *mev-1* (Complex II), *clk-1* (coenzyme Q) and *isp-1* (Complex III).

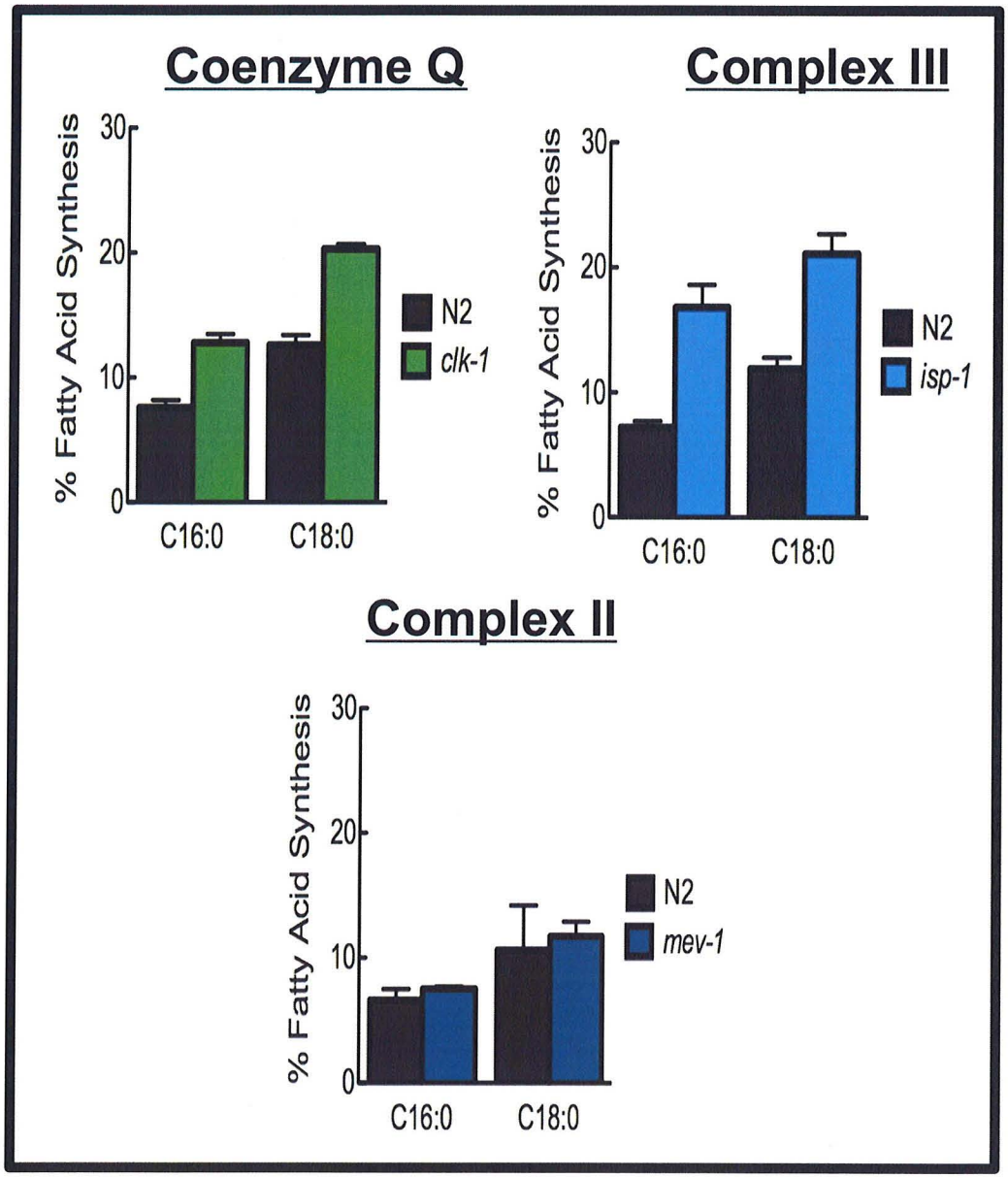

Figure 5.2. Decreased Mitochondrial Respiration Leads to Increased Synthesis: Inhibition of complex I (by rotenone), coenzyme Q (*clk-1*) and complex III (*isp-1*) all lead to increased synthesis. However, inhibition of complex II (*mev-1*) results in normal palmitate synthesis suggesting that lipogenesis is linked to imbalance of NADH:NAD+ levels and not by $FADH_2$:FAD. SEM is shown.

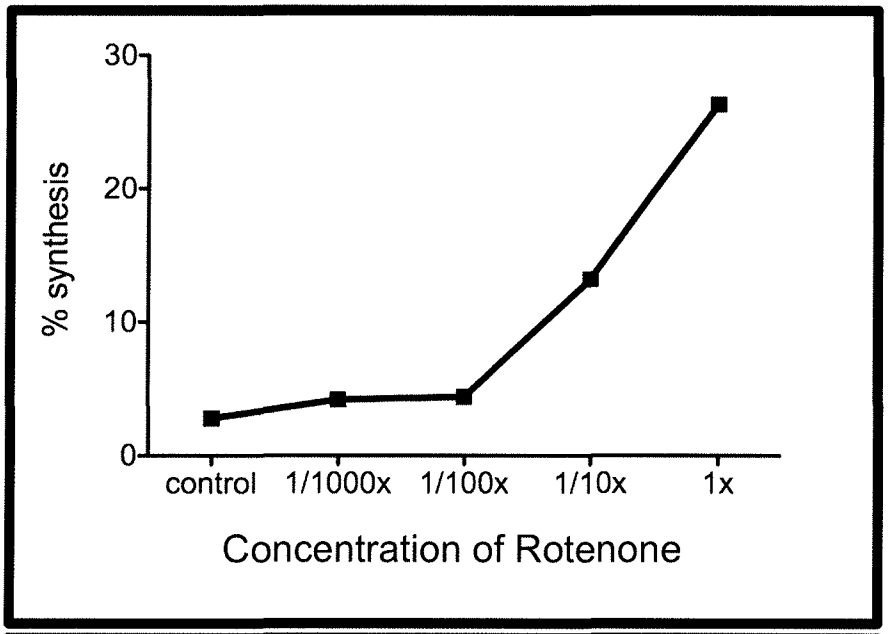

Figure 5.3. Dose-dependent Increase in Lipogenesis With Inhibition of Complex I: In order to test the requirement of Complex I activity on *de novo* fatty acid synthesis, we grew animals on rotenone, a Complex I inhibitor. We found that not only does palmitate synthesis increase with rotenone treatment, but it does so in a dose-dependent manner. The curve shown is from one experimental set, but the trend has been reproduced multiple times. (Ix = 0.5mg/ml)

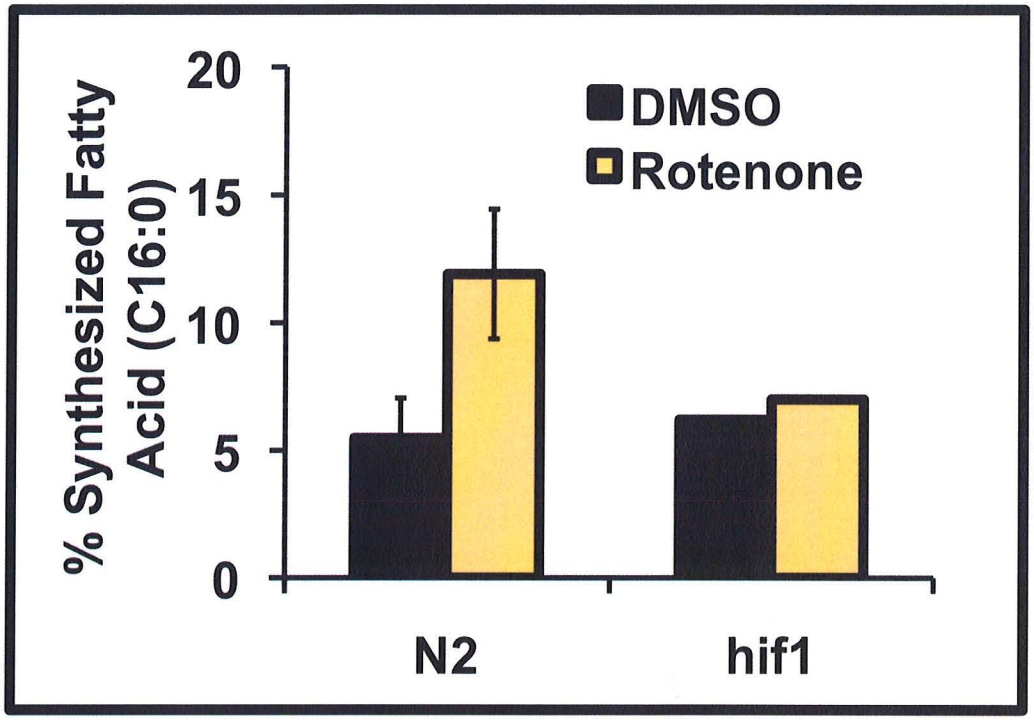

Figure 5.4. HIF1 is Required for Rotenone Induced Lipogenic Increase: In wild-type (N2) animals, rotenone treatment results in a >2-fold increase in C16:0 synthesis. However, *hif-1(ia04)* animals do not have increased synthesis on rotenone (~1.1-fold). Data shown is a compilation of 3 replicates for N2 animals,but only 2 replicates for the *hif-1* animals.

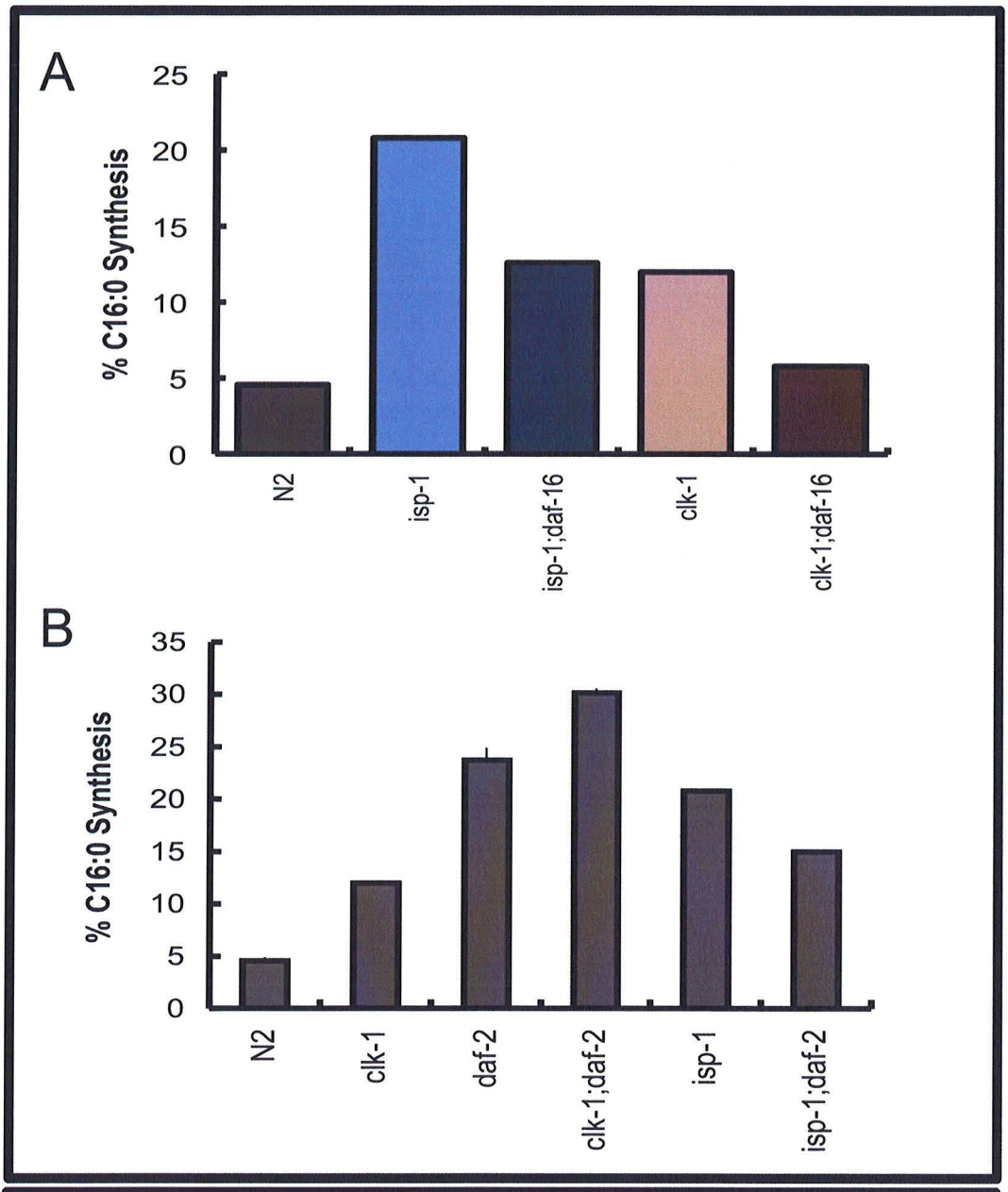

Figure 5.5. Interaction Between the ETC and Insulin Signaling Pathway: (A) Using double mutants, we have found that *daf-16* function is required for the increased lipogenesis of ETC mutants. (B) The *clk-1;daf-2* animals demonstrate that these pathways are partially additive; however, the *isp-1;daf-2* animals have lower synthesis than either parent. Although these experiments need to be repeated, it suggests that *clk-1* and *isp-1* may be regulating synthesis differently. Confirmation of these interactions is needed as most strains have only been assayed two times.

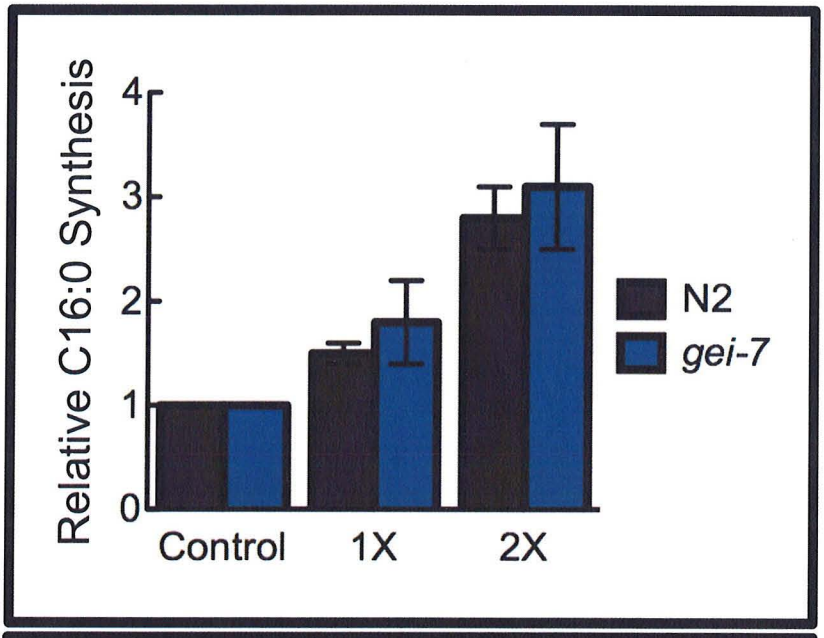

Figure 5.6. *gei-7* Mutants Increase Synthesis With Rotenone Treatment: We found that the *gei-7(ok531)* mutant responds normally to rotenone treatment. Synthesis rates were normalized to the control plates. Data from a minimum of 3 experiments with SEM shown.

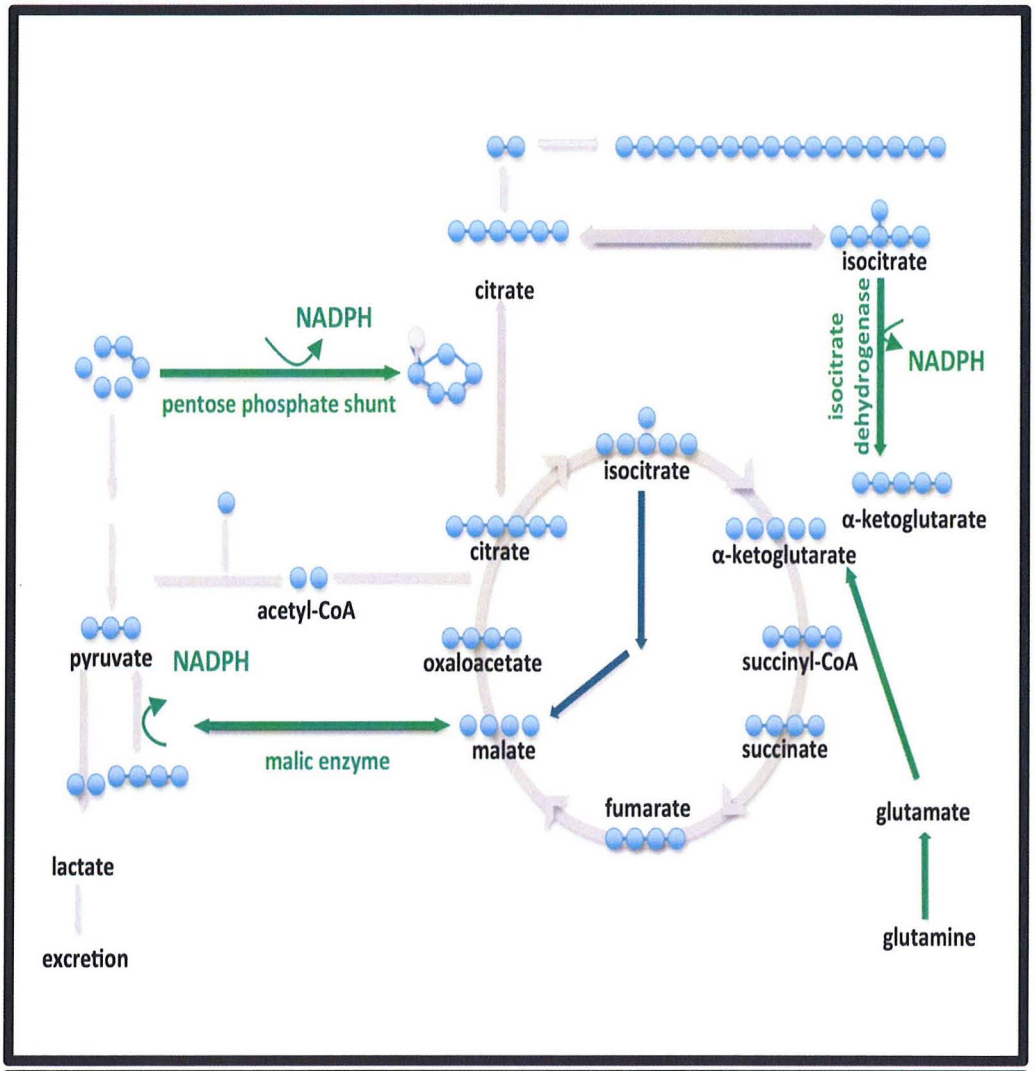

Figure 5.7. NADPH Generating Pathways: There are multiple enzymes that can be used to generate NADPH needed for lipid synthesis (highlighted in green). Other pathways including the glutamine pathway and glyxoylate shunt can also be tested for their role in cancer cell metabolism using the nematode and rotenone inhibition. Combining genetic mutants with reduction of ETC activity will allow us to begin to understand the relative importance of each of these metbaolic pathways.

CHAPTER VI: Conclusions and Future Directions

Summary

We believe that the implementation of stable isotope technology in a model organism such as *C. elegans* will allow for the exploration of many fundamental questions about fatty acid metabolic regulation that have not yet been able to be addressed. We have demonstrated that the mixed labeling technology can be utilized to learn more about how known regulatory pathways like the insulin/IGF signaling pathway impact fatty acid metabolism. Additionally, this strategy can also be implemented to identify previously unrecognized connections such as the role of electron transport chain activity and reproduction in the regulation of *de novo* synthesis. Not only can these isotope labeling strategies be used to continue to understand fatty acid metabolism pathways, but the implementation of feeding stable isotopes in the nematode can also be expanded to address different aspects of fatty acid metabolism and to quantify changes in other cellular components like proteins and DNA.

Origins of Fatty Acids in *C. elegans*

In this work, we have been able to define the sources of fatty acids in wild-type *C. elegans* for the first time. We have established that, like mammals, the worm derives the majority of its fat directly from the diet, and the proportion of *de novo* synthesized fatty acids is minimal for most fatty acid species. Because we can achieve high levels of isotope enrichment in the animal, we can measure the contribution of synthesis to all the different types of fatty acids. In doing so, we have found an enrichment in synthesized fatty acid in the polyunsaturated species (PUFAs) which suggests that *de novo* fatty acid synthesis may play an important role in the generation of membrane lipids. Future work is necessary to fully establish this function as high fragmentation of longer chain PUFAs in the mass spectrometer makes their analysis difficult.

Because the development and lifespan of the nematode is relatively short, *C. elegans* offers a unique opportunity to study how fatty acid metabolism changes over development and aging. Thus far, we have found a dramatic shift in how an animal processes its diet as a larva and as a reproductive adult. However, it will be important to characterize how an organism processes its diet at all life stages. In particular, the aged animal has a tremendous reduction in feeding rate, and it will be important to define which lipid processing pathways are intact at that stage.

Characterization of Fat Storage Mutants

In addition to characterizing fatty acid metabolism in wild-type *C. elegans*, this mixed labeling approach can also be used to determine how fat storage genes impact metabolic pathways. This ability may be particularly useful because there have been hundreds of genes identified that impact fat accumulation; however, defining how each gene impacts lipid physiology is essential for the continued understanding of the regulation of fat storage. We have demonstrated that the mixed isotope technology can be used to determine if a high fat mutant has increased fat absorption, increased fatty acid synthesis or decreased fat utilization. Moreover, we have used the mixed labeling approach to characterize the cause of the altered fat accumulation in several mutant backgrounds (Figure 6.1). For example, we have determined that the elevated fat storage observed in *daf-2* animals can be largely attributed to the increased fatty acid synthesis seen in these mutants. Not only will this method allow for these genes to be defined much more quickly than through standard transcriptional analysis, but the large amount of data will also allow for a more thorough understanding of how each gene impacts the lipid physiology of the nematode.

Additionally, we have undertaken a limited screen of high fat mutants and have identified several new regulators of *de novo* fatty acid synthesis including peroxisomal β-oxidation genes (Appendix I). Because the majority of the key metabolic pathways including *de novo* synthesis, β-oxidation, and fat absorption are homologous to mammalian systems, we believe that the definition of genes in nematodes will impact the understanding of obesity and metabolic disease in humans. In that regard, we have established that chemicals that inhibit mammalian metabolic pathways, like rotenone and orlistat, also are efficacious in *C. elegans.*

***C. elegans* As a Model System for Studying Fat Metabolism**

We believe that the capability to conduct isotope flux analysis will be critical in the continued development of the nematode as a model for studying fat storage and metabolism. This is especially true in light of the fact that many of the current tools available for measuring fat storage have come under scrutiny as of late. Lipophilic dyes like Nile Red have been utilized to characterize fat storage and to screen for new regulators of fat storage; however, recent studies have shown that this dye primarily stains lysosome-related organelles, which are not the primary fat stores of the nematode (O'Rourke et al., 2009;

Zhang et al., 2010). Nile red screen shave identified many genes that have impacts on fat metabolism that have been confirmed by other methods including biochemical analysis; therefore, the mixed isotope labeling method that we described may contribute to a better understanding of other fat storage tools by allowing us to look directly at the dynamics of the fatty acids themselves.

Furthermore, we can look at defined populations of lipid molecules to characterize the metabolism of triglycerides and phospholipids separately. Because we combine metabolic labeling with gas chromatography/mass spectrometry, we can quantify the relative ratio of synthesized and absorbed fatty acids, the composition of the fatty acids in the TAG and in the PL, and the TAG:PL, a preferred method for measuring fat storage, all in a single sample. For these reasons, we believe that this method will be useful in determining how particular genes and pathways disrupt fat metabolism.

Identification of Genes and Pathways that Impact Fatty Acid Metabolism

The implementation of flux analysis in the fat of the nematode has allowed us to further define how key regulatory pathways impact fatty acid metabolism. In this work, we have expanded the knowledge of fat metabolism by studying the impact of genetic pathways on total dynamics. We were able to define how the insulin signaling pathway impacts lipid metabolism more accurately by tracing the utilization of the diet as opposed to relying only on transcriptional changes. We believe that this method will continue to be useful in describing complex genetic pathways that regulate fat metabolism.

This type of isotope analysis has also allowed us to determine how changes in metabolite balances impact interacting metabolic pathways. The best example of this type of study is the interrogation of how oxidative phosphorylation impacts fatty acid metabolism where we uncovered a relationship between the ratio of NADPH to NAD+ and the rate of fatty acid synthesis. However, there is much more to learn about how different pathways interact in animals. For example, we do not know which enzymes are important for the generation of acetyl-CoA from TCA intermediates. Using RNAi in conjunction with isotope tracers, it is possible to monitor how perturbations in one pathway impact other metabolic fluxes.

The Impact of Fatty Acid Synthesis on Fat Storage and Lifespan

One of the major advances of this work was the description of how *de novo* fatty acid synthesis impacts fat storage and lifespan. We found that the levels of fatty acid synthesis have a dramatic influence on the total fat stores of the animal. Although it is not surprising that making more fat would result in elevated fat stores, the impact on total fat accumulation was larger than expected. Because *de novo* fatty acid synthesis is normally quite minimal, even modest increases in the rates of synthesis (~30 to 50% total) account for more than 60% of the increased fat stores. In fact, we believe that this number is conservative as increased lipogenesis can feed back and inhibit mitochondrial β-oxidation resulting in reduction of fat utilization as well.

Our studies also allowed for us to genetically separate fatty acid synthesis and longevity. Because many pathways like the insulin/IGF pathway regulate both lifespan and fat metabolism, it made intuitive sense that the changes in fat metabolism might be essential for the increased longevity. However, our studies with a series of *daf-2* mutant alleles allowed us to determine that lifespan and fat synthesis were genetically separable. This result is encouraging for the future development of drugs that can target fat storage without negatively impacting longevity and vice versa. However, we and others have established a potential role for *de novo* fatty acid synthesis in reproduction (Chirala et al., 2003). Also, in our studies, we have found an additional role for *fasn-1* in regulating adult lifespan which will need to be considered before attempting such interventions.

A Role for *De Novo* Fatty Acid Synthesis in Reproduction and Adult Survival

In addition to probing known genetic pathways, we also used this technology to understand the role of lipogenesis at various life stages in the animal. In these studies, we found a key role for altered fat metabolism at the onset of reproduction. We believe that these studies have major implications for how the field thinks about fat metabolism. There are many instances where the function of a gene or pathway is assumed to be constant throughout its growth and development; however, we believe that this represents a need to consider developmental stage in comparative studies.

Additionally, when the key fatty acid synthesis gene, *FASN-1*, is inhibited, we found a reduction of adult lifespan. Besides the generation of fatty acids when fat is not present in the diet, an essential role for fatty acid synthesis in the adult animal has not been described in any species. These experiments led us to a model that suggests a key role for altered fat metabolism in allowing animals to survive reproduction. We believe that the role of fatty

acid synthesis in lifespan after reproduction should be considered in the development of therapeutics that alter fatty acid metabolism.

The Impact of Oxidative Phosphorylation on *De Novo* Fat Synthesis

We have also employed the mixed labeling strategy to define how perturbations in metabolic pathways can influence overall fat metabolism. In cancer cells, there is a lipogenic shift that results in the vast majority of fatty acids coming from *de novo* fatty acid synthesis. The redox balance model suggests that the high levels of fatty acid synthesis are a necessary compensation mechanism to generate adequate levels of NAD+ to run glycolysis. Using the nematode, we have found that increased fatty acid synthesis is a result of decreased electron chain activity. We have used this model to identify genes that are required for this transition and have established roles for the HIF-1 and DAF-16 transcription factors. There are many open questions about the relative contributions of certain metabolic pathways to cancer cell metabolism, and the establishment of *C. elegans* as a model for studying aerobic glycolysis will allow the relative impacts of pathways like NADPH generation to be defined.

Defining the Impact of Fatty Acid Synthesis

Using the isotope labeling technology, we have been able to define several genes and conditions that impact the levels of *de novo* fatty acid synthesis; however, the next step is to define the importance of fat synthesis in these processes. We believe that increased *de novo* synthesis is an essential component for efficient reproduction and for survival with decreased electron chain function; however, to address these questions, inhibition of fatty acid synthesis in these states would be essential. Additionally, our studies with *fasn-1* RNAi have already established a role for fatty acid synthesis in adult lifespan. Next, it will be important to define the function of this pathway in adults.

Further Development of Isotope Technology in *C. elegans*

The feeding of a stable isotope labeled diet has many more potential applications in the nematode. Stable isotope labeling can be used to map other features of lipid metabolism like fatty acid turnover and food choice as well as monitoring the synthesis, turnover and dynamics of almost any other cellular molecule (Appendix II). Molecules that contain carbon or nitrogen, like proteins and DNA, can be studied with the same labeling techniques we

have described. Preliminary studies have indicated that heavy water, D_2O, can be incorporated into the agar plates that the nematodes live on. Because the nematode gets its water from the plate, we have been able to monitor the incorporation of deuterium into the lipids of starved nematodes. This and other types stable isotope incorporation studies will allow for metabolism to be explored in unique contexts. The study of metabolic flux and turnover in the worm with stable isotopes has several advantages including cost effectiveness and genetic tractability; however, studies in other systems like mammalian cell culture can also be done with modified techniques.

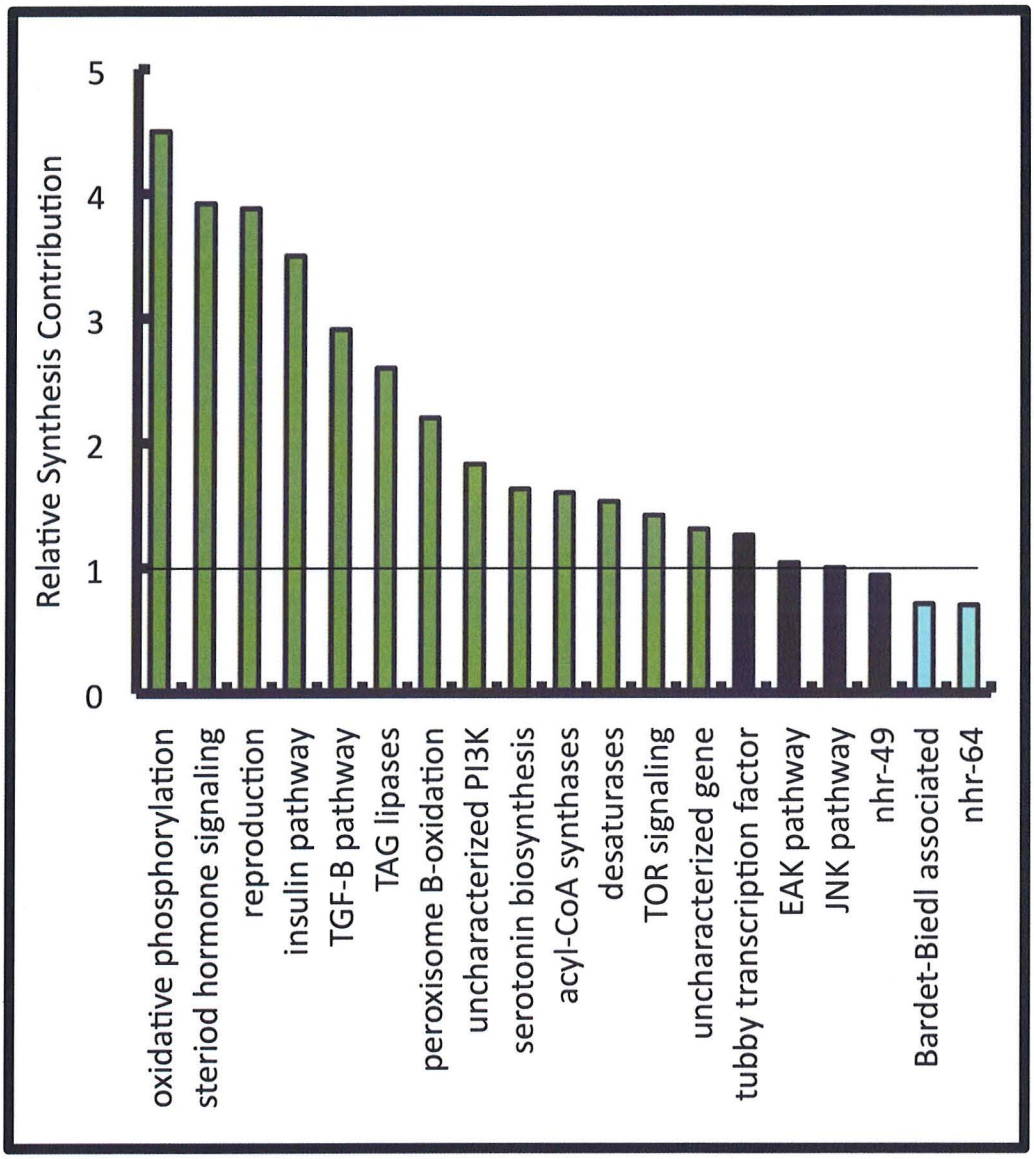

Figure 6.1. Summary of Screened Mutants: Over the course of these studies, we have investigating the impact of a number of genes, pathways and processes on fatty acid synthesis. This graph represents the relative contribution of these studies with disruptions leading to increased relative synthesis (green), no change in synthesis (black) and decreased relative synthesis (blue). It should be noted that the data here was collected using different methods including mutant strains, drug treatment and overexpression lines.

Appendix I: Novel Regulators of Fatty Acid Synthesis

Summary

In order to define new regulators of *de novo* fatty acid synthesis, we screened a number of genes that have been previously implicated in the regulation of fat storage or longevity. Through these efforts, we have identified a number of novel regulators of *de novo* synthesis including genes encoding enzymes in peroxisomal β-oxidation, acyl-CoA metabolism, and oxidative phosphorylation. Additionally, this screening approach has identified two novel genes which we have named *high lipid synthesis (hls)* genes. One of these novel genes, *hls-1*, encodes a Type I PI3-Kinase which may function in the insulin signaling pathway. Here, we describe the progress we have made to further understand these regulators and the pathways that they function in.

Screen of Mutants with Elevated Nile Red Staining

A genome-wide RNAi screen identified a set of genes that when knocked down resulted in changes in fat storage as assayed by Nile Red staining (Ashrafi et al., 2003). We first identified genes that resulted in increased Nile Red staining that had available homozygous mutant strains. Then, we quantified the amount of fatty acid synthesis for these strains and identified three novel regulators of fatty acid synthesis, *maoc-1 (MAO-C-like dehydratase domain), hls-1 (high lipid synthesis)* and *hls-2*.

Peroxisomal β-oxidation Pathway Regulates Lipogenesis

The most notable of the screen hits was the *maoc-1* strain which encodes an ortholog of human hydroxysteroid (17-beta) dehydrogenase 4 (HSD17B4) which is a multifunctional enzyme that functions in the peroxisomal β-oxidation pathway (Moller et al., 1999). The peroxisomal-β oxidation pathway is responsible for the oxidation of long chain fatty acids (C15-C20), very long chain fatty acids (>C20) and branched fatty acids (Figure A.1A). The products of this oxidation are then exported to the mitochondria where they can be fully oxidized to produce energy. Once *maoc-1* was identified in the screen, we wanted to assay if elevated synthesis was inherent to all peroxisomal β-oxidation mutants. To do this, we assayed synthesis in deletion strains for other genes that encode other enzymes in the pathway, *dhs-28(tm2581) and daf-22(m130)* (Figure A.1B). We found an increased

synthesis phenotype in all these strains which is the first time a connection between peroxisome β-oxidation and *de novo* lipogenesis has been identified.

In *C. elegans*, the peroxisomal-β oxidation pathway has recently been implicated in the biosynthesis of the dauer pheromone (Butcher et al., 2009; Joo et al., 2009). The dauer pheromone called daumone is continuously secreted into the environment by the nematodes where is used to assess population density, and animals with mutations in peroxisome β-oxidation genes fail to produce the normal pheromones. Because these mutants cannot synthesize daumone, they are not capable of inducing the dauer formation when unfavorable growth conditions including high population density and low food availability are encountered. Dauer formation is known to be regulated by multiple signaling pathways that orchestrate changes in fat metabolism, stress resistance and longevity genes, so we next wanted to assess whether the increased fatty acid synthesis we see in these mutants is due to a failure to regulate dauer signaling pathways. Because the role of the insulin pathway in dauer formation is well established, we addressed this question by looking at role of insulin signaling in this response by constructing a *maoc-1;daf-16* worm strain. In these animals, the synthesis increase is intact suggesting that the impact of peroxisomal β-oxidation of fatty acid synthesis is independent of insulin signaling (Figure A.1C). We believe that daumone is acting downstream of the insulin pathway on the nuclear hormone receptor, DAF-12, and we are currently investigated that possibility. However, we also cannot exclude the alternate model that the impact of peroxisome β-oxidation of fatty acid synthesis is independent of daumone synthesis entirely.

A New PI3-Kinase Regulates Lipogenesis in Nematodes

In our screening effort, we found a novel gene, F39B1.1, which we named *high lipid synthesis (hls-1)* but has subsequently been named *piki-1(phosphoinositide-3-kinase)*. This gene has homology to a mammalian Type II PI3-Kinase (P13KC2α), and we have established that HLS-1 has kinase activity *in vitro* (data not shown). In mammalian systems, Type II P13-Kinases have been shown to respond to insulin (Brown et al., 1999). Therefore, we are currently testing whether *hls-1* functions downstream of DAF-2 to regulated lipogenesis. Preliminary studies have found that the regulation of fatty acid synthesis by *hls-1* requires the activity of *daf-16* (Figure A.2A). We are currently investigating whether *hls-1* may specifically regulate *de novo* fatty acid synthesis downstream of the insulin signaling pathway (Figure A.2B).

A Novel Worm Specific Regulator of Fatty Acid Synthesis

From our screen of high fat mutants, we also identified a previously uncharacterized gene, M70.1 that we since named *high lipid synthesis* (*hls-2*). This gene includes a WSN (worm specific N terminal) domain and has no identifiable human homolog; however, the protein is predicted to be localized to the membrane. When fatty acid synthesis is measured across fatty acid species, we found that the synthesis increase is not uniform and becomes more dramatic as the fatty acids become increasingly polyunsaturated (Figure A.3A). By constructing a *hls-2;daf-16* double mutant and assaying its rates of lipogenesis, we found that the increase in fat synthesis is mediated by the DAF-16 transcription factor (Figure A.3B).

Acyl-CoA Synthase

In a non-biased mutagenesis screen utilizing the lipophilic dye, Nile Red, one of the nematode acyl-CoA synthase genes, *acs-3,* was identified as a regulator of fat storage. In order to determine the source of the excess fat staining, we measured fat uptake and fatty acid synthesis in *acs-3* mutant animals in collaboration with the Ashrafi lab. These studies revealed that *acs-3* animals have both increased dietary fat uptake as measured by BODIPY labeled fatty acid incorporation and increased fatty acid synthesis as quantified by mixed ^{13}C isotope labeling (Figure A.4A and (Mullaney et al., 2010)).

Because asc-3 animals are sensitive to LY294002, a broad spectrum phosphatidylinositol 3-kinase (PI3-Kinase), we performed a screen to identify suppressors of the LY294002-induced developmental arrest of the asc-3 mutants. This screen identified three suppressors: a long-chain acyl-CoA dehydrogenase (acdh-11), a medium-chain acyl-CoA dehydrogenase (acdh-10) and a fatty acid elongase (elo-6). All three suppressors can rescue the fatty acid uptake and fat storage phenotypes; however, only elo-6 can suppress the increased fatty acid synthesis phenotype (Figure A.4).

A Role for TORC2 in Regulating Lipogenesis

In a screen for mutants of altered lipid storage, the Ashrafi lab isolated two alleles of the *C. elegans* rictor homolog which they named *lpo-6* (*lipophilic dye abnormal*). The *lpo-6* gene encodes Rictor which functions in the TOR (target of rapamycin) pathway as the binding partner of the TORC2 complex (Jones et al., 2009). We tested the role of *lpo-6* in

regulating lipogenesis and found that there is a significant enrichment in synthesized fatty acids. We have found that the increase in synthesis is not seen in palmitate, but in the other fatty acid species of the worm (Figure A.5)

Reduced Fatty Acid Synthesis in *bbs-1* Animals

Mutations in the human *bbs-1* gene have been associated with Bardet-Biedl syndrome. Because Bardet-Biedl syndrome is characterized by an increased propensity for obesity, there has been interest in defining how the *bbs-1* gene may impact lipid metabolism pathway. When we assayed these animals for synthesis, we found a decreased abundance in synthesized fatty acids (Figure A.5). Because these animals are high in fat, this result suggests an increase in dietary fatty acid absorption consistent with gene expression analysis (Mak et al., 2006).

Overexpression of *nhr-69* Eliminates Lipogenic Increase Seen at Adulthood

We measured *de novo* fatty acid synthesis in a worm strain that overexpresses the *nhr-69* (generated and provided by D Gems) and found that these animals fail to upregulate synthesis between L4 and adulthood (Figure A.6A). These animals allowed us to test the importance of this increase by assaying lifespan and brood production in animals that fail to upregulate synthesis. We found that these animals have severely compromised brood production and a shortened lifespan, supporting the model we presented in Chapter IV (Figure A.6B). Although further study is needed, this suggests that there is genetic regulation of the increase in adults.

Appendix II: Other Stable Isotope Labeling Strategies in *C. elegans*

Summary

The implementation of stable isotope technology has many potential utilizations in the nematode including RNAi screening, fat turnover studies and food discrimination studies. Additionally, other elements can be labeled depending on the types of hypotheses tested. For example, we have used heavy H_2O to look at label incorporation in starved animals where we cannot introduce label via the diet. Here, we also describe our efforts to expand the utility of isotope labeling approaches in nematodes by adapting the isotope strategies to be compatible with RNAi feeding technologies.

Compatibility with RNAi Feeding Platforms

Our current analysis has been limited to assaying the regulatory role of genes that have mutant strains available; however, there are many genes of interest that do not yet have developed strains. We therefore sought to expand this technology to be compatible with RNAi feeding. The primary hurdle to RNAi feeding compatibility is that mixed isotope feeding plates are prepared with agarose media to eliminate excess unlabeled carbon incorporation by growing bacteria. Because RNAi induction by IPTG requires actively growing bacteria, we have approached this problem in two distinct ways to with some success. First, we have experimented with induction of RNAi production in liquid cultures before plating on agarose plates. This method has shown success with several RNAi strains including *fat-7* RNAi as shown; however, this strategy does not sustain long-tern RNAi inhibition and may not be suitable for RNAi of all genes.

The second strategy that we have employed is to isotope label worms on NGM growth plates. We have done preliminary experiments with the *daf-2* (*e1370*) strain to establish that the isotope patterns are intact despite the presence of unlabeled ^{12}C in the plates. This strategy will allow us to ensure induction of RNA interference; however, it will require further processing of the data. Additionally, both of these methods will ultimately require the growth of small individual bacterial cultures.

Lipid Turnover Studies

In order to measure fatty acid turnover rates, a population of fully ^{13}C bacteria were fed to the nematodes for a defined period. In these studies, we have found that extremely high

levels of fatty acid turnover especially in that phospholipids of the animal (Figure A.6). We next wanted to determine if turnover of fatty acids are constant over aging, and we found that fatty acid turnover rates decrease as the animals age (Figure A.7). We are currently investigating the role of membrane turnover in the aging process.

Food Discrimination Assays

Previous studies have found that the nematodes preferentially move to bacterial lawns of "high quality" food sources (Shtonda et al., 2006). However, it is not known whether the nematodes respond only to populations of bacteria or whether the nematode can distinguish between individual bacterium. To test these possibilities, we labeled a population of *P. aeruginosa* with 99% ^{13}C and found that we could determine the preference for the bacteria by quantifying the amount of ^{13}C in the lipids of the worms. We extended these studies to find that when we mixed the ^{13}C-labeled *P. aeruginosa* with ^{12}C-labed *E. coli* the nematodes still favored the *E. coli* population (Figure A.8).

$^{2}H_2O$ Studies in Nematodes

One of the limitations of the ^{13}C-labeled food incorporation is that the animals must be eating in order to be exposed to the stable isotope. Because we are also interested in measuring metabolic pathways in starved animals, we made use of the fact that nematodes get water directly from their feeding plates. We then poured growth plates with heavy water, $^{2}H_2O$ and put worms on unseeded plates. In these preliminary studies, we saw a small but significant accumulation of deuterium in the animals suggesting this labeling approach will be useful in studying metabolic flux in starved worms.

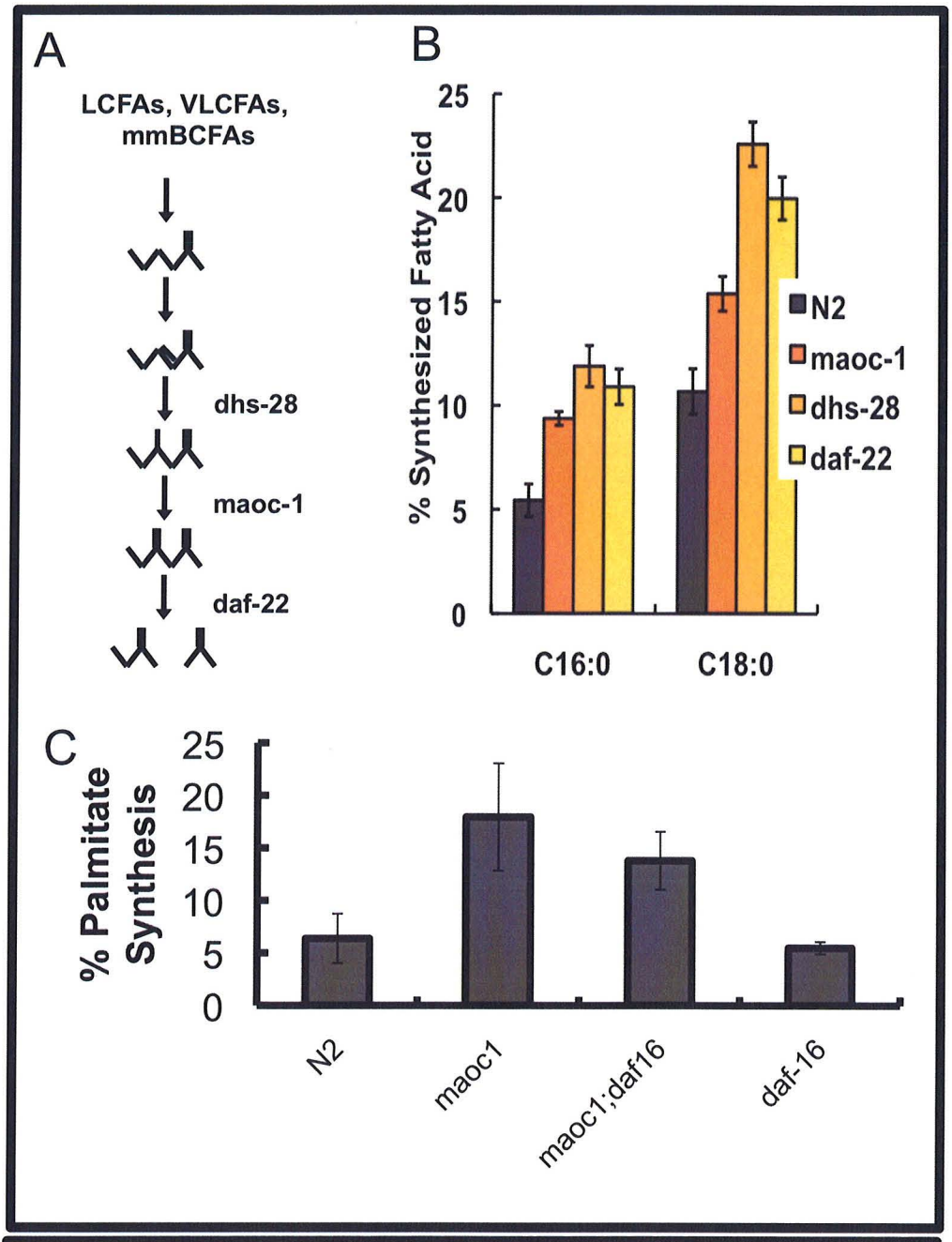

Figure A.1: Mutations in the peroxisomal β-oxidation pathway have increased lipogenesis. (A) Diagram of the peroxisome β-oxidation pathway. (B) Mutations in each component tested has elevated fatty acid synthesis in total lipid. (C) Epistatic studies have found that the increased synthesis observed in the *maoc-1* animals does not require the presence of *daf-16.*

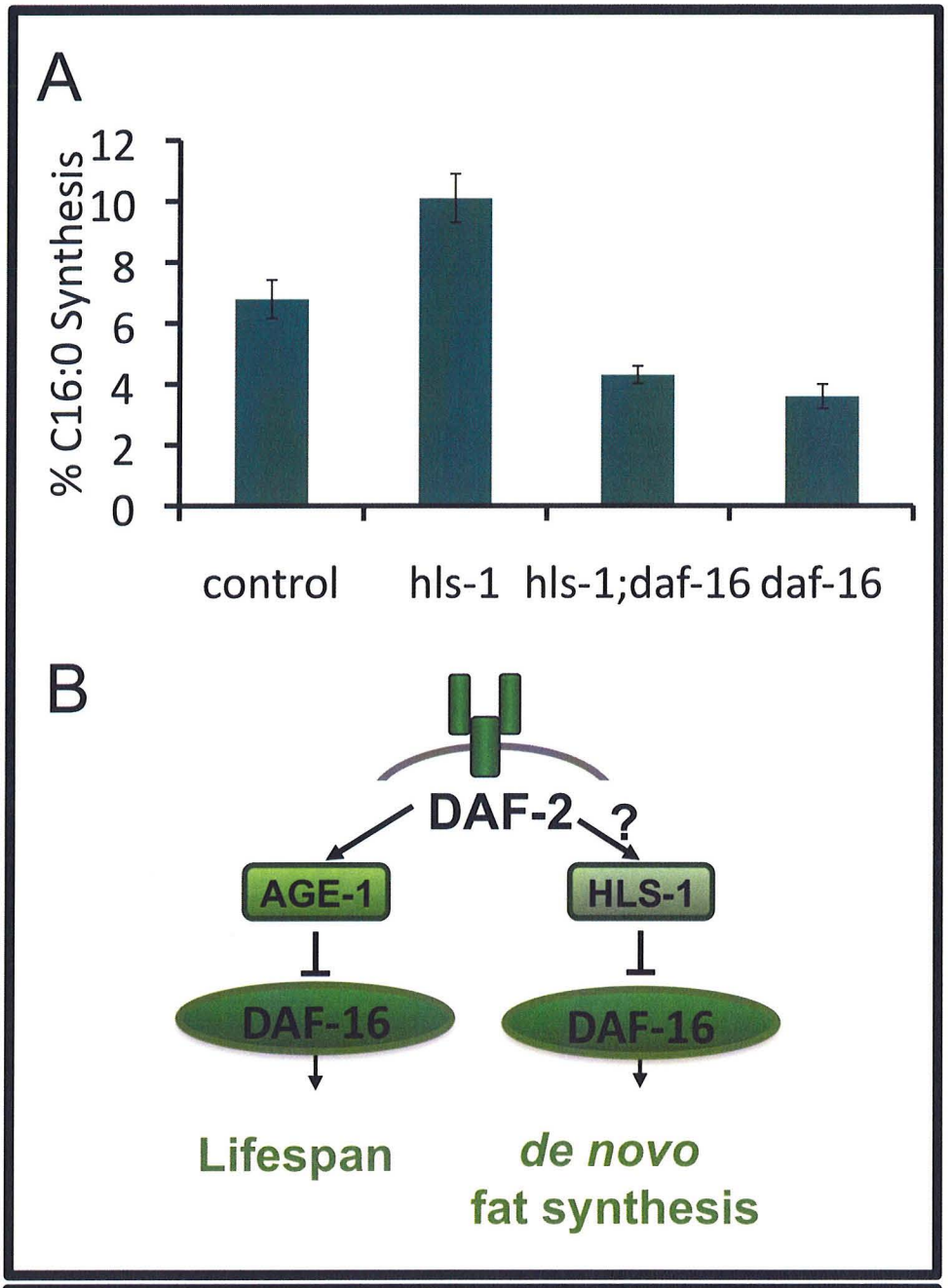

Figure A.2: *hls-1* animals have elevated fatty acid synthesis dependent on *daf-16*. (A) Fatty acid synthesis is increased in the *hls-1* mutants as shown with palmitate synthesis. In *hls-1;daf-16* double mutants, synthesis rates are rescued suggesting that *hls-1* interacts with the insulin signaling pathway. (B) We are currently testing the role of HLS-1 in regulating fat synthesis downstream of DAF-2.

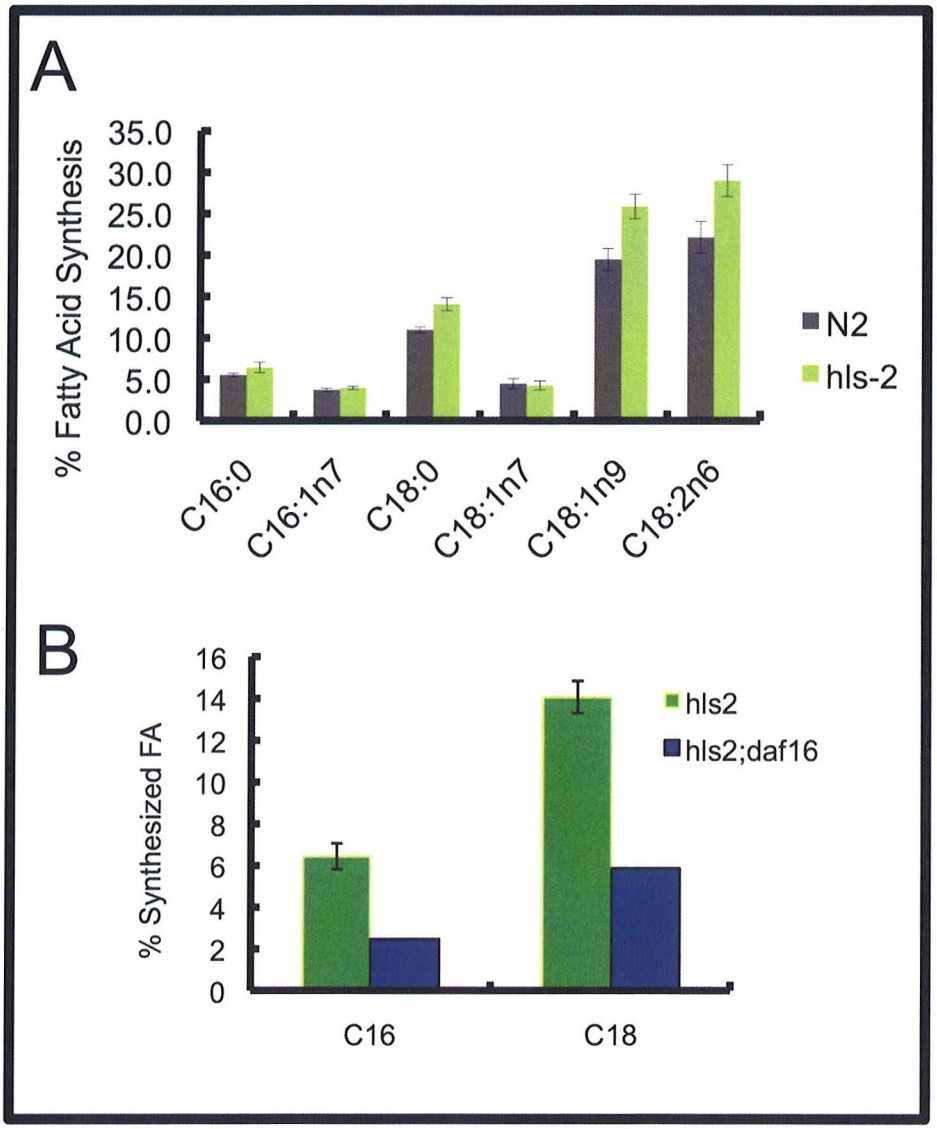

Figure A.3: HLS-2 regulates lipogenesis. (A) *hls-2* animals have increased synthesis especially in longer fatty acids. Data are shown as percentage of synthesized fatty acid ± SEM. (B) Preliminary experiments have established that the increased synthesis observed in *hls-2* animals depends on DAF-16 as *hls-2;daf-16* animals (purple) have reduced synthesis. Data from *hls-2;daf-16* animals is compiled from 2 replicates.

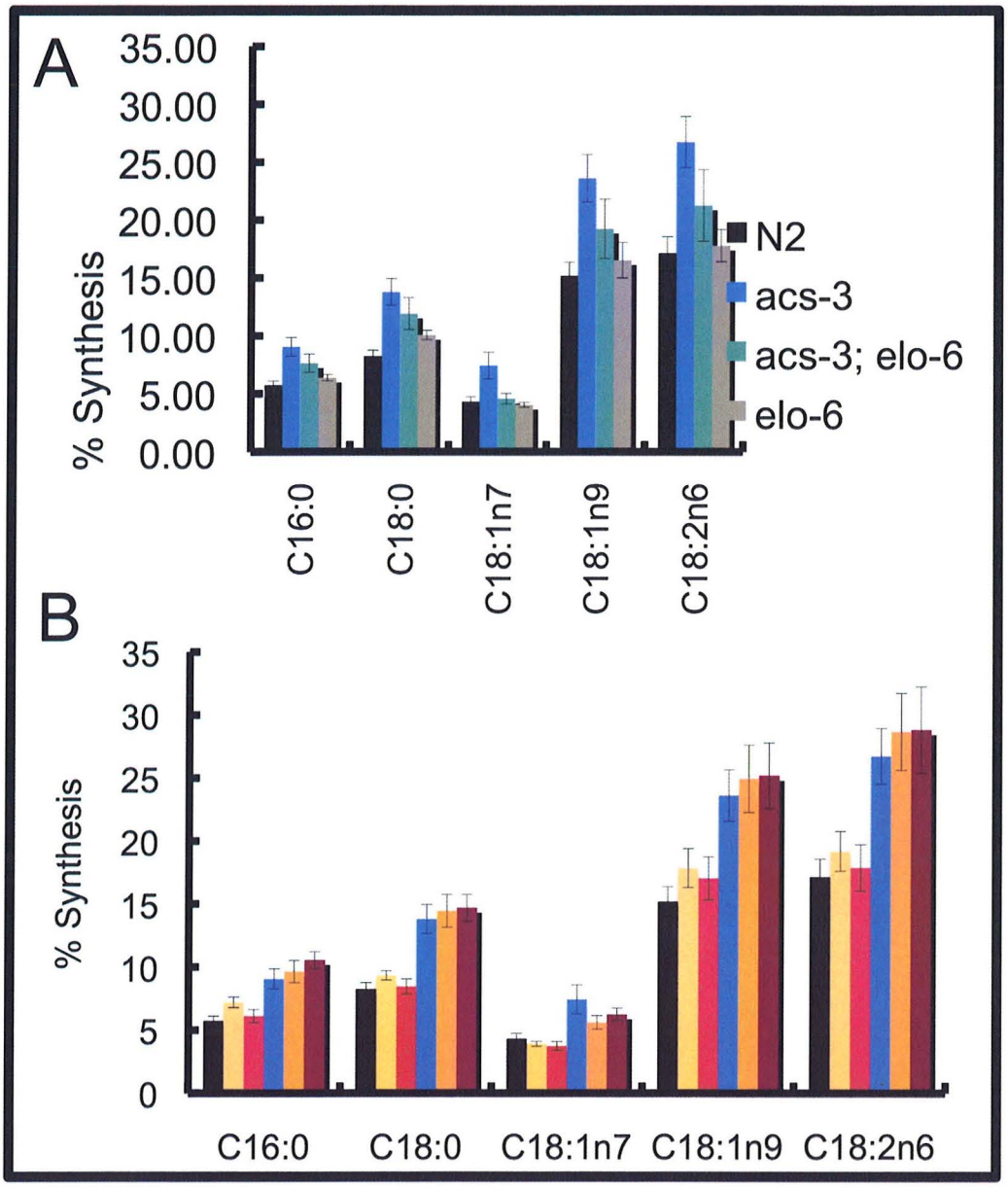

Figure A.4. ACS-3 Increases Fat Synthesis in ELO-6 Dependent Manner: (A) The acs-3 animals show increase fatty acid synthesis in all fatty acid species measured (blue). The acs-3;elo-6 (green) animals are partially rescued with synthesis levels slightly above wildtype (black). elo-6 anmsils have WT synthesis (grey). (B) ACS-3 Increases Fat Synthesis independent of ACDH-10 and ACDH-11. The levels of fatty acid synthesis are elevated in acs-3 (blue), acs-3;acdh-10 (orange), and acs-3;acdh-11 (red) animals. The levels of synthesis are normal in acdh-10 (light orange) and acdh-11 (light red) single mutants. Data shown is from a minimum of 5 experiments with SEM shown.

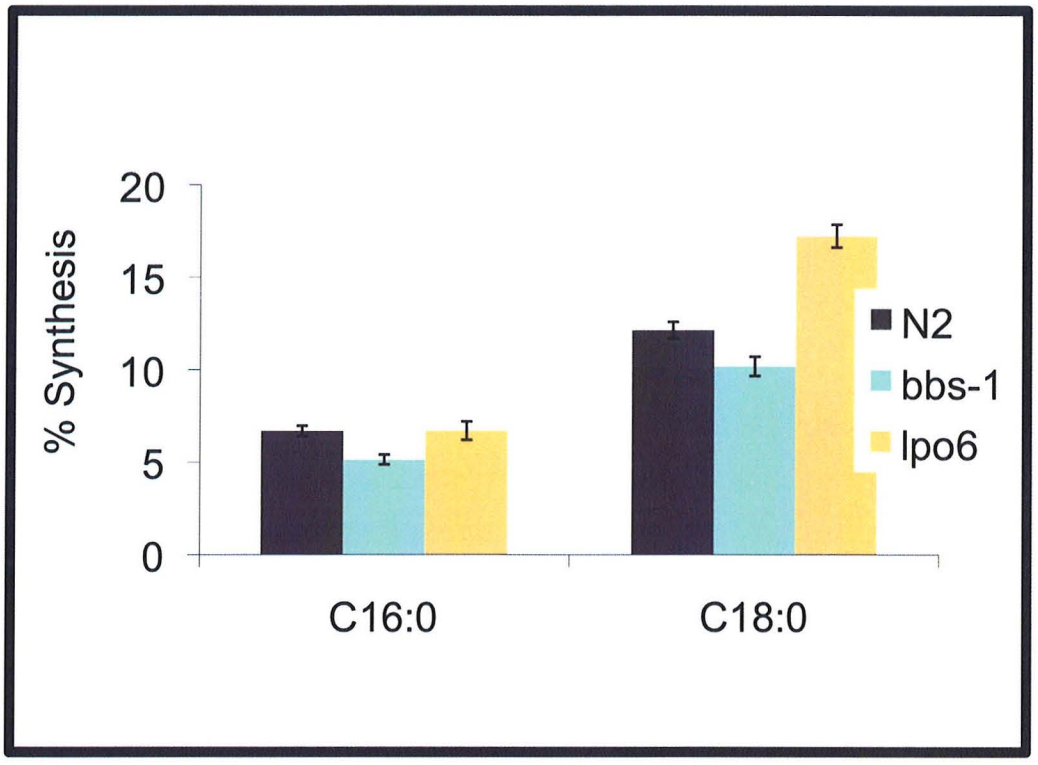

Figure A.5. Synthesis Quantification in *bbs-1* and *lpo-6* Mutants: We quantified *de novo* fatty acid synthesis in other animals that have been implicated in fat storage regulation. We found increased synthesis in *lpo-6* (yellow) and decreased synthesis in *bbs-1* (blue).

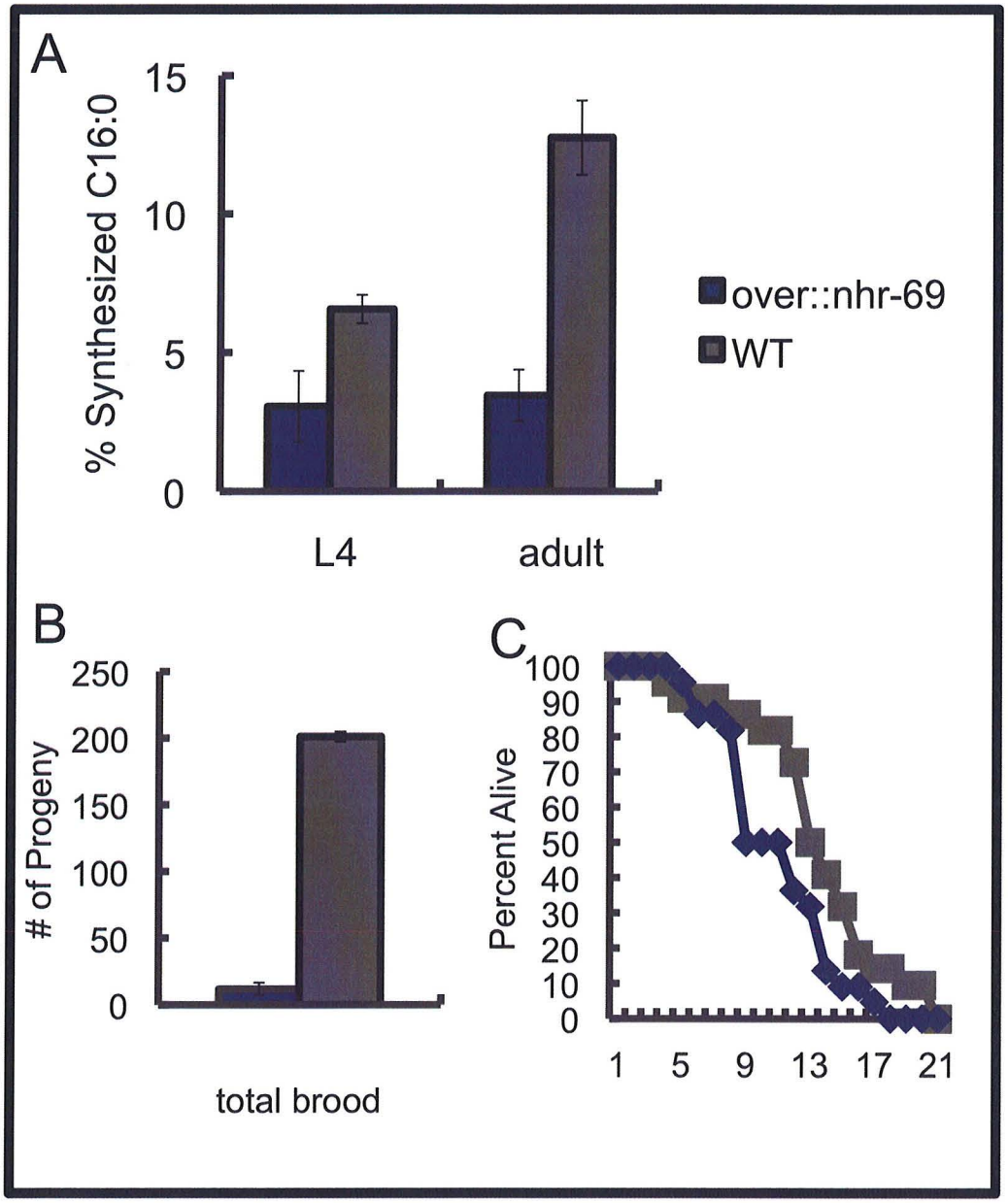

Figure A.6. Overexpression of *nhr-69* Eliminates Lipogenic Increase Seen in Adults: (A) We quantified *de novo* fatty acid synthesis in *over::nhr-69* animals (purple). These animals also had a reduced brood (B) and a short lifespan (C).

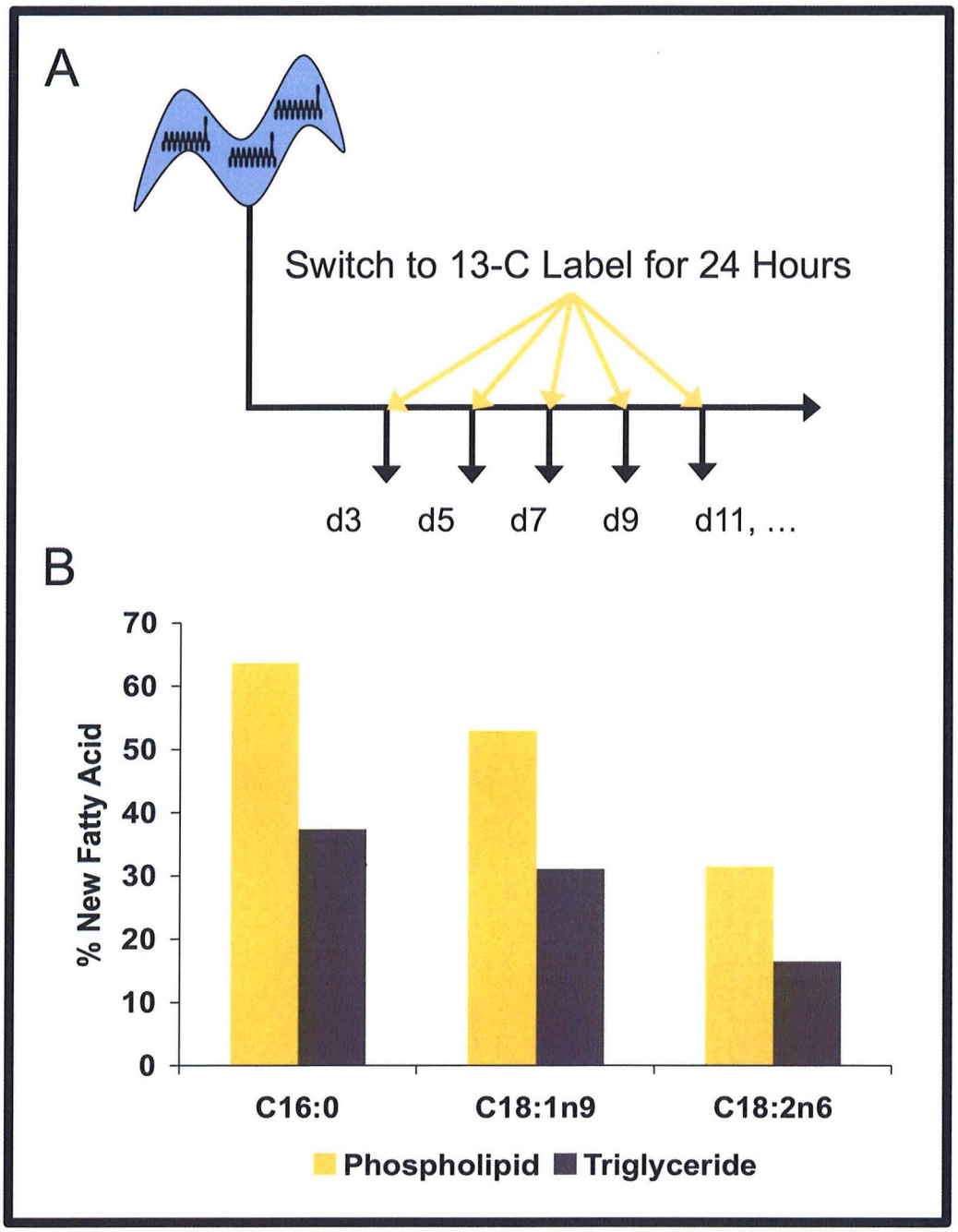

Figure A.7. Use of Stable Isotopes to Monitor Fatty Acid Turnover: (A) In order to quantify fatty acid turnover, we grew worms on unlabeled ^{12}C bacteria until early adulthood. We then transferred those animals to 99% ^{13}C bacteria for a 24 hour period. (B) In young adults, we found very high levels of fatty acid turnover in both phospholipids (yellow) and triglyceride (black).

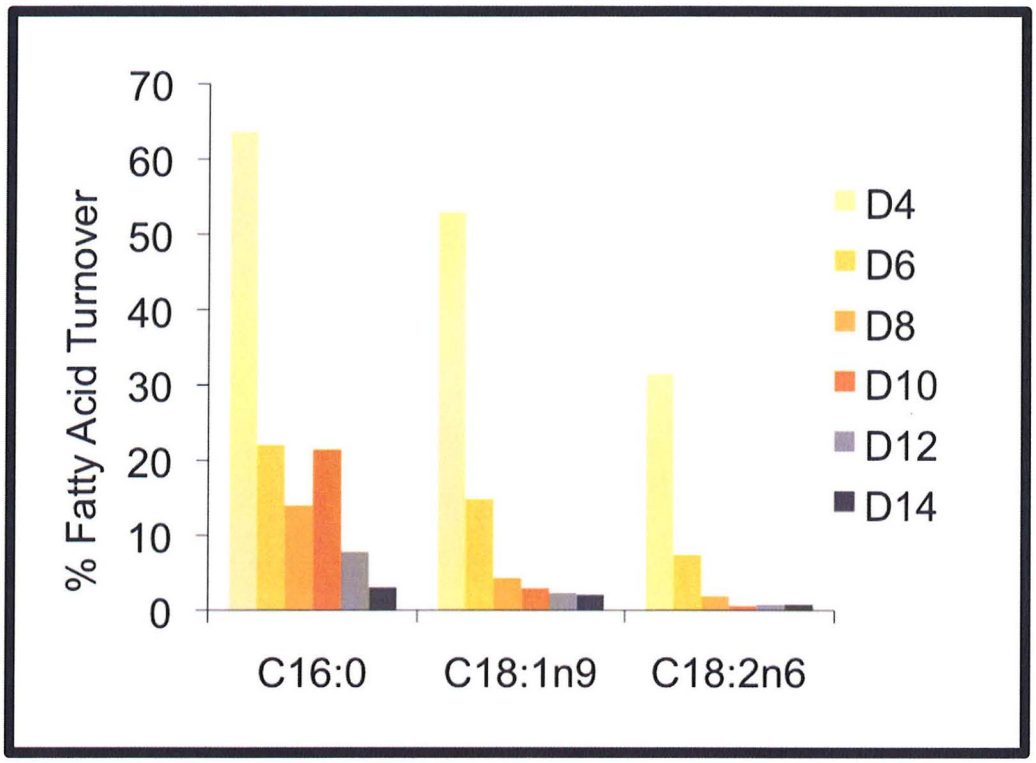

Figure A.8. Fatty Acid Turnover Decreases Over Aging: Although rates of fatty acid turnover start off quite high, there is an aging dependent decrease in fat turnover. Data is shown from one data set of purified phospholipids but the trend has been repeated multiple times.

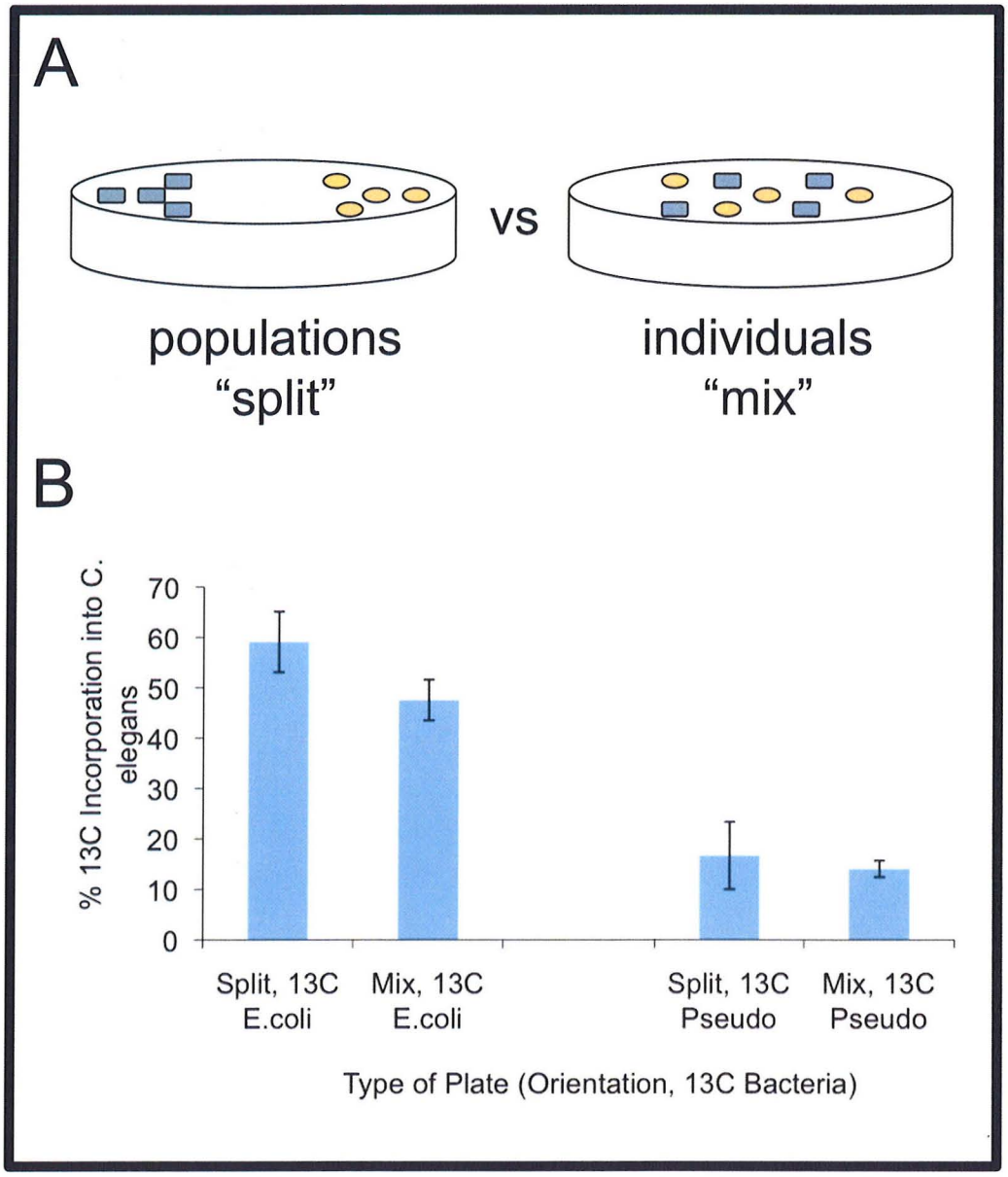

Figure A.9. Isotope Based Food Discrimination Studies: (A) In order to determine if the nematodes had a preference for a specific food source, we labeled one food source with 99% ^{13}C and monitored the incorporation of label into the worm's fats. This allowed us to determine if the animals could only distinguish *E. coli* (circles) from *Pseudomonas aeriginosa* (rectangles) in a "split" plating where populations of bacteria could be sensed or if the distinction could still be made based on an individual bacterium in the "mix" plating. (B) We found that the worms preferred the *E. coli* regardless of the plating format. The type of bacteria labeled with ^{13}C was also switched with the same results.

References

Arantes-Oliveira, N., Apfeld, J., Dillin, A., and Kenyon, C. (2002). Regulation of life-span by germ-line stem cells in Caenorhabditis elegans. Science *295*, 502-505.

Ashrafi, K. (2007). Obesity and the regulation of fat metabolism. WormBook, 1-20.

Ashrafi, K., Chang, F.Y., Watts, J.L., Fraser, A.G., Kamath, R.S., Ahringer, J., and Ruvkun, G. (2003). Genome-wide RNAi analysis of Caenorhabditis elegans fat regulatory genes. Nature *421*, 268-272.

Bluher, M., Michael, M.D., Peroni, O.D., Ueki, K., Carter, N., Kahn, B.B., and Kahn, C.R. (2002). Adipose tissue selective insulin receptor knockout protects against obesity and obesity-related glucose intolerance. Dev Cell *3*, 25-38.

Braeckman, B.P., Houthoofd, K., and Vanfleteren, J.R. (2009). Intermediary metabolism. WormBook, 1-24.

Brock, T.J., Browse, J., and Watts, J.L. (2006). Genetic regulation of unsaturated fatty acid composition in C. elegans. PLoS Genet *2*, e108.

Brown, R.A., Domin, J., Arcaro, A., Waterfield, M.D., and Shepherd, P.R. (1999). Insulin activates the alpha isoform of class II phosphoinositide 3-kinase. J Biol Chem *274*, 14529-14532.

Brunengraber, H., Kelleher, J.K., and Des Rosiers, C. (1997). Applications of mass isotopomer analysis to nutrition research. Annu Rev Nutr *17*, 559-596.

Bruning, J.C., Gautam, D., Burks, D.J., Gillette, J., Schubert, M., Orban, P.C., Klein, R., Krone, W., Muller-Wieland, D., and Kahn, C.R. (2000). Role of brain insulin receptor in control of body weight and reproduction. Science *289*, 2122-2125.

Bruning, J.C., Michael, M.D., Winnay, J.N., Hayashi, T., Horsch, D., Accili, D., Goodyear, L.J., and Kahn, C.R. (1998). A muscle-specific insulin receptor knockout exhibits features of the metabolic syndrome of NIDDM without altering glucose tolerance. Mol Cell *2*, 559-569.

Burnell, A.M., Houthoofd, K., O'Hanlon, K., and Vanfleteren, J.R. (2005). Alternate metabolism during the dauer stage of the nematode Caenorhabditis elegans. Exp Gerontol *40*, 850-856.

Butcher, R.A., Ragains, J.R., Li, W., Ruvkun, G., Clardy, J., and Mak, H.Y. (2009). Biosynthesis of the Caenorhabditis elegans dauer pheromone. Proc Natl Acad Sci U S A *106*, 1875-1879.

Chirala, S.S., Chang, H., Matzuk, M., Abu-Elheiga, L., Mao, J., Mahon, K., Finegold, M., and Wakil, S.J. (2003). Fatty acid synthesis is essential in embryonic development: fatty acid synthase null mutants and most of the heterozygotes die in utero. Proc Natl Acad Sci U S A *100*, 6358-6363.

Dorman, J.B., Albinder, B., Shroyer, T., and Kenyon, C. (1995). The age-1 and daf-2 genes function in a common pathway to control the lifespan of Caenorhabditis elegans. Genetics *141*, 1399-1406.

Drew, B.S., Dixon, A.F., and Dixon, J.B. (2007). Obesity management: update on orlistat. Vasc Health Risk Manag *3*, 817-821.

Flatt, T. (2009). Ageing: Diet and longevity in the balance. Nature *462*, 989-990.
Flavin, R., Zadra, G., and Loda, M. (2011). Metabolic alterations and targeted therapies in prostate cancer. J Pathol *223*, 283-294.

Flegal, K.M., Carroll, M.D., Ogden, C.L., and Curtin, L.R. (2010). Prevalence and trends in obesity among US adults, 1999-2008. JAMA *303*, 235-241.

Furuta, E., Pai, S.K., Zhan, R., Bandyopadhyay, S., Watabe, M., Mo, Y.Y., Hirota, S., Hosobe, S., Tsukada, T., Miura, K., *et al.* (2008). Fatty acid synthase gene is up-regulated by hypoxia via activation of Akt and sterol regulatory element binding protein-1. Cancer Res *68*, 1003-1011.

Gems, D., Sutton, A.J., Sundermeyer, M.L., Albert, P.S., King, K.V., Edgley, M.L., Larsen, P.L., and Riddle, D.L. (1998). Two pleiotropic classes of daf-2 mutation affect larval arrest, adult behavior, reproduction and longevity in Caenorhabditis elegans. Genetics *150*, 129-155.

Greer, E.R., Perez, C.L., Van Gilst, M.R., Lee, B.H., and Ashrafi, K. (2008). Neural and molecular dissection of a C. elegans sensory circuit that regulates fat and feeding. Cell Metab *8*, 118-131.

Halaschek-Wiener, J., Khattra, J.S., McKay, S., Pouzyrev, A., Stott, J.M., Yang, G.S., Holt, R.A., Jones, S.J., Marra, M.A., Brooks-Wilson, A.R., *et al.* (2005). Analysis of long-lived C. elegans daf-2 mutants using serial analysis of gene expression. Genome Res *15*, 603-615.

Hanahan, D., and Weinberg, R.A. (2011). Hallmarks of cancer: the next generation. Cell *144*, 646-674.

Hellerer, T., Axang, C., Brackmann, C., Hillertz, P., Pilon, M., and Enejder, A. (2007). Monitoring of lipid storage in Caenorhabditis elegans using coherent anti-Stokes Raman scattering (CARS) microscopy. Proc Natl Acad Sci U S A *104*, 14658-14663.

Hertweck, M., Gobel, C., and Baumeister, R. (2004). C. elegans SGK-1 is the critical component in the Akt/PKB kinase complex to control stress response and life span. Dev Cell *6*, 577-588.

Hilvo, M., Denkert, C., Lehtinen, L., Muller, B., Brockmoller, S., Seppanen-Laakso, T., Budczies, J., Bucher, E., Yetukuri, L., Castillo, S., *et al.* (2011). Novel Theranostic Opportunities Offered by Characterization of Altered Membrane Lipid Metabolism in Breast Cancer Progression. Cancer Res *71*, 3236-3245.

Holzenberger, M., Dupont, J., Ducos, B., Leneuve, P., Geloen, A., Even, P.C., Cervera, P., and Le Bouc, Y. (2003). IGF-1 receptor regulates lifespan and resistance to oxidative stress in mice. Nature *421*, 182-187.

Horiguchi, A., Asano, T., Ito, K., Sumitomo, M., and Hayakawa, M. (2008). Pharmacological inhibitor of fatty acid synthase suppresses growth and invasiveness of renal cancer cells. J Urol *180*, 729-736.

Hsin, H., and Kenyon, C. (1999). Signals from the reproductive system regulate the lifespan of C. elegans. Nature *399*, 362-366.

Hull, F.E., and Whereat, A.F. (1967). The effect of rotenone on the regulation of fatty acid synthesis in heart mitochondria. J Biol Chem *242*, 4023-4028.
Ioannides-Demos, L.L., Piccenna, L., and McNeil, J.J. (2011). Pharmacotherapies for obesity: past, current, and future therapies. J Obes *2011*, 179674.

Jones, K.T., Greer, E.R., Pearce, D., and Ashrafi, K. (2009). Rictor/TORC2 regulates Caenorhabditis elegans fat storage, body size, and development through sgk-1. PLoS Biol *7*, e60.

Joo, H.J., Yim, Y.H., Jeong, P.Y., Jin, Y.X., Lee, J.E., Kim, H., Jeong, S.K., Chitwood, D.J., and Paik, Y.K. (2009). Caenorhabditis elegans utilizes dauer pheromone biosynthesis to dispose of toxic peroxisomal fatty acids for cellular homoeostasis. Biochem J *422*, 61-71.

Katic, M., Kennedy, A.R., Leykin, I., Norris, A., McGettrick, A., Gesta, S., Russell, S.J., Bluher, M., Maratos-Flier, E., and Kahn, C.R. (2007). Mitochondrial gene expression and increased oxidative metabolism: role in increased lifespan of fat-specific insulin receptor knock-out mice. Aging Cell *6*, 827-839.

Kelleher, J.K. (2001). Flux estimation using isotopic tracers: common ground for metabolic physiology and metabolic engineering. Metab Eng *3*, 100-110.

Kenyon, C. (2010). A pathway that links reproductive status to lifespan in Caenorhabditis elegans. Ann N Y Acad Sci *1204*, 156-162.

Kenyon, C., Chang, J., Gensch, E., Rudner, A., and Tabtiang, R. (1993). A C. elegans mutant that lives twice as long as wild type. Nature *366*, 461-464.

Kniazeva, M., Crawford, Q.T., Seiber, M., Wang, C.Y., and Han, M. (2004). Monomethyl branched-chain fatty acids play an essential role in Caenorhabditis elegans development. PLoS Biol *2*, E257.

Kompare, M., and Rizzo, W.B. (2008). Mitochondrial fatty-acid oxidation disorders. Semin Pediatr Neurol *15*, 140-149.

Kuhajda, F.P. (2000). Fatty-acid synthase and human cancer: new perspectives on its role in tumor biology. Nutrition *16*, 202-208.

Kusakabe, T., Maeda, M., Hoshi, N., Sugino, T., Watanabe, K., Fukuda, T., and Suzuki, T. (2000). Fatty acid synthase is expressed mainly in adult hormone-sensitive cells or cells with high lipid metabolism and in proliferating fetal cells. J Histochem Cytochem *48*, 613-622.

Kusakabe, T., Nashimoto, A., Honma, K., and Suzuki, T. (2002). Fatty acid synthase is highly expressed in carcinoma, adenoma and in regenerative epithelium and intestinal metaplasia of the stomach. Histopathology *40*, 71-79.

Larsen, P.L., Albert, P.S., and Riddle, D.L. (1995). Genes that regulate both development and longevity in Caenorhabditis elegans. Genetics *139*, 1567-1583.

Lee, R.Y., Hench, J., and Ruvkun, G. (2001). Regulation of C. elegans DAF-16 and its human ortholog FKHRL1 by the daf-2 insulin-like signaling pathway. Curr Biol *11*, 1950-1957.

Lee, S.J., Hwang, A.B., and Kenyon, C. (2010). Inhibition of respiration extends C. elegans life span via reactive oxygen species that increase HIF-1 activity. Curr Biol *20*, 2131-2136.

Mabon, M.E., Scott, B.A., and Crowder, C.M. (2009). Divergent mechanisms controlling hypoxic sensitivity and lifespan by the DAF-2/insulin/IGF-receptor pathway. PLoS One *4*, e7937.

Mak, H.Y., Nelson, L.S., Basson, M., Johnson, C.D., and Ruvkun, G. (2006). Polygenic control of Caenorhabditis elegans fat storage. Nat Genet *38*, 363-368.

McCabe, B.J., and Previs, S.F. (2004). Using isotope tracers to study metabolism: application in mouse models. Metab Eng *6*, 25-35.

McElwee, J., Bubb, K., and Thomas, J.H. (2003). Transcriptional outputs of the Caenorhabditis elegans forkhead protein DAF-16. Aging Cell *2*, 111-121.

McElwee, J.J., Schuster, E., Blanc, E., Thornton, J., and Gems, D. (2006). Diapause-associated metabolic traits reiterated in long-lived daf-2 mutants in the nematode Caenorhabditis elegans. Mech Ageing Dev *127*, 458-472.

McPherson, R. (2007). Genetic contributors to obesity. Can J Cardiol *23 Suppl A*, 23A-27A.
Menendez, J.A., and Lupu, R. (2007). Fatty acid synthase and the lipogenic phenotype in cancer pathogenesis. Nat Rev Cancer *7*, 763-777.

Min, K.J., Hogan, M.F., Tatar, M., and O'Brien, D.M. (2006). Resource allocation to reproduction and soma in Drosophila: a stable isotope analysis of carbon from dietary sugar. J Insect Physiol *52*, 763-770.

Moller, G., Leenders, F., van Grunsven, E.G., Dolez, V., Qualmann, B., Kessels, M.M., Markus, M., Krazeisen, A., Husen, B., Wanders, R.J., *et al.* (1999). Characterization of the HSD17B4 gene: D-specific multifunctional protein 2/17beta-hydroxysteroid dehydrogenase IV. J Steroid Biochem Mol Biol *69*, 441-446.

Mooijaart, S.P., Brandt, B.W., Baldal, E.A., Pijpe, J., Kuningas, M., Beekman, M., Zwaan, B.J., Slagboom, P.E., Westendorp, R.G., and van Heemst, D. (2005). C. elegans DAF-12,

Nuclear Hormone Receptors and human longevity and disease at old age. Ageing Res Rev *4*, 351-371.

Mukhopadhyay, A., Deplancke, B., Walhout, A.J., and Tissenbaum, H.A. (2005). C. elegans tubby regulates life span and fat storage by two independent mechanisms. Cell Metab *2*, 35-42.

Mullaney, B.C., and Ashrafi, K. (2009). C. elegans fat storage and metabolic regulation. Biochim Biophys Acta *1791*, 474-478.

Mullaney, B.C., Blind, R.D., Lemieux, G.A., Perez, C.L., Elle, I.C., Faergeman, N.J., Van Gilst, M.R., Ingraham, H.A., and Ashrafi, K. (2010). Regulation of C. elegans fat uptake and storage by acyl-CoA synthase-3 is dependent on NR5A family nuclear hormone receptor nhr-25. Cell Metab *12*, 398-410.

Murata, S., Yanagisawa, K., Fukunaga, K., Oda, T., Kobayashi, A., Sasaki, R., and Ohkohchi, N. (2010). Fatty acid synthase inhibitor cerulenin suppresses liver metastasis of colon cancer in mice. Cancer Sci *101*, 1861-1865.

Murphy, C.T., McCarroll, S.A., Bargmann, C.I., Fraser, A., Kamath, R.S., Ahringer, J., Li, H., and Kenyon, C. (2003). Genes that act downstream of DAF-16 to influence the lifespan of Caenorhabditis elegans. Nature *424*, 277-283.

Murphy, E.J. (2006). Stable isotope methods for the in vivo measurement of lipogenesis and triglyceride metabolism. J Anim Sci *84 Suppl*, E94-104.

O'Brien, D.M., Min, K.J., Larsen, T., and Tatar, M. (2008). Use of stable isotopes to examine how dietary restriction extends Drosophila lifespan. Curr Biol *18*, R155-156.

O'Rourke, E.J., Soukas, A.A., Carr, C.E., and Ruvkun, G. (2009). C. elegans major fats are stored in vesicles distinct from lysosome-related organelles. Cell Metab *10*, 430-435.

Ogg, S., Paradis, S., Gottlieb, S., Patterson, G.I., Lee, L., Tissenbaum, H.A., and Ruvkun, G. (1997). The Fork head transcription factor DAF-16 transduces insulin-like metabolic and longevity signals in C. elegans. Nature *389*, 994-999.

Ookhtens, M., Kannan, R., Lyon, I., and Baker, N. (1984). Liver and adipose tissue contributions to newly formed fatty acids in an ascites tumor. Am J Physiol *247*, R146-153.

Partridge, L., Gems, D., and Withers, D.J. (2005). Sex and death: what is the connection? Cell *120*, 461-472.

Patel, D.S., Garza-Garcia, A., Nanji, M., McElwee, J.J., Ackerman, D., Driscoll, P.C., and Gems, D. (2008). Clustering of genetically defined allele classes in the Caenorhabditis elegans DAF-2 insulin/IGF-1 receptor. Genetics *178*, 931-946.

Perez, C.L., and Van Gilst, M.R. (2008). A 13C isotope labeling strategy reveals the influence of insulin signaling on lipogenesis in C. elegans. Cell Metab *8*, 266-274.

Piper, M.D., Skorupa, D., and Partridge, L. (2005). Diet, metabolism and lifespan in Drosophila. Exp Gerontol *40*, 857-862.

Pizer, E.S., Chrest, F.J., DiGiuseppe, J.A., and Han, W.F. (1998). Pharmacological inhibitors of mammalian fatty acid synthase suppress DNA replication and induce apoptosis in tumor cell lines. Cancer Res *58*, 4611-4615.

Rappleye, C.A., Tagawa, A., Le Bot, N., Ahringer, J., and Aroian, R.V. (2003). Involvement of fatty acid pathways and cortical interaction of the pronuclear complex in Caenorhabditis elegans embryonic polarity. BMC Dev Biol *3*, 8.

Rottiers, V., and Antebi, A. (2006). Control of Caenorhabditis elegans life history by nuclear receptor signal transduction. Exp Gerontol *41*, 904-909.

Shi, Y., and Burn, P. (2004). Lipid metabolic enzymes: emerging drug targets for the treatment of obesity. Nat Rev Drug Discov *3*, 695-710.

Shtonda, B.B., and Avery, L. (2006). Dietary choice behavior in Caenorhabditis elegans. J Exp Biol *209*, 89-102.

Strawford, A., Antelo, F., Christiansen, M., and Hellerstein, M.K. (2004). Adipose tissue triglyceride turnover, de novo lipogenesis, and cell proliferation in humans measured with 2H2O. Am J Physiol Endocrinol Metab *286*, E577-588.

Sze, J.Y., Victor, M., Loer, C., Shi, Y., and Ruvkun, G. (2000). Food and metabolic signalling defects in a Caenorhabditis elegans serotonin-synthesis mutant. Nature *403*, 560-564.

Taghibiglou, C., Martin, H.G., Rose, J.K., Ivanova, N., Lin, C.H., Lau, H.L., Rai, S., Wang, Y.T., and Rankin, C.H. (2009). Essential role of SBP-1 activation in oxygen deprivation induced lipid accumulation and increase in body width/length ratio in Caenorhabditis elegans. FEBS Lett *583*, 831-834.

Van Gilst, M.R., Hadjivassiliou, H., Jolly, A., and Yamamoto, K.R. (2005). Nuclear hormone receptor NHR-49 controls fat consumption and fatty acid composition in C. elegans. PLoS Biol *3*, e53.

Vander Heiden, M.G., Cantley, L.C., and Thompson, C.B. (2009). Understanding the Warburg effect: the metabolic requirements of cell proliferation. Science *324*, 1029-1033.

Wang, M.C., Min, W., Freudiger, C.W., Ruvkun, G., and Xie, X.S. (2011). RNAi screening for fat regulatory genes with SRS microscopy. Nat Methods *8*, 135-138.

Wang, M.C., O'Rourke, E.J., and Ruvkun, G. (2008). Fat metabolism links germline stem cells and longevity in C. elegans. Science *322*, 957-960.

Warburg, O., Wind, F., and Negelein, E. (1927). The Metabolism of Tumors in the Body. J Gen Physiol *8*, 519-530.

Watts, J.L. (2009). Fat synthesis and adiposity regulation in Caenorhabditis elegans. Trends Endocrinol Metab *20*, 58-65.

Watts, J.L., and Browse, J. (2002). Genetic dissection of polyunsaturated fatty acid synthesis in Caenorhabditis elegans. Proc Natl Acad Sci U S A *99*, 5854-5859.

Wolkow, C.A., Kimura, K.D., Lee, M.S., and Ruvkun, G. (2000). Regulation of C. elegans life-span by insulinlike signaling in the nervous system. Science *290*, 147-150.

Yamawaki, T.M., Berman, J.R., Suchanek-Kavipurapu, M., McCormick, M., Maria Gaglia, M., Lee, S.J., and Kenyon, C. (2010). The somatic reproductive tissues of C. elegans promote longevity through steroid hormone signaling. PLoS Biol *8*.

Yen, K., Le, T.T., Bansal, A., Narasimhan, S.D., Cheng, J.X., and Tissenbaum, H.A. (2010). A comparative study of fat storage quantitation in nematode Caenorhabditis elegans using label and label-free methods. PLoS One *5*.

Zhang, S.O., Trimble, R., Guo, F., and Mak, H.Y. (2010). Lipid droplets as ubiquitous fat storage organelles in C. elegans. BMC Cell Biol *11*, 96.

Curriculum Vitae

Carissa Perez Olsen

Education

University of Washington/Fred Hutchinson Cancer Research Center, Seattle, WA — 2005 - 2011
Molecular and Cellular Biology

Cornell University, Ithaca, NY — 2001 - 2005
Bachelor of Arts, Biological Sciences

Research Experience

Fred Hutchinson Cancer Research Center, Seattle, WA
Graduate Student, Van Gilst Laboratory, Basic Sciences Division March 2006-Present

- Thesis research (March 2006 – April 2011): Isotope, lipid biochemistry and genetic studies on the regulation of *de novo* fatty acid synthesis using the model organism *C. elegans (Advisor: Dr. Marc van Gilst)*

- Lab rotation (*Jan 2006 – March 2006)*: Biochemical and molecular studies of human papillomavirus genus β viral proteins and human tumor suppressors that link the virus's involvement in cancer formation *(Dr Denise Galloway)*

- Lab rotation (*Sept 2005 – Dec 2005)*: Genetic, immunohistochemistry and cell biology studies to explore the role of the E2F:DP complex in regulating the cell cycle exit at terminal differentiation in the pupal wing of *Drosophila melanogaster (Dr Bruce Edgar)*

Student Research Assistant, Wolfner Laboratory 2004 - 2005
Department of Genetics and Development
Cornell University, Ithaca, NY

- Primary research: Genetic and molecular studies to explore the feasibility of using *Drosophila Melanogaster* as a model system for studying human laminopathy diseases

Student Research Assistant, Linster Laboratory 2002 - 2004
Department of Neurobiology and Behavior
Cornell University, Ithaca, NY

- Primary research: Behavior and electrophysiology studies of habituation and learning in rats using odor discrimination tasks

Cornell Biomedical Research Apprentice, Suarez Laboratory 2000
Department of Biochemical Science

Cornell University, Ithaca, NY

- Primary research: Biochemistry and molecular studies to characterize of fucose-binding protein involved in bovine oviductal sperm reservoirs

---

Teaching Experience

2009	**Undergraduate Research Mentor,** Fred Hutchinson Cancer Research Center, Seattle WA
2008	**High School Student Mentor,** Fred Hutchinson Cancer Research Center, Seattle WA
Spring 2007	**Teaching Assistant,** Science Education Partnership/Fred Hutchinson Cancer Research Center, Seattle WA
Fall 2006	**Teaching Assistant** (*Undergraduate Biology Course)*, University of Washington, Seattle, WA

Fellowships & Awards

2007 - 2010	**Cellular & Molecular Biology Training Grant,** University of Washington, Seattle WA
2009	**Keystone Symposium Scholarship,** Hypoxia: Molecular Mechanisms of Oxygen Sensing and Response Pathways, Keystone, CO
2007	**Keystone Symposium Scholarship,** Bioactive Lipids in the Lipodomic Era, Taos, NM
2001 - 2005	**Cornell Presidential Research Scholar,** Cornell University, Ithaca, NY
2004	**Hughes Scholar**, Cornell University, Ithaca, NY

Presentations

January 20, 2010	Exposure to Hypoxic Environments Results in Elevated *de novo* Fatty Acid Synthesis as Revealed by a 13C Isotope Labeling Strategy Hypoxia: Molecular Mechanisms of Oxygen Sensing and Response Pathways Keystone Symposium, Keystone, CO

August 4, 2008	A Novel 13C Labeling Strategy Identifies Insulin/IGF Receptor Mutations that Selectively Modulate de novo Fatty Acid Synthesis and Longevity *C. elegans* Aging, Stress, Pathogenesis, and Heterochrony Topic Meeting, University of Wisconsin, Madison, WI
June 29, 2008	Using Metabolic Tracers to Quantify Fatty Acid Synthesis, Absorption, and Expenditure 16th International *C. elegans* Meeting, UCLA, Los Angeles, CA
October 12, 2007	Use of metabolic tracers to quantify fatty acid synthesis in *C. elegans* Isotope Tracers in Metabolic Research: Principles & Practice of Kinetic Analysis Course, University of Arkansas, Little Rock, AK
April 20, 2007	Defining the Regulation of Fatty Acid Synthesis by Insulin/IGF Signaling Seattle/Vancouver Worm Meeting, Seattle, WA
Feb 24, 2007	Metabolic Labeling Assays of Fatty Acid Synthesis and Turnover in *C. elegans* Keystone Symposia: Bioactive Lipids in the Lipidomics Era, Taos, NM

Publications

Morrish F, Noonan J, **Perez C.L.**, Gafken P.R., Fitzgibbon M.P., Kelleher J.K., Van Gilst M.R., and Hockenbery D.M. (2010) MYC-dependent mitochondrial generation of acetyl-coa contributes to fatty acid biosynthesis and histone acetylation during cell cycle entry. *Journal of Biological Chemistry* .

Mullaney B.C., Blind R.D., Lemieux G.A., **Perez C.L.,** Elle I.C., Faergeman N.J., Van Gilst M.R., Ingraham H.A. and Ashrafi K. (2010) Regulation of *C. elegans* Fat Uptake and Storage by Acyl-CoA Synthase-3 Is Dependent on NR5A Family Nuclear Hormone Receptor *nhr-25. Cell Metabolism 12:* 398-410.

Perez C.L., and Van Gilst M.R. (2008) A ^{13}C isotope labeling strategy reveals the influence of insulin signaling on lipogenesis in *C. elegans. Cell Metabolism* 8(3):266-274.

Greer E.R., **Perez C.L.**, Van Gilst M.R., Lee B.H., and Ashrafi K. (2008) Neural and molecular dissection of a *C. elegans* sensory circuit that regulates fat and feeding. *Cell Metabolism* 8(2):118-131.

Buttitta L.A., Katzaroff A., **Perez C.L.**, de la Cruz A.F., and Edgar B.A. (2007). A double-assurance mechanism controls cell cycle exit upon terminal differentiation in Drosophila. *Developmental Cell* 12:631-643.

Ignotz G.G., Lo M.C., **Perez C.L.,** Gwathmey T.M., and Suarez S.S. (2001). Characterization of a fucose-binding protein from bull sperm and seminal plasma that may

be responsible for formation of the oviductal sperm reservoir. *Biology of Reproduction* 64: 1806-1811.